بسم الله الرحمن الرحيم

IN THE NAME OF ALLAH

THE MERCIFUL THE COMPASSIONATE

BIOPHYSICAL MECHANISM OF RADIATION DAMAGE TO MAMMALIAN CELLS BY HEAVY CHARGED PARTICLES.

MUHAMMAD JAMAL BIN MD. ISA

M.Sc.

Department of Physics,
University of St. Andrews.

November 1986

"The more Knowledge I gained, the more I know of my Ignorance"

Imam Al-Ghazali.

CONTENTS

2.5.2/

3.4.3/

3.9.4/

Page

CHAPTER VII

DISCUSSIONS, CONCLUSIONS AND PROPOSALS FOR FUTURE WORK

ACKNOWLEDGEMENTS

The author wishes to acknowledge the following for their invaluable help:-

Dr. D.E. Watt	:	for his guidance, supervision and much understanding
Dr. A.C. Riches Dr. I.V. Chapman Professor D. Brynmor Thomas Professor J.H. Martin	:	members of staff who gave lectures in the course

Finally, I wish to express my gratitude to my employer, The Director General of the Nuclear Energy Unit, Prime Minister's Department and The Government of Malaysia for granting a study leave and financial sponsorship to make it possible for me to carry out this work.

DECLARATION

I Muhammad Jamal Bin Md. Isa hereby certify that this thesis has been composed by myself, that it is a record of my own work, and that it has not been accepted in partial or complete fulfilment of any other degree or professional qualification.

November 1986

ABSTRACT

This work is divided into two parts: the first being the discussion of the most basic tool needed in studying the survival of cells irradiated by charged particles i.e. the particle accelerator; and the second being the analysis of already published information on cell survival to extract a satisfactory physical mechanism responsible for radiation damage to mammalian cells.

Intrinsic efficiencies for the inactivation of mammalian cells, V79 Chinese hamster cells in particular, irradiated by accelerated heavy charged particles have been determined by re-analysing published data on the survival of mammalian cells.

Results from this work point to the significance of the 1.8 nanometer mean free path between primary ionizations of the incident radiation. It was concluded that the dominant physical mechanism of damage in the inactivation of mammalian cells with double stranded DNA is determined by the 'matching' of the mean free path between primary ionizations to the strand separation in the DNA.

Contrary to the widely accepted view, this work also seems to suggest that the contribution of damage due to delta-rays when mammalian cells are irradiated by heavy charged particles may not be as significant as thought hither to. This follows the observed lack of any clear/

clear relationship between the energy of the delta-rays, E_δ, and the total intrinsic efficiency for inactivation, ϵ_R, of the incident radiation; and also between E_δ and the calculated intrinsic efficiency for inactivation of the delta-rays, $\bar{\epsilon}_j$, (beyond the saturation condition i.e. $1/\bar{I}_s < 1.8$ nm) themselves.

Results also show that for all the cell lines investigated, there is an optimum value for LET of between 150 and 190 eV/nm beyond which the increase in the efficiency for inactivation per increase in LET is drastically reduced.

Finally, a discussion on future experimental and theoretical work is presented.

LIST OF FIGURES

CHAPTER VI/

6.11/

LIST OF TABLES

CHAPTER I

GENERAL INTRODUCTION

There can hardly be any doubt that radiation will continue to be an important factor in our lives. Present and future advances in nuclear technology urgently require further work in research and development in the field of radiation biophysics if the maximum benefit is to be obtained at minimal risk from the various kinds of radiation that form a major by-product of nuclear processes. The rapid development of nuclear research and technology as well as the wide range of applications of radiations in the treatment of disease; in widely differing industrial production processes; for the sterilization of drugs and medical appliances; for experiments in the food industry; and also the use of nuclear reactors and radioactive isotopes, makes it essential to elucidate the mechanisms by which radiations act.

It is interesting to look back at some of the historical aspects of development of basic research in radiation biophysics. As with most new lines of research, its development was initiated by quite accidental observations once the scene had been set by the discovery of ionizing radiations. A good example is that of Becquerel, who absent-mindedly carried a radium preparation around in his waistcoat pocket;/

pocket; this caused an inflamation of the skin, which he found healed only with difficulty. After the discovery of X-rays there were many scientists who, marvelling at their penetrating power, never tired of looking at images of the skeleton of their own hands. However, their enjoyment was soon dampened by the observation of peculiar changes in the exposed skin. Such phenomena stimulated interest in the action of ionizing radiations.

Progress in physics, chemistry and biology led to the application of mathematical and statistical methods to the interpretation of these observations. Simply put, this involved the study of the action of radiation as a function of the absorbed radiation energy i.e. as a function of dose. From a statistical analysis of the shape of the dose-response curves obtained, attempts were made to draw conclusions about the nature of the effective mechanisms. This interest in the nature of the action of radiation led to the introduction of the various radiation parameters in order to explain the observed effects.

Radiotherapists were the first large group of practising scientists to require a method for specifying the quality of the various energies of the X and gamma-rays used in therapy. Radiations of different types or of the same type at different energies can, for equal absorbed doses, produce different/

different degrees of effects as measured by some specified biological end-point. Therefore, at least one or possibly more parameters, in addition to absorbed dose, is required if the biological effectiveness of the radiation field is to be quantified. This parameter (or parameters) determines the quality of the radiation i.e. an inherent property of the radiation manifested by its interaction with matter. The quality is the measure of the 'ability' with which a certain 'quantity' (e.g. dose) of the radiation can produce a specified biological end-point (e.g. cell death).

As the physical processes of radiation absorption have become better understood and with the introduction of more parameters, attempts to express quantitatively the biological effects induced by ionizing radiations in terms of these physical parameters descriptive of the initial radiation field were made. This led to the formulation of the many known radiation damage models descriptive of the biological action of ionizing radiations.

Radiation damage models, in general, attempt to describe the damage caused by ionizing radiation to higher cells (mammalian in particular) and are usually of similar form, containing two and sometimes three unknown parameters. Since the initial models were mainly used as a way of describing the shape of the survival/

survival curves, there is a conventional form most models ascribe to:-

Surviving Fraction = f (some measurable variable of the energy transference)

where the energy variable may be Dose, LET, etc., for example,

$$S.F. = \exp(-K_1 D)[1-(1-\exp(K_2 D))^n] \quad \text{(Katz et al 1971)}$$

$$S.F. = \exp(\alpha D + \beta D^2) \quad \text{(Rossi-Kellerer 1971)}$$

where D is the absorbed dose and $K_1, K_2, n, \alpha, \beta$ are parameters defined by the authors.

Although much effort has been expended in the quest for a viable model descriptive of the biological action of ionizing radiation, to date none of these have been completely successful. Indeed, it is doubtful if a perfect model can ever be formulated. To do so would require a complete understanding and a qualitative analysis of every stage in the vast complexity of events that evolve between the initial physical passage of the radiation and the ultimate biological effect. The best approach is then to identify the main processes which dominate in the chain of events and which determine the ultimate biological action and to attempt to incorporate these quantitatively into a model which, at best, must be approximate yet as realistic as possible.

PART I.

CHAPTER II

PARTICLE ACCELERATORS

2.1 Introduction

Particle accelerators are built for the sole purpose of endowing nuclear particles with large quantity of kinetic energy so that they may serve as projectiles to alter the structure of other nuclei or to act as probes to discover relevant information on the forces that hold nuclei together. When Rutherford demonstrated in 1919 that the nitrogen nucleus could be disintegrated by the naturally occuring alpha-particles from radium and thorium, a new era was opened in physics. For the first time man was able to modify the structure of the atomic nucleus and physicists began to recognize the need for artificial sources of much more energetic accelerated particles to disintegrate nuclei of heavier atoms. Ever since then, the particle accelerator has been used mainly in the field of particle and nuclear physics. Not until quite recently, has its used been extended to other fields of science such as solid state physics, radiation chemistry, biology and medicine, aerospace technology to name a few.

In few/

In few fields of science has progress been so spectacular. In a relatively short time, particle accelerators have undergone a tremendously rapid development. Particle energies available for research have increased from a few keV to many billion (10^9) eV. Research on nuclear physics and the properties of fundamental particles owes much of its progress to the continuously increasing energy achieved by a series of electronuclear machines, each larger and more effective than its predecessor. Initially, the particles most often used for acceleration are electrons and nuclei of light elements such as protons, deuterons and alpha-particles but with the ever increasing acceleration capabilities of later machines, heavier nuclei such as those of carbon, beryllium, oxygen, neon, argon, etc., have also been accelerated.

2.2 The Fundamental Principles of Particle Acceleration

The basic structure of a particle accelerator can be represented very schematically by a diagram such as that of figure 2.1. There are three fundamental components: the ion source or electron gun (according to the type of particle to be accelerated) in which the particles are produced; an acceleration chamber under high vacuum where the acceleration is performed; and a target on which the high velocity particles impinge.

Besides/

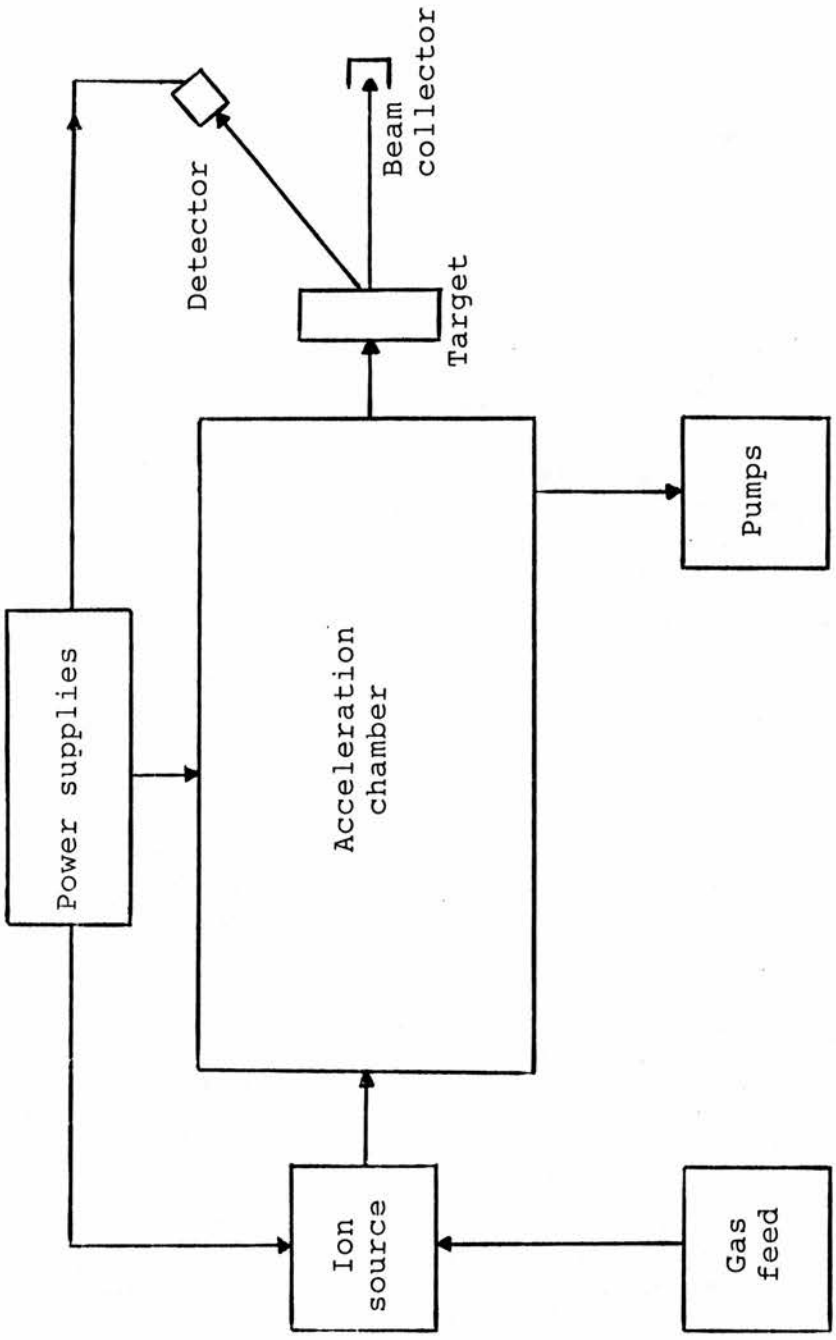

Fig. 2.1 Schematic diagram of a particle accelerator.

Besides these basic components some machines require power generators to energize the coils of a large magnet, high voltage supplies, generators of oscillating electric fields, etc. All these items have been grouped together as power supplies in figure 2.1. Vacuum pumps are obviously needed to remove the air from the acceleration chamber, thus allowing the acceleration to proceed unperturbed. The acceleration chamber may have widely different shapes in different types of machines but the physical principles underlying the acceleration of particles, namely the laws of mechanical motion and interaction of charged particles with electromagnetic field, are the same in all cases.

2.2.1 Laws of Motion

If a particle moves, its position vector, $\underline{r}$, will change in magnitude and direction with time. This is expressed mathematically by

$$\underline{r} = r(t) \qquad 2.1$$

The velocity, $\underline{v}$, of a particle is defined as the rate of change of $\underline{r}$ with time. That is to say, if the distance travelled by a particle in time Δt is Δr, the mean velocity, $\bar{v}$, is given by

$$\bar{v} = \Delta r/\Delta t \qquad 2.2$$

whilst the instantaneous velocity is defined as the limit to which the ratios $\Delta r/\Delta t$ tends when the interval Δt is made shorter and shorter, approaching the value zero,

$$\text{i.e.} \quad \underline{v} = \lim_{\Delta t \to 0} \frac{\Delta \underline{r}}{\Delta t} = \frac{d\underline{r}}{dt} = \dot{\underline{r}} \qquad 2.3$$

Similarly, the acceleration $\underline{a}$ is the rate of change of velocity with time,

$$\underline{a} = \lim_{\Delta t \to 0} \frac{\Delta \underline{v}}{\Delta t} = \frac{d\underline{v}}{dt} = \dot{\underline{v}} = \ddot{\underline{r}} \qquad 2.4$$

and is directed along the increment of velocity dv in time dt.

The problem is then how to produce acceleration. According to the fundamental laws of dynamics, due to Newton, a particle of mass, m, will experience an acceleration, $\underline{a}$, when subject to a force, $\underline{F}$, i.e.

$$\underline{F} = m\underline{a} \qquad 2.5$$

It is this force, $\underline{F}$, that is provided by the interaction of the charge on the particle and the electromagnetic field of the acceleration chamber that gives the particle the necessary acceleration.

2.2.2 The Electron Volts

In dealing with acceleration and in discussing the energy of nuclear or atomic phenomena, it has been found convenient to introduce the electron-volt (eV) as a unit of energy. The amount of energy gained by any particle bearing a charge as large as that of an electron in falling freely across a one-volt potential difference is called one electron-volt. Since an electron has 1.6×10^{-19} coulomb of charge, then

$$1 \text{ eV} = 1.6 \times 10^{-19} \text{ coulomb} \times 1 \text{ volt}$$
$$= 1.6 \times 10^{-19} \text{ joule}$$

A proton has a charge exactly as large as does an electron (though of positive rather than of negative electricity), therefore, one could equally well speak of "proton-volts" as of electron-volts; but custom has settled on the latter terminology.

If either a proton or an electron falls freely through one-volt, it will acquire 1 eV or 1.6×10^{-19} joule. A doubly ionized helium atom, bearing two electron charges, in falling through one-volt will gain 2 eV or 3.2×10^{-19} joule.

2.2.3 Relativity

Only a limited amount of the theory of relativity required to understand particle accelerators is necessary/

necessary but absolutely crucial. Classically, kinetic energy is given by the expression $\frac{1}{2}M_o v^2$, so a body of mass M_o, will quadruple its kinetic energy if the velocity, v, is doubled. Since there seems to be nothing to prevent one from adding as much energy as one pleases, it looks as though any velocity whatsoever should be attainable. But the theory of relativity, due to Einstein, declares that the velocity of light is the ultimate and that mass and energy are interconvertible. An increase in kinetic energy is associated with an increase in both mass and velocity, the change in the former being small when velocity is low; but as the limiting velocity of light is approached, a larger and larger fraction of the energy increment appears as a gain in mass.

The relativistic statement for the mass as a function of velocity states that

$$M = \frac{M_o}{(1-v^2/c^2)^{\frac{1}{2}}} \qquad 2.6$$

Here, c is the velocity of light i.e. 3×10^8 m sec^{-1}, M_o is the rest mass (the mass as measured by an observer with respect to whom the body is at rest), while M is the mass as measured by an observer with respect to whom the body has velocity v. The difference between M and M_o is utterly negligible for ordinary man-made projectiles, but it becomes distinctly noticeable/

noticeable for electrons and ions; even in small accelerators truly high velocities can be reached.

2.2.4 Kinetic Energy

Einstein introduced the concept that mass and energy are interconvertible, the ratio of energy to mass being c^2. Thus a body of mass M_o, at rest with respect to an observer, represents a supply of energy (its so called rest mass energy) given by E_o, where

$$E_o = M_o c^2 \qquad 2.7$$

Now let this mass be given some kinetic energy, T; the total energy, E, is then

$$E = E_o + T \qquad 2.8$$

$$\text{i.e. } E = M_o c^2 + T \qquad 2.8a$$

It is possible to express this total energy in terms of a total mass, M, through the expression

$$E = Mc^2 \qquad 2.9$$

so that

$$Mc^2 = M_o c^2 + T \qquad \text{(by equation 2.8a)}$$

giving

$$M = M_o + \frac{T}{c^2} \qquad 2.10$$

This mass, M, of a body in motion with respect to an observer/

observer is identical with its initial mass, as seen by the same observer. Owing to the enormous value of c^2, the kinetic energy must be very large indeed in order for M to be noticeably different from M_o. Solving equation 2.10 for T, gives

$$T = c^2(M - M_o) \qquad 2.11$$

and substituting the value of M from equation 2.6, gives

$$T = M_o c^2 \left[\frac{1}{(1-v^2/c^2)^{\frac{1}{2}}} - 1\right] \qquad 2.12$$

If v is very small compared with c, this may be expanded in a power series in v/c;

$$\text{i.e.} \quad T = M_o c^2 [1 + \tfrac{1}{2}(v/c)^2 + 3/8(v/c)^4 + \ldots\ldots \ldots - 1] \qquad 2.13$$

and if the exceedingly minute terms in $(v/c)^4, (v/c)^6$, etc., are neglected, this reduces to

$$T = \tfrac{1}{2}M_o v^2 \qquad 2.14$$

which is the elementary expression for the kinetic energy of mass, M_o, as mentioned earlier.

It has been found convenient to measure velocity as a fraction of that of light by defining the dimensionless quantity, β, as follows

$$\beta = v/c \qquad 2.15$$

This is/

This is equivalent to the aeronautical Mach number, which measures speed in terms of that of sound. But, whereas Mach numbers greater than unity can be attained, this is not true of β; nothing but light can reach $\beta=1$, though this figure can be approached very closely by particles of sufficient energy. The relativistic expression for kinetic energy then becomes

$$T = E_o\left[\frac{1}{(1-\beta^2)^{\frac{1}{2}}} - 1\right] \qquad 2.16$$

solving for β yields

$$\beta^2 = 1 - \frac{1}{(1 + T/E_o)^2} \qquad 2.17$$

which shows that if a particle has a kinetic energy equal to its rest energy i.e. $T=E_o$, then $\beta=0.886$.

Since $T=E-E_o$, equation 2.17 can be written in the very useful form of

$$\beta^2 = \frac{E^2 - E_o^2}{E^2} \qquad 2.18$$

2.3 Types of Particle Accelerators

There exist today many different kinds of particle accelerators. They can generally be categorised into two types. One, is the straightforward way of accelerating a charged particle by letting it fall through a potential drop (or rise depending on the charge/

charge of the particle) and machines which do this are known as DC accelerators. The other is by continuously accelerating the particle through an alternating electric field such that its change during the flight of the particle is of importance and machines which perform this kind of acceleration are known as cyclic accelerators.

2.4 DC Accelerators

The technique of endowing charged particles with kinetic energy by allowing them to fall in a vacuum through an electrostatic potential had been known for years, in the production of X-rays and in the early work on the measurement of the charge-to-mass ratio of electrons and positively charged isotopes. In priciple it was only necessary to apply these techniques at higher and higher voltages. But there are difficulties, primarily of insulation, both with respect to the voltage producing device and to the discharge tube through which the particles pass. This tube must be of insulating material, for the full voltage is applied to it from end to end, the ion source being at one end and the target at the other. It must be well evacuated, not only to prevent an arc or glow dicharge within it, but also to permit free passage for the ions as they gain energy in falling down the potential hill.

The problem/

The problem of insulation becomes more acute with the advent of the Van de Graaff electrostatic generator (initially high voltage was generated by a succession of voltage-multiplying rectifier circuits) which could generate much higher potentials. From observations, it became evident that, left to itself, a high voltage generally will not be distributed to form a uniform gradient to ground, across intervening space or insulating materials. It is much more likely for a gentle gradient to develop across the majority of the distance, followed by a large potential drop across the remaining small space, thus initiating flash-over. By forcing intermediate positions to be held at intermediate potentials, a distribution of voltage much nearer to the uniform ideal can be attained, with consequent improvement in voltage holding ability. This may be achieved by breaking up insulating columns and discharge tubes into short segments separated by metal pieces which are connected to appropriate points on a potential dividing system between the high voltage terminal and ground.

In modern Van de Graaff machines, a cylindrical volume of relatively uniform gradient is produced by a large number of coaxial hoops maintained in the above manner at successively graded potentials. Inside this region are located the segmented structured members, the segmented discharge tube and the charging belt. Finally/

Finally the entire assembly is encased in a steel shell filled with several atmospheres of nitrogen or a mixture of other gases which inhibit breakdown. By these means, developed over the years with much painstaking effort, the Van de Graaff technique now yields nuclear projectiles of unsurpassed precision and stability of energy up to 10 million electron-volts. This seems to be just about the limit, for insulation problems become intractable at higher voltage.

Further development has introduced the two-stage "tandem" Van de Graaff machines. In this machine, as shown by figure 2.2, positive ions produced at ground potential are accelerated to a few kilovolts and then sent through a channel containing a gas, where an appreciable fraction of the positive ions pick up two electrons and become negatively charged. These are then accelerated by perhaps 5 million volts to the high voltage terminal, where they pass another gas-filled chamber. Both electrons become stripped off, leaving a positive ion which is further accelerated (through a second discharge tube) back to ground potential, thereby gaining, over all, an energy twice that of the potential of the high-voltage terminal.

2.5 Cyclic Accelerators

With the exception of the "tandem" Van de Graaff, all the/

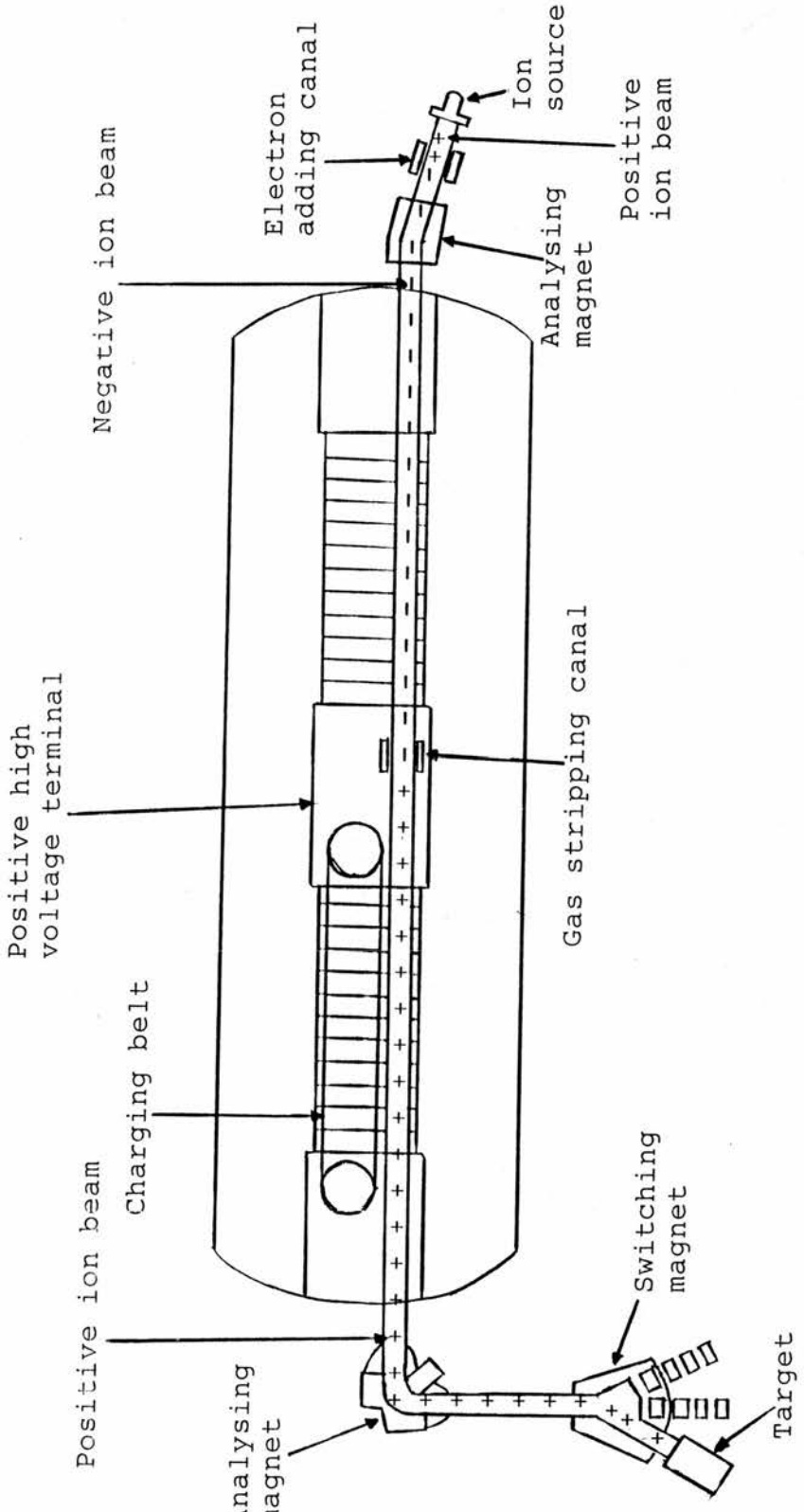

Fig. 2.2 Two-stage "tandem" Van de Graaff accelerator.

all the DC accelerators produce a single value of potential i.e. in falling across which, the particle acquires its full kinetic energy. On the other hand, cyclic accelerators, as the name suggests, are devices in which a low voltage is used over and over again with the result that the final energy equals that gained in one passage through the voltage generator multiplied by the number of such traversal.

The development of such cyclic acceleration has opened up a whole new world of laboratory exploration, for particles are now available with energies millions of times greater than that produced by the application of steady electrostatic potentials.

2.5.1 The Linear Accelerator

The simplest of the cyclic accelerators is the linear accelerator, a device in which high energy is attained by the repeated application of a small accelerating force and in which the particles travel in a straight line.

It basically consists of a series of hollow metal "drift tubes" which are aligned along the axis of a cylindrical glass vacuum envelope as shown in figure 2.3. Alternative tubes are connected to the terminals of an AC generator running at constant frequency, so that even-numbered tubes are positively charged when the odd-numbered tubes are negative, and vice-versa.

Suppose/

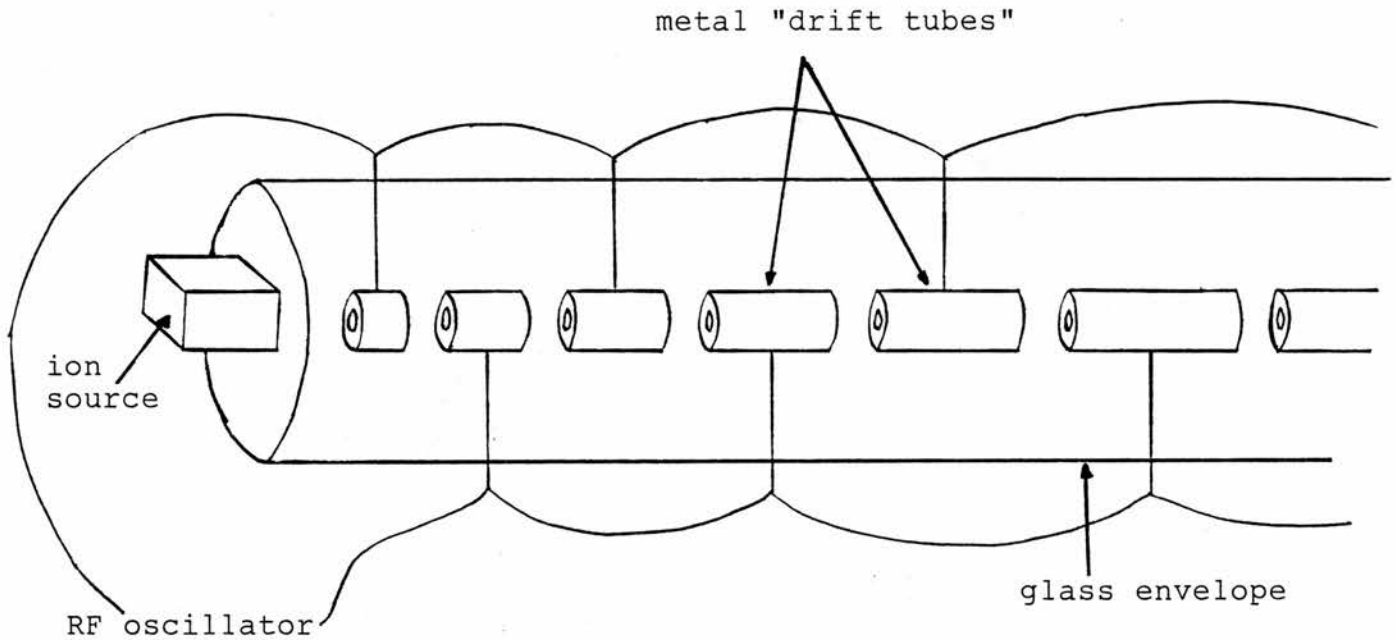

Fig. 2.3 The Wideroe linear accelerator. (Each drift tube becomes charged to the opposite sign from that of its neighbours. The distance from gap-to-gap is travelled in a half-period of the oscillator.)

Suppose a positive ion is emitted from a source at one end of this array at the moment when the first drift tube is at its peak negative potential. The electric field between source and tube will accelerate the ion until it plunges into the interior of the tube, where upon the particle finds itself in a field-free* region and coasts on at a steady velocity. With the proper ratio of the tube length to particle velocity, the ion will reach the gap between the first and second tubes exactly one-half cycle later when the potentials of all tubes have reversed, so that a second acceleration is experienced in crossing the second gap. This process proceeds along the whole length of the device, the final energy being the sum of all the energy increments gained in all the gaps.

Since the particle goes faster and faster, while the time for the reversal of the field is fixed at a constant value, it is apparent that the successive drift tubes must increase in length in an appropriate manner. Hence, it is not surprising that linear accelerators of enormous total length have been built in order to produce the most energetic of particles.

2.5.2 The Cyclotron

The cyclotron may be considered as a linear accelerator which has been wrapped up into a flat spiral and encased/

---

*It is a well-known physical fact that there is no electric field inside a hollow conductor, no matter what its potential as a whole may be.

and encased in an evacuated chamber, with the addition of a steady magnetic field perpendicular to its plane. The effect of the field on the moving ions is to cause their paths to become circular, with greater radius after each energy increment. The drift tubes are now replaced by two semicircular hollow electrodes (fig. 2.4) known as 'dees' (because of their shape); and they are connected to a source of alternating voltage of fixed frequency, as were the drift tubes in the linear accelerator.

In a linear accelerator, each drift tube must be of a particular length so that the speeding-up ions will traverse each in equal time. In a cyclotron there are no specific drift tubes, the length of time a particle is sheltered from the electric field depended on the length of path it follows inside a dee. The success of the machine as an accelerator depends on the fortunate circumstance that fast particles take longer paths i.e. larger radius, and slow particles shorter ones, so that the time required to traverse any path is the same (though there is a limitation to the validity of this statement; see Appendix I).

The acceleration action is much as before. A positive ion released from a centrally located source between the dees is acted on by the electric field between them, being attracted towards whichever dee is negatively charged. The ion then coasts at constant speed/

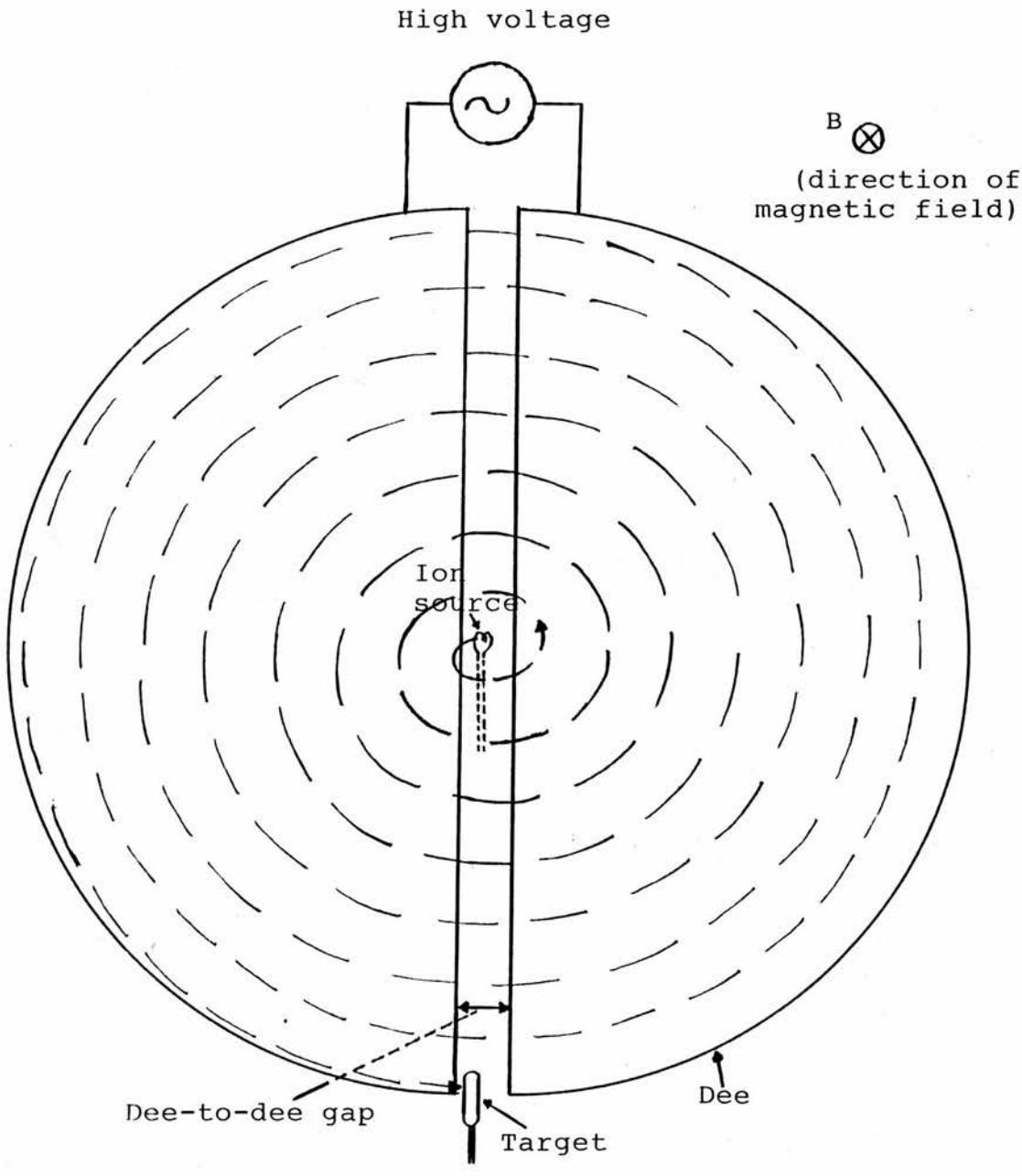

Fig. 2.4 Principle of operation of a cyclotron.

speed in the region within the dee, free of electric forces. The magnetic field bends the path into a semicircle and when the inter-electrode gap is again reached, the potentials have reversed, leading to a second acceleration. This process continues, the projectile spiralling outward towards the bounds of the magnetic field and the resulting final energy being the sum of all the individual contributions.

2.6 Ion Sources

A very important integral part of any particle accelerator is the ion source. Basically, the purpose of ion sources is to produce a volume of atoms and/or molecules with a net positive or negative charge. The material of interest is introduced into the ion source and ionized near an aperture through which the charged particles can be extracted. Many types of ion sources are available to produce either positive or negative, light or heavy ion beams such that several classes or types of source can be recognized; grouped according to the nature of the discharge phenomena or the different physical arrangements used to produce the ionization:

1) Cold-cathode canal-ray tube
2) Spark discharge
3) Low-voltage capillary arc
4) Hot/

4) Hot cathode arc

5) Discharge in an axial magnetic field

6) Radiofrequency (r.f.) electrodeless discharge

7) Electron oscillation discharge

Even so, all ion sources utilize the ionization produced in a gaseous discharge, it is only the mechanisms for producing this ionization and for concentrating the discharge into a small, parallel beam that vary considerably.

2.6.1 Properties of a Gaseous Discharge

In all ion sources the ionization is produced by electron impact in a gaseous discharge. The general requirements are: a source of electrons, a small region of a relatively high gas pressure separated from the accelerating tube, an electric field to accelerate the electrons and to maintain the discharge and some mechanism for concentrating the discharge and for pulling positive ions out in a parallel beam. Parameters of an ion source that are adjustable are the electron emission, gas pressure, voltage across the discharge, magnetic field, size of the exit hole, geometry and surface properties of the electrodes and the general shapes and dimensions of the enclosing discharge chamber.

Ionization occurs in gases when the electron energy equals or exceeds the ionization potential of the gas. The ionization potential of the hydrogen molecule,

forming/

forming H_2^+, is 15.6 volts; that for the formation of atomic ions H^+ from H atoms is 24.5 volts; and for He^{++} it is 54 volts. Ionization probability increases with electron energy, having a maximum for hydrogen at about 75 volts. Electrons make collisions in the gas, their average energy depends on the energy acquired in a mean free path between collisions and so varies inversely with pressure.

2.7 The S.A.M.E.S. (Société Anonyme De Machines Electrostatiques) Ion Accelerator

Quite a considerable part of this work was involved with the re-assembling of the 600 kV (now reduced to 300 kV) SAMES Ion Accelerator. It was hoped that once the machine has been commissioned, experimental work on the inactivation of biological targets such as enzymes, mammalian cells, etc., by charged particles could be carried out. However, mainly due to the lack of time, this was unfortunately not achieved. It is sincerely hoped that work on the re-assembling of the accelerator will continue and once commissioned further relevant experimental work by other workers may be carried out.

2.7.1 General Description of the SAMES Ion Accelerator

Basically, the machine is a simple DC type of accelerator and (when fully re-assembled) should comprised/

comprise the followings (see figure 2.5):

1) The high voltage electrostatic generator the value (voltage) of which determines the energy of the accelerated particles; though as was mentioned earlier the maximum possible voltage should now be 300 kV due to the insulation of the high voltage electrode to ground now being half the original value i.e. it has been reduced from a two stage to only a one stage insulating tube, mainly because of the lack of space (height clearance of the room).

2) The accelerator itself, which composed of,
   i) The high voltage electrode which includes the electron gun or the ion source and their associated power supplies; a generator for focussing voltage; and an alternator. The whole assembly is supported by an insulating tube through which pass the drive shaft of the alternator and the remote control rods.
   ii) The constant field accelerator tube or acceleration chamber. Potential distribution is assured by a resistance divider i.e. each segment of the tube is separated electrically by an insulator of approximately 350 mega-ohms resistance.
   iii) The pumping unit which provides the required vacuum for the system. It consists of the backing pump, oil diffusion pump, freon cooled traps, Penning and Pirani gauges for reading vacuum.
   iv) The/

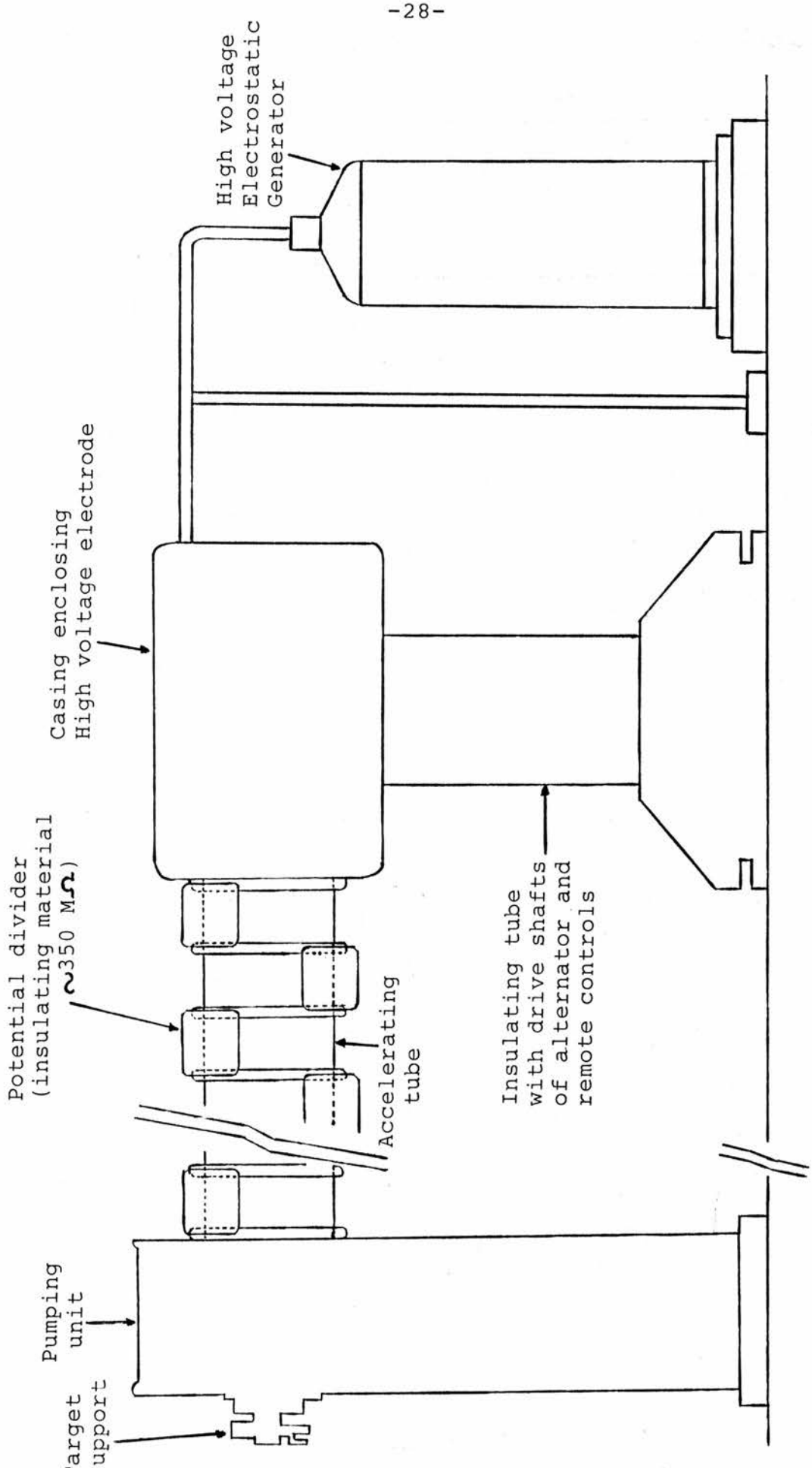

Fig. 2.5 General layout of the S.A.M.E.S Particle Accelerator.

iv) The target support device with the necessary accessories such as the gate valve for rapid target changing without interfering with the vacuum of the system; diaphragm and secondary electron suppressor (operation in ions); centering and sweeping device; thin aluminium alloy window; and anti-cathode (operation in electrons).

3) The general control bay which contains the respective controls of the high voltage generator, the vacuum pumps, the ion source or electron gun, the extraction voltage and the focussing voltage.

It should be noted that the machine should be in a very well shielded room as when in operation a large amount of radiation will be produced. As specified by the manufacturer: at its full potential of 600 kV; electron dose of 10^9 rad sec^{-1} and X-ray dose of 1000 Roentgen sec^{-1} is produced.

2.8 Conclusion

It is unavoidable that in order to obtain data on the survival study of any biological system exposed to heavy charged particles there is a need for a particle accelerator as a source for the heavy charged particles. Hence, it can be seen for the necessity of the above mentioned particle accelerator to be re-commissioned as early as possible so that informative work may be carried out.

PART II.

CHAPTER III

INTRODUCTION AND REVIEW OF RELEVANT WORK

3.1 General Purpose of Work

It is of fundamental importance, especially in radiation protection, to have the maximum possible knowledge on both the physical and biological action of ionizing radiation. Only through this knowledge will one be able to properly specify the quality of ionizing radiation. However, to do this, it is necessary to study in detail all the physical and biological mechanisms in the array of events that follow the initial physical interaction of the radiation resulting in the ultimate biological effect. It should be realized that this is a very tall order indeed and it is doubtful if it can ever be achieved. The next best approach would be to identify only the main mechanisms which dominate in the chain of events and which make significant contributions to the ultimate biological effect.

The study of the interaction of radiation with matter is fundamental to many aspects of radiation biophysics, for example, many radiation damage models attempt to predict the ultimate biological effects of radiation from a knowledge of the initial interaction processes/

processes which can contribute to the radiation action. However, in this work the study of the action of heavy charged particles (p,α,C,O,N,etc.) on mammalian cells is made with the aim of assessing and identifying the main mechanisms responsible for radiation damage in the cells so that it may be incorporated into future models.

3.2 Charged Particles and Ions

To begin with it would be appropriate to clarify the differences or similarities between charged particles and ions. Charged particles refer to any of the particles of modern physics which are positively or negatively charged such as muons ($\mu^{\pm}$), pions ($\pi^{\pm}$), kaons ($K^{\pm}$), protons, electrons, to name a few and of course ions. Ions, on the other hand, are charged particles; and they are atoms with one or more of their electrons stripped, hence being positively charged, as a result of a process known as ionization (see section 3.4.3).

3.2.1 Heavy Ions

As mentioned above, heavy ions are charged particles and as such are directly ionizing. The primary cause of biological damage in living tissue is the production of ions by radiation when it interacts with the tissue.

The path /

The path of a heavy ion through matter is described as a solid column of ionizations, which will increase in density as the particle slows down toward the end of its range. Outside of the central core, there are regions of less dense ionization caused by delta-rays, which are simply electrons knocked out of atoms of the absorbing material and given a great deal of kinetic energy. The overall appearance of the track is rather like a test tube brush: a solid central core of ionization surrounded by long range delta-rays which are ejected predominantly in the forward direction.

3.2.2 Contrast Between Heavy Ions and Photons

X and gamma-rays are indirectly ionizing but give rise to fast-moving secondary electrons. Fast neutrons are also indirectly ionizing but they give rise to recoil protons, alpha-particles and heavier nuclear fragments.

The electrons set in motion when photons are absorbed are relatively very light, negatively charged particles. By contrast, the particles set in motion when neutrons, pions or heavy ions are absorbed are heavy and densely ionizing. They also for the most part, carry a positive rather than a negative charge, though this difference appears to be trivial biologically. A proton for example, has a mass almost 2000 times greater than an electron; an alpha-particle has a/

has a mass four times larger still, while nuclear fragments may be an order of magnitude larger in mass again. Hence, the pattern of ionizations and excitations along the tracks of these various charged particles is very different; in particular the density of ionization is greater for neutrons, pions and heavy ions than is the case for X and gamma-rays and this accounts for the dramatic differences in the biological effects observed.

3.3 Interaction of Charged Particles with Matter

There is an important difference in the sizes of interaction cross-sections for charged and for uncharged radiations. Those for photons and neutrons are very small because interaction of these radiations with matter through which they pass are relatively rare events. On the other hand, the cross-sections for charged particles are very large because these particles are almost certain to interact with every atom near which they pass.

For heavy charged particles with kinetic energies up to the order of their rest mass energy, $M_o c^2$ (e.g. protons $\leq$938 MeV; ^{6}Li $\leq$5601 MeV; ^{12}C $\leq$11174 MeV; etc.), it is possible to separate the major interactions between particles and matter into three broad groups:

i) interactions with the individual electrons of the atoms or molecules,

ii) interactions/

ii) interactions with the nuclei, and

iii) interactions with the atoms/molecules as a whole.

The electric field of a charged particle will interact with that of the atoms/molecules of the absorbing material in the vicinity of its path. The interaction process can be simplified by figure 3.1, which shows a charged particle passing an atom. Here it can be seen that as the particle approaches the atom, the electric field at the site of the atom, hence the forces acting on the atom, increase, and once the particle has passed, decrease again. It can also be seen that a slow particle acts on an atom over a much longer period of time than a fast particle, thereby giving the atom a larger momentum.

Although rather simple, the picture describes correctly some of the most important aspects of energy transfer between the atoms of the absorbing material and the charged particle, like:

i) the interference caused by a passing particle is greater for slow particles than for fast ones,

ii) the energy transfer increases with the charge of the particle, and

iii) the mass of the particle has no influence on the amount of energy transferred.

A characteristic feature of the absorption of heavy charged particles is that they have a definite range in matter/

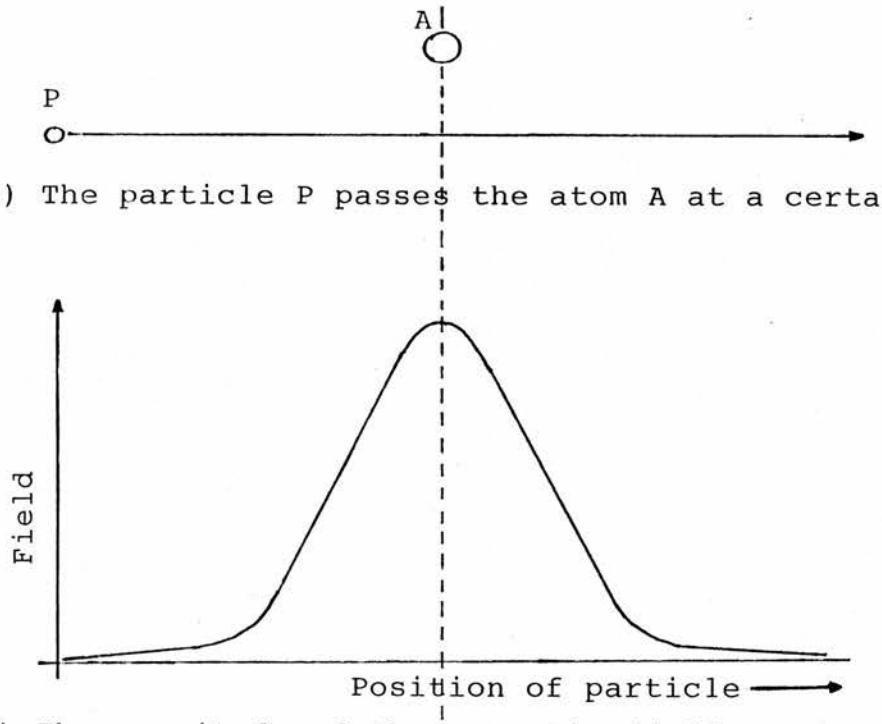

(a) The particle P passes the atom A at a certain distance.

(b) The magnitude of the magnetic field at the site of the atom as a function of distance (velocity-independent).

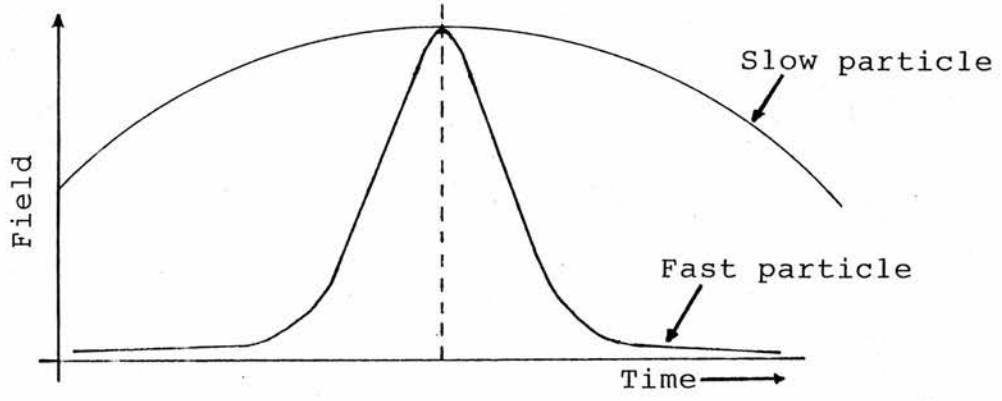

(c) The same field as a function of time (velocity-dependent).

Fig. 3.1 Schematic representation of the interaction between a charged particle and an atom.

matter. This is in contrast to the absorption of photons or neutrons, which is exponential, or of electrons which have only an ill-defined range in matter.

Energy losses due to ionization are now relatively well understood and quantitatively, the differential energy loss (or stopping power) of a charged particle i.e. the loss of energy per unit track length, is given by the Bethe-Bloch equation:

$$-\frac{dE}{dx} = \frac{4\pi e^2 (ze)^2}{mv^2} nZ\left[\ln\left(\frac{2mv^2}{I}\right) - \ln(1-\beta^2) - \beta^2\right] \quad 3.1$$

where m and e are the mass and charge of the electron respectively; v and ze the velocity and charge of the particle respectively; Z and I the effective atomic number and mean ionizing potential of the absorbing material respectively; n the number of atoms per cm^3 of the absorbing material and $\beta = v/c$ (c being the velocity of light).

The above equation is also sometimes expressed as:

$$-\frac{dE}{dx} = \frac{4\pi (ze^2)^2}{mc^2\beta^2} N\left[\ln\left(\frac{2mc^2\beta^2}{I}\right) - \ln(1-\beta^2) - \beta^2\right] \quad 3.1a$$

where here, v is now equated to $c\beta$ (from $\beta = v/c$) and $N = Zn$ is the electron density of the absorbing material.

Since all the charged particles dealt with in this work are categorised as 'fast' particles, therefore, a slightly/

slightly more detailed discussion on the energy loss processes by the so called 'fast' particles is made in the following section.

3.3.1 Interaction of Fast Heavy Charged Particles

A heavy charged particle or ion is categorised as 'fast' when its velocity, v_i, is large compared with the orbital velocity, v, of the electrons which the ion is capable of carrying. On the basis of the Thomas-Fermi estimates, v is given by

$$v = v_o Z_i^{2/3} \qquad 3.1c$$

and $v_o = e^2/\hbar = 2.18 \times 10^6$ m sec^{-1}

is the orbital velocity of the ground state electron in the hydrogen atom and Z_i is the atomic number of the incident ion; e the electronic charge and $\hbar = h/2\pi$ where h is Planck's constant.

For fast heavy charged particles, energy is lost primarily in collisions with the orbital electrons in the target atoms of the absorber. Sufficient energy may be transferred to a bound target electron either to raise it to a higher excited state (excitation) or to remove it completely from the parent atom (ionization). The latter type of ionization is known as primary ionization and the energetic electrons produced are called delta-rays and they are sufficiently energetic to produce/

to produce further ionization called secondary ionization. If the fast charged particle passes close to the target nucleus it may experience a sudden acceleration or deceleration accompanied by the emission of radiation called bremsstrahlung.

Since the encounter is most commonly between the massive ion and the much lighter target electron it follows that there will be a very small momentum transfer and the trajectory of the incident particle will be undeviated by the collision. Therefore, the trajectories of fast heavy charged particles are usually straight lines with well defined ranges. It should be noted that the delta-rays produced in ionization can have appreciable velocities despite the small momentum involved i.e. kinetic energy $\doteqdot 4\frac{m}{M}.E$, where m is the electronic mass, M and E the mass and energy of the incident particle respectively.

Although fast ions mainly collide with the orbital electrons in the target atoms of the absorber, nevertheless, there are some rare occasions when the incident particle passes near the nucleus of the target atom and the interaction is described by a simple Coulomb interaction between the respective nuclei. This is the historically important Rutherford scattering and here large momentum transfers occur causing appreciable deflections of the incident particle along its track.

3.4 Important/

3.4 Important Parameters in the Specification of Radiation Quality and Quantity

3.4.1 Linear Energy Transfer (LET)

Because of its great importance in the specification of radiation quality, the differential coefficient dE/dx given by equations 3.1 and 3.1a, has been given a special name. It is known as the "Linear Energy Transfer" (LET), and is defined by the ICRU as follows:

"The linear energy transfer (L) of charged particles in a medium is the quotient of dE_L by dl where dE_L is the average energy locally imparted to the medium by a charged particle of specified energy in traversing a distance of dl".

$$\text{i.e.} \quad L = \frac{dE_L}{dl} \qquad 3.2$$

It is usually measured in keV per micron (keV/μm) and dividing this by the density, ρ, of the material, the quantity L/ρ, which is independent of density is obtained. This quantity is generally known as the mass stopping power of the material and is measured in $MeV.cm^2/gm$.

From the Bethe-Bloch equation, it can be clearly seen that the LET of a charged particle is inversely proportional to the square of its kinetic energy, $(1/v^2)$ but directly proportional to the square of its charge, $(ze)^2$ and/

$(ze)^2$ and also that it is independent of its mass. In addition it is also found to be directly proportional to N, the mean electron density in the absorbing material.

The LET for different kinds of radiation may vary by several orders of magnitude and it is to be expected that radiation with such different physical properties will also differ in their biological effectiveness and this is indeed so. However, one very serious drawback of LET as a quality parameter is the fact that, as has been shown experimentally, different kinds of radiation having the same LET do not necessarily produce the same biological or chemical effect. There are many factors which may contribute to this observation. An important factor being the idealised assumption that particles travel in straight tracks of negligible width and depositing energy continuously rather than discretely which is never realised in practice. Allowance must be made for the spatial distribution of energy deposited by, for example, delta-rays; even though whose range is short compared with the range of the primary particle but it may be significant compared with the dimensions of a sensitive structure in which case energy lost by the primary particle inside the structure is expended predominantly outside the structure.

The concept of LET as a quality parameter also does not/

does not allow for fluctuations in the number of particles which may penetrate a sensitive structure when the medium is irradiated to a given absorbed dose. Also, the manner by which energy is transferred may be a factor in causing biological effect. For example, energy transferred in elastic collisions may act with different damaging efficiency from energy transferred by ionizing collisions, even for particles of the same type and same LET.

Therefore, it can be realised that even though LET has been and will continue to be a very important quality parameter, there is a need for other parameters to specify properly the quality of radiation.

3.4.2 Absorbed Dose and Radiobiological Effectiveness (RBE)

A discussion on parameters for the specification of radiation quantity will not be complete without including the most basic of these parameters, namely absorbed dose. The biological effects of radiation are often quantitatively described in terms of the absorbed dose needed to produce a certain biological end-point. The absorbed dose due to any ionizing radiation is defined as the energy imparted to matter by the ionizing particles per unit mass of irradiated material at the point of interest. The unit of absorbed dose used to be (and is still widely used in textbooks) the 'rad' and is equal to an energy absorption of 100 ergs/gm. The rad has now been replaced/

replaced by another unit, the 'gray' (Gy), and is equal to an energy absorption of 1 joule/kg (1 Gy ≡ 100 rad).

Like LET, it is well known that different absorbed doses are often needed to produce a given end-point with different kinds of radiation; and so the concept of "Relative Biological Effectiveness" (RBE), is introduced. It is defined as follows:

"The RBE of any radiation type A with respect to that of type B is defined as the ratio of the absorbed dose D_B to the absorbed dose D_A required to produce the same degree of biological response in the same biological system under identical conditions",

$$\text{i.e.} \quad RBE_{A \text{ wrt } B} = \frac{D_B}{D_A} \qquad 3.3$$

Usually, the reference radiation type B is taken as 250 kV-peak X-rays or ^{60}Co gamma-rays but is not necessarily so. It is always essential to specify the reference radiation if RBE values are to have any definite meaning.

3.4.3 Ionization Potential, I, and Average Energy per Ion Pair, W.

An atom is ionized when one or more of the orbital electrons is removed and is usually the result of the collision between a high velocity charged particle with the atomic electrons of a material. The ionization potential/

potential, I, for an atom is that minimum amount of energy required to remove one of its electrons and produce an ion-pair i.e. a positive ion plus a free electron. The value of I is given approximately by the relationship

$$I = 13.5Z \quad (eV) \qquad 3.4$$

where Z is the atomic number of the material.

Hence, the energy required to ionize a hydrogen atom, with Z=1, is 13.5 eV. For a multi-electron atom, it is necessary to specify the shell from which the electron is being removed, since the ionization potential is different for different shells; only a few eV may be required to remove an outer-shell electron but removal of a K-shell electron may require several tens of thousands of eV. After ionization, the ion will eventually encounter a free electron and recombination will occur. It is during recombination that the atom gives up the ionization energy, usually as a single photon with an energy equal to the ionization potential.

In practice, when a charged particle interacts with matter, a large amount of ionizations occur and therefore a large number of ion-pairs are produced. The energy of the charged particle, E, is related to the ionizations produced through the quantity W, which is defined as the energy expended in a gas per ion-pair formed/

formed. Thus,

$$E = WN_i \qquad 3.5$$

where N_i is the number of ion-pairs produced when a charged particle of energy E is absorbed. The value of W in a gas is always larger than the ionization potential, I, since some energy goes into non-ionizing processes such as excitation.

A very useful quality parameter in specifying radiation quality is the specific primary ionization, defined as the number of ion-pairs formed by primary ionization per unit length of track of the charged particle and is usually measured in 'per micron' (μm^{-1}). It should be noted that the secondary ionizations caused by the associated delta-ray emission is not included here and that there is no simple formula for calculating the total specific ionization.

In this work the reciprocal of specific primary ionization i.e. length of track per ion-pair produced by primary ionization or much better known as the mean free path between primary ionizations is highlighted to be a very important parameter in the specification of the quality of radiation.

3.4.4 Cross-Sections

Many quantities used in radiation dosimetry and in the qualitative evaluation of radiation effects are fundamentally dependent on a knowledge of cross-sections, e.g. dose/

e.g. dose, dose distribution, target theory, design of irradiation facilities and detectors, etc. Although cross-section is acknowledged as an extremely important concept in describing the interactions of particles, it has often played lesser roles when it comes to the specification of the quality of radiation.

Cross-sections are used to express the probability that a particle or particles will produce a specified effect (e.g. to produce ionization, excitation, etc.) due to interaction with a target nucleus, atom or molecule per unit area in a medium.

Consider a beam of particles of intensity I particles/cm^2sec., incident upon a thin slab of absorber of thickness dx. If the absorbing medium contains N nuclei per cm^3, then the number of incident particles interacting, dI, will be proportional to both I and Ndx;

$$\text{i.e.} \quad -dI \propto INdx$$

$$\text{or} \quad -dI = \sigma NIdx \qquad 3.6$$

where σ is a constant of proportionality, representing the effective interaction cross-section of each nucleus. Integrating equation 3.6 gives

$$I(x) = I(0)e^{-Ndx} \qquad 3.7$$

where I(x) is the particle intensity at depth x and I(0) is the/

is the incident particle intensity.

The product $N\sigma$ is often called the absorption coefficient, denoted by μ

$$\text{i.e.} \quad \mu = N\sigma \qquad 3.8$$

and its reciprocal known as an attenuation length, often denoted by λ,

$$\text{i.e.} \quad \lambda = 1/\mu = 1/N\sigma \qquad 3.9$$

λ is also known as the mean free path between interactions i.e. it represents the mean distance travelled by the particle between collisions.

3.5 Models for the Biophysical Action of Ionizing Radiation

Although there are many models of radiation action, to date well over seventy of them, published in the literature, generally they can almost all be categorised into three main groups:

i) hit and target
ii) two-component
iii) dual-action

All of these models are based on the reasonable premise that ionizing radiation transfers its energy in discrete amounts/

amounts and at random along the radiation tracks i.e. Poisson statistical theory is assumed to apply.

3.6 Hit and Target Model

The concept of a biological 'target' which must be 'hit' by the radiation to produce a specified biological effect is based on the assumptions that:

i) the interaction of radiation with matter occurs randomly and discretely,
ii) the interactions are independent of each other but their probability of occurrence is adequately described by the Poisson distribution of probabilities, and
iii) the effect is produced if the biological target receives a defined integral number, n, of hits.

Currently, a 'hit' is taken to be either a certain minimum amount of energy (often $\sim$60 eV, the mean 'W-value' of condensed hydrocarbons) or a specified physical interaction (e.g. breaking of a molecular bond) required to initiate the test effect. The 'target' is defined as a radiosensitive region within the biological entity and it is still the subject of active research to identify what the radiosensitive region is.

The most general formula for the hit and target theory is the case in which m number of targets must be hit n times to produce the specified biological effect/

effect. If the expectancy value for the number of hits i.e. the number of hits per target, is h, then the observed surviving fraction $F_{n,m}$ can be written as:

$$F_{n,m} = 1 - (1-F_{n,1})^m \qquad 3.10$$

$$= 1 - \left[1-e^{-h}\sum_{r=0}^{n-1}\frac{h^r}{r!}\right]^m \qquad 3.10a$$

where

$$F_{n,1} = e^{-h}\sum_{r=0}^{n-1}\frac{h^r}{r!} \qquad 3.11$$

is the Poisson probability of any one target surviving after being hit n times,

i.e. $F_{1,1}=e^{-h}$; $F_{2,1}=(1+h)e^{-h}$; $F_{3,1}=(1+h+\frac{h^2}{2!})e^{-h}$; etc.

Examination of these expressions indicate that the mean number of hits, h, is a suitable parameter with which to quantify the biological action. In fact it is a complete representation of the radiation quality and quantity within the limitations of target theory (Sect. 3.6.4). However, it is not convenient to measure 'h' in practice, so experimentalists usually study the probability of survival as a function of absorbed dose, D, (or of the radiation fluence, ϕ) which is more accessible to direct measurement.

3.6.1 Relationship Between the Mean Number of Hits, 'h', and the Absorbed Dose, D

Since D (and ϕ) is a parameter for radiation quantity and not quality, it is necessary to know the relationship between D and h.

If W is defined as the mean energy required to produce a hit, then for an absorbed dose D, the concentration of hits per unit mass of the medium is $\frac{D}{W}$. Let ν be the geometric mass of the target, then for an absorbed dose D, the energy deposited in the target is νD and the mean number of hits is given by

$$h = \nu\frac{D}{W} \qquad 3.12$$

$$= \nu\mu D \qquad 3.12a$$

[ν in kg, D in J kg^{-1}(Gy), W in J and μ in J^{-1}].

where $\mu=1/W$ is called the energy action coefficient and represents the efficiency with which the biological effect is produced per unit energy expended in the target. The product $\nu\mu$ is often known as radiosensitivity (sometimes denoted by k) and represents the radiosensitive mass of the target.

3.6.2 Single Hit, Single Target (n=1, m=1)

In the special case of single hit, single target action, the surviving fraction is a pure exponential given by

$$F_{1,1}/$$

$$F_{1,1} = e^{-h} \qquad 3.13$$

and therefore

$$\ln(F_{1,1}) = -h \qquad 3.13a$$

If $\ln(F_{1,1})$ is plotted against h, a straight line of gradient equal to -1 will be obtained

In equation 3.13a, if the mean number of hits per target, h, is equal to 1 i.e. one hit per target, then

$$\ln(F_{1,1}) = -1$$

therefore $F_{1,1} = e^{-1} = 1/e = 0.3679 = 37\%$

The value of h and D corresponding to a survival fraction of 1/e is denoted by h_{37} and D_{37} respectively, where

$$h_{37} = 1$$

therefore from equation 3.12

$$D_{37} = 1/\mu\nu = 1/k \qquad 3.14$$

In some experiments e.g. in track segment experiments where the thickness of the target material irradiated is small compared with the range of the charged particle tracks, the effect cross-section, σ, can be measured.

Since/

Since $h = \sigma\phi$

Therefore when $h=1$ i.e. $\phi = \phi_{37}$,

$$\sigma = 1/\phi_{37} \qquad 3.15$$

For the track segment situation, $D=\phi.L$ where

ϕ = the fluence in cm^{-2}

and L = the linear energy transfer in energy $cm^2\ gm^{-1}$

Therefore $F_{1,1} = e^{-h} = e^{-\sigma\phi}$

and $\sigma = 1/\phi_{37} = L/D_{37} = kL = \mu\rho L \qquad 3.15a$

If μ is assumed to be constant for any particular biological system, therefore as LET increases one expects

$\sigma(L) \longrightarrow \sigma_g$, the geometric cross-section

This prediction was, however, found to be untrue and that target theory must allow for the fact that μ may not be constant; and can depend on both the radiation type and biological system.

3.6.3 Single Hit, Multi-Target (n=1, m)

In this special case of a single hit in each of m targets

i.e. $F_{1,m} = 1 - (1-F_{1,1})^m$

$$= 1 - (1-e^{-h})^m \qquad 3.16$$

This is/

This is a curve typical of the survival of mammalian cells irradiated by low LET radiation e.g. gamma-rays. The trend of the survival fraction at a large number of hits (large dose) can be easily seen by expanding the binomial term, thus

$$F_{1,m} = 1 - (1-me^{-h} + \ldots\ldots \pm e^{-mh})$$

which for large h becomes

$$F_{1,m} = me^{-h} \qquad 3.17$$

and therefore

$$\ln(F_{1,m}) = \ln(m) - h \qquad 3.17a$$

There are several interesting features to notice about this special case (see figure 3.2):

i) At large values of h the surviving fraction becomes pure exponential with a final slope given by

$$\left.\frac{\partial(\ln F_{1,m})}{\partial h}\right|_{h \text{ large}} = -1 \qquad 3.18$$

ii) If the final slope is extrapolated backwards it will intercept the ordinate at the value m. Hence, m is often called the extrapolation number. Theoretically it represents the target multiplicity.

iii) For a survival fraction of 1/e, the hit number, h, corresponding/

Fig. 3.2 Survival curve for the special case of a single hit in each of m targets (n=1, m).

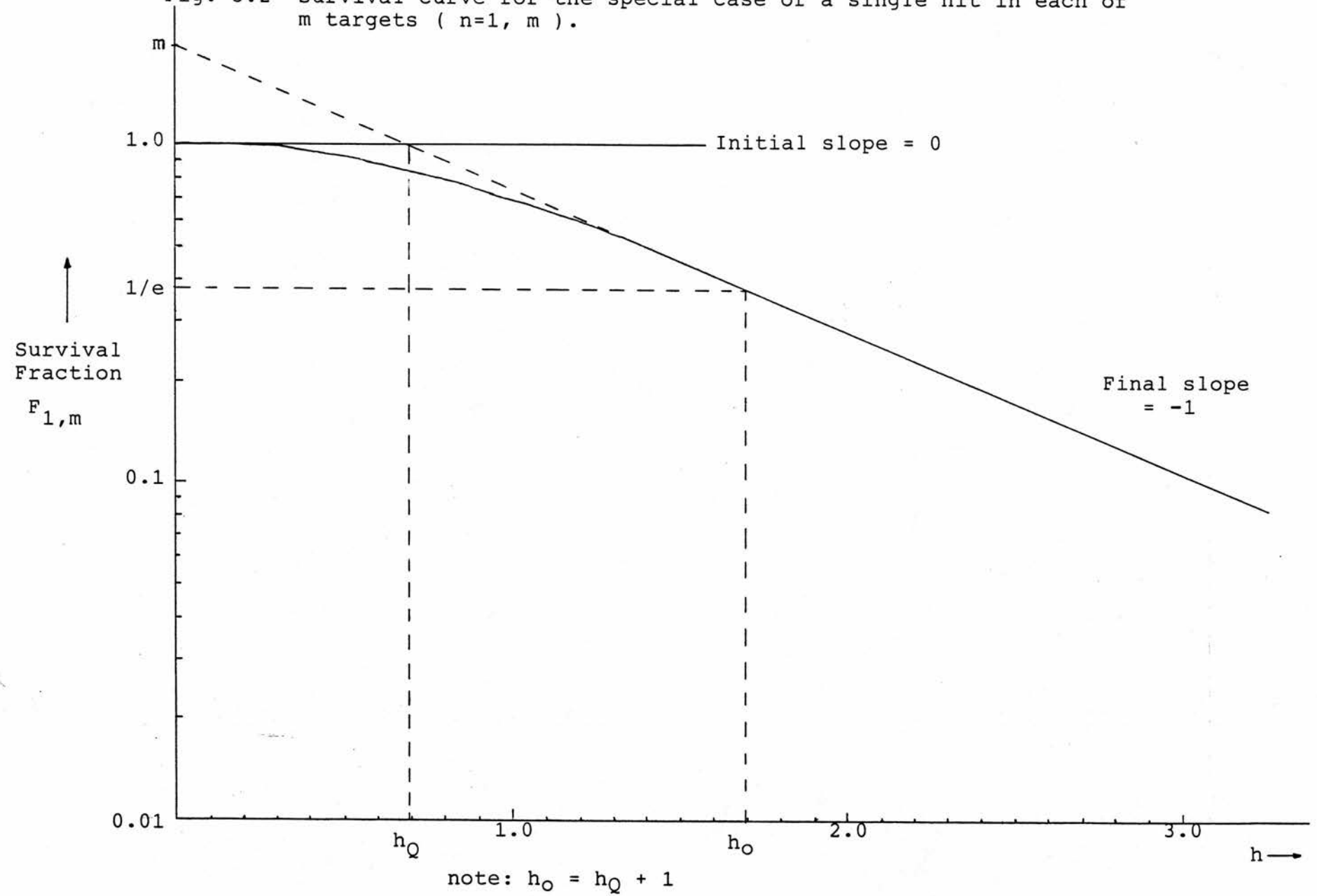

corresponding to 37% survival is given by

$$\left.\begin{aligned} h_o &= \ln m + 1 \\ \text{or} \quad D_o &= 1/\nu\mu\ (\ln m + 1) \end{aligned}\right\} \quad 3.19$$

Note that this extrapolated h_{37} for sigmoid curves is denoted by h_o (or D_o). D_o is also sometimes called the mean lethal dose or characteristic dose.

iv) The intercept between the horizontal line at 100 % survival and the extrapolated final slope corresponds to a hit value denoted by h_Q

$$\text{i.e.} \quad h_Q = \ln m \qquad 3.20$$

$$\text{and} \quad h_o = h_Q + 1 \qquad 3.21$$

v) The final slope is zero.

3.6.4 Limitations to the Basic Target Theory

Basic target theory reveals very little about the detailed mechanisms of radiation action. It nevertheless, successfully incorporates statistical concepts to reproduce the general shapes of the survival curves. In principle, the single hit, single target model is adequate for describing the observed exponential survival; and the single hit, multi-target form, gives a good enough representation of the general trend of cellular survival to low LET radiation.

However,/

However, a number of serious difficulties demonstrated by experimental observations remain because the theory does not take into account the saturation or overkill effects and the influence of the spatial distribution of delta-rays which greatly increase the efficiencies of radiation action. The theory predicts that: different radiations with the same LET should produce identical effects; the initial slope of the response curve for the multi-target models should be zero; the cross-section for the production of biological effect for single hit, single target inactivation should saturate at the geometric cross-section; none of which are supported experimentally.

3.7 Two-Component Models

The two-component radiation damage models meet the requirements for the possibility of a non-zero initial slope of the dose-response curve and also the all important cumulative action of delta-rays to produce the biological effect. It also retained the basic tenets of the hit and target theory but now, the action of radiation is split into a high LET component associated with the pure exponential survival characteristics which are typical of non-cumulative damage, and a low LET component which acts cumulatively on multiple targets to produce the biological effect. There are many models which fall into this category, particularly those of Todd (1964)/

of Todd (1964), Wideroe (1966), etc., but the one being most significant is that of Katz's (1968).

3.8 The Katz Two-Component Cellular Model of Radiation Action By Heavy Ions

Katz attributed the radiation action of accelerated heavy ions to the specific yield and radial distribution of the associated delta-rays. In his cellular model, Katz allows for the possibility of both cumulative and non-cumulative damage by separating the radial distribution of the dose due to the delta-rays into a 'track width regime' which if present occurs very close to the ion path; and a 'grain count regime' which occurs at greater radial distances from the ion path.

In the track width regime i.e. in the immediate vicinity of the ion path, there is a sufficient high density of delta-rays such that all targets situated within this region are inactivated in a manner described purely by exponential survival characteristics. The delta-ray density is so great that even if 'm' targets per cell have to be 'hit' to produce the biological effect, this is accomplished in the passage of a single ion and exponential survival characteristics are obtained instead of the sigmoid (one hit, m targets) survival which would have been observed for gamma-irradiation. This track width regime is a saturation region and the non-cumulative damage observed/

observed in this region is termed 'ion-kill' by Katz.

In the grain count regime i.e. at greater radial distances from the ion path or for very fast particles (low LET), the dose becomes smaller in magnitude and the density of the delta-rays is much less. Here the damage is a cumulative type of action which requires the passage of more than one ion to induce the effect and therefore the survival curve is sigmoid as typical of gamma irradiation. This type of inactivation is termed as 'gamma-kill' in Katz terminology. It should be noted that ion-kill may also be present in the grain count regime because there is a finite probability that in the passage of a single ion, m targets within a single cell may be simultaneously inactivated by time coincident delta-rays.

Therefore in the Katz two-component model, the fraction, F_D, of cells surviving a given dose, D, of heavy ion irradiation is the product of the fraction, F_i, described by the pure exponential component (ion-kill) and the fraction, F_γ, described by the sigmoid component (gamma-kill)

$$\text{i.e.} \quad F_D = F_i . F_\gamma \qquad 3.22$$

3.8.1 F_i, The Fraction of Cells Surviving Ion-Kill and F_γ, The Fraction Surviving Gamma-Kill

For cells, the effect probability, $P_i(t)$, is calculated/

calculated as a function of the radial distance, 't', for single hit, multi-target action. Thus

$$P_i(t) = (1 - e^{-h_i})^m \qquad 3.23$$

where $h_i = \varepsilon_i(t)/\varepsilon_{\gamma,o}$

$\varepsilon_i(t)$ is the mean energy deposition (or reduced dose) by delta-rays in an individual target at distance t and $\varepsilon_{\gamma,o}$ is the reduced dose for which there is on average one hit per target and the probability of the inactivation occurring is equal to 63%. $\varepsilon_{\gamma,o}$ is used as the reference dose to separate quantitatively the grain count regime from the track width regime associated with heavy ion tracks.

The total ion-kill cross-section, σ_i, after integration to the maximum extremity, τ, of the delta-rays, is given by

$$\sigma_i = \int_o^{\tau} 2\pi t . P_i(t)\, dt \qquad 3.24$$

and the fraction surviving the ion-kill mode of damage is

$$F_i = e^{-\sigma_i \phi} = e^{-h_{nc}} \qquad 3.25$$

where $h_{nc}=\sigma_i \phi$ is the number of hits in non-cumulative damage and ϕ the particle fluence.

The fraction/

The fraction of cells surviving gamma-kill (cumulative) action is given by

$$F_\gamma = 1 - (1-e^{-h_\gamma})^m \qquad 3.26$$

where h_γ is the mean number of hits per target.

To find h_γ, P_L the limiting value of P_i is used, where

$$P_L = (1-e^{-h_L})^m \qquad 3.27$$

and h_L the fraction of the reduced dose, $\mathcal{E}_D$, deposited in the non-cumulative damage mode is given by

$$h_L = \mathcal{E}_L / \mathcal{E}_{\gamma,o} \qquad 3.28$$

Therefore, h_γ is given by

$$h_\gamma = (1-P_L).D/D_{\gamma,o} \qquad 3.29$$

$$= (1-P_L).\mathcal{E}_D/\mathcal{E}_{\gamma,o} \qquad 3.29a$$

and by equation 3.27,

$$\text{therefore} \quad h_\gamma = [1 - (1-e^{-h_L})^m].\mathcal{E}_D/\mathcal{E}_{\gamma,o} \qquad 3.29b$$

with

$$\mathcal{E}_D = D.\frac{\beta_i^2}{z^{*2}}.a_o^2 \quad \text{and} \quad \mathcal{E}_{\gamma,o} = D_{\gamma,o}.\frac{\beta_i^2}{z^{*2}}.a_o^2$$

where/

where $D_{\gamma,o}$ is the reduced extrapolated dose for sigmoid survival (or the $D_{\gamma,37}$ for pure exponential survival); β^2 the ratio of the velocity, v_i, of the particle to that of light i.e. $\beta^2 = v_i^2/c^2$; z^* the effective charge of the particle; and a_o the radius of the target.

Therefore, the total surviving fraction, F_D, from equation 3.22 is

$$F_D = F_i \cdot F_\gamma$$

$$= e^{-h_{nc}} [1 - (1-e^{-h_\gamma})^m] \qquad 3.30$$

This model shows that at the same velocity but with increasing effective charge on the ions, there will be an increasingly filled core and that the track width is related in a complex way to z^{*2}/β_i^2 and β_i^2.

3.8.2 Success and Limitations of the Two-Component Model

The two-component models satisfy the requirements for the possibility of a non-zero initial slope of the survival curves and it also takes into consideration the cumulative action of the delta-rays to produce the biological effect. The Katz model for cellular inactivation by heavy ions copes with saturation effects through the use of the probability functions $P_i(t)$ and/

$P_i(t)$ and P_L. This particular model also explicitly includes the size of the radiosensitive target through a_o.

One basic assumption of the two-component model is that the radiosensitivity to delta-rays is identical to that defined by the extrapolated dose for secondary electrons from gamma-rays. Evidence from theoretical and experimental microdosimetry findings, particularly the experimental observation that tritium β-rays are much more damaging than ^{60}Co gamma-rays per unit dose, suggest that the assumption is probably a very crude approximation.

The two-component models always have a linear final slope at high doses in the dose-response curve. This doesn't quite agree with experimental observations which show that often there is a continuous curvature even at very high doses.

Even though the two-component models satisfy the requirements for the probability of a non-zero initial slope of the dose-response curve, it gets into difficulties when explaining the observed survival curves for cells with and without repair capabilities. In the two-component model there will always be a zero initial slope in the absence of a track core (non-cumulative ion-kill) i.e. at lower z^{*2}/β_i^2 values, which is not consistent with experimental observations in the absence of repair. On the other hand if there is a track/

a track core, there will always be a finite initial slope, which is not observed experimentally in cells with repair capabilities.

3.9 Dual Action Models

Most models of radiation action assume the existence of two basic mechanisms: a) a pure exponential (single hit, single target) component of survival fraction and is independent of the dose-rate, and b) a sigmoid (single hit, multi-target) component, which at low doses, is dose-rate dependent. Each of the components can occur separately or in various proportions. At high doses the survival tends toward a pure exponential dose-effect curve, conflicting with detailed experimental observations which often reveal a dose-effect relation which continues to curve with decreasing surviving fraction i.e. at high doses. This situation is overcome in the so called 'Dual Action Model'.

In the dual action models, instead of invoking two separate modes of radiation action, it assumes that the primary lesions produced depend on the local energy concentration in a manner which comprises two components of damage, namely, a linear component and a quadratic component. The linear component of damage is attributed to lesions produced along an individual particle track and is therefore

proportional/

proportional to dose, D; and the quadratic component is attributed to the interactions of lesions produced along separate charged particle tracks and therefore proportional to the square of the dose, D^2. This mechanism gives rise to the dual action formulae

$$\text{Survival Fraction, } F = e^{-y} \qquad 3.31$$

where y, the yield of lesions is given by

$$y = k(\xi D + D^2) \qquad 3.32$$

$$\text{or} \quad y = (\alpha D + \beta D^2) \qquad 3.32a$$

There are three main dual action models: those of Neary (1965); Rossi and Kellerer (1971); and Chadwick and Leenhouts (1974). Each of these are very similar in concept; Neary's model was developed to explain chromosome aberrations, Rossi-Kellerer's model is more general as it can be applied to any sensitive targets and can be related directly to the theory of microdosimetry, and Chadwick-Leenhouts model is applied to the DNA molecule.

3.9.1 Neary's Theory of Chromosome Aberrations

Neary postulated that (i) a primary lesion can be caused by the deposition of a single primary ionization within a chromosome, and (ii) an aberration results from the interaction of two chromosomes in a region/

region where each has a primary lesion.

If p, is the probability of a single energy loss event in a target chromosome to produce a primary lesion; s the specific primary ionization and W the mean energy expenditure per ionization in the chromosome medium, then

$$s = L/W \qquad 3.33$$

where L is the LET of the radiation.

The probability, k, that a track forms a lesion in a chromosome is given by

$$k = 1 - e^{-pst} \qquad 3.34$$

where t is the chromosome thickness (mean chord length)

Neary deduces that the yield, y, of aberrations for the cell nucleus is

$$y = NE[1-e^{-mgk^2}(1-(1-e^{-(mk+mgk^2)})^2)] \qquad 3.35$$

where

N is the number of sites per nucleus

E is the probability that two chromosomes in a site, each having a primary lesion, will undergo exchange to form an aberration

$m=\frac{AD}{L}$ is the mean number of tracks through area A, and D is the absorbed dose

A is the/

A is the mean projected area of the chromosome segment of length 'l' within a site of radius h

i.e. $A = ht$

g is the probability that a track which has traversed one target chromosome of a site will also traverse the other; and is given by

$$g = \frac{A}{\pi h^2} = \frac{t}{\pi h}$$

By expanding the exponential terms in equation 3.35 and neglecting all terms with powers greater than k^4, the following is obtained

$$y = \frac{NEA^2k^2}{(16L)^2}\left[(1-gk)^2 - \frac{g^2k^2}{2}\right]\left[\frac{16gL}{A\left((1-gk)^2 - \frac{g^2k^2}{2}\right)}D + D^2\right] \qquad 3.36$$

which is the general formulae for Neary's theory of chromosome aberration; and is generally known in the form

$$y = k(\xi D + D^2) \qquad 3.36a$$

where

$$k = \frac{NEA^2k^2}{(16L)^2}\left[(1-gk)^2 - \frac{g^2k^2}{2}\right] \quad Gy^{-2} \qquad 3.37$$

and $$\xi = \frac{16gL}{A\left((1-gk)^2 - \frac{g^2k^2}{2}\right)} \quad Gy \qquad 3.37a$$

3.9.2/

3.9.2 The Dual Action Model of Rossi and Kellerer

From studies in microdosimetry Rossi and Kellerer found that (i) for low doses of fast neutrons, cells are very unlikely to be traversed by more than one charged particle track and consequently radiation effects within the cell can be initiated by passage of a single densely ionizing particle through the cell and (ii) the frequency of elementary lesions depends on the square of the specific energy imparted, z, in sub-cellular regions called sites whose diameter is $\gtrsim 1$ μm. From the analysis of experimental results for RBE plotted as a function of neutron dose for various biological end-points, Rossi and Kellerer found that the equation

$$RBE = \lambda_n^{\frac{1}{2}} D_n^{-\frac{1}{2}} \qquad 3.38$$

(where $\lambda_n^{\frac{1}{2}}$ is a constant of proportionality)

represents the general trend although there are exceptions where some types of mammalian cells and simple organisms such as bacteria and spores, show an RBE which is constant with dose.

For low doses, the yield, ε, of elementary lesions is proportional to the absorbed dose, D

$$\text{i.e. } \varepsilon = k_n D_n \qquad 3.39$$

Using/

Using the defination of RBE (i.e. RBE=D_x/D_n ; where D_x is the equivalent reference dose of X-rays), and equation 3.38,

$$\text{Therefore,} \quad \frac{D_x}{D_n} = \frac{\lambda_n^{\frac{1}{2}}}{D_n^{\frac{1}{2}}}$$

$$\text{giving} \quad D_n = \frac{D_x^2}{\lambda_n} \qquad 3.40$$

Therefore equation 3.39 now becomes

$$\varepsilon = k_n D_n = k_n \frac{D_x^2}{\lambda_n} = k D_x^2 \qquad 3.41$$

where $k = \frac{k_n}{\lambda_n}$

It is concluded that the yield, ε, of elementary lesions is proportional to D_x^2 in the dose range where single track action for low energy neutrons occurs. This is valid for certain dose range though it should be noted that this range of validity is broad and that the same characteristic dependence is observed for a wide spectrum of biological end-points. It is therefore a likely hypothesis that the primary mechanisms underlying a variety of radiation induced biological effects are related or identical. It may be assumed that the equations for the primary damage in the case of neutrons/

neutrons and X-rays i.e.

$$\mathcal{E} = k\lambda_n D_n \quad \text{and} \quad \mathcal{E} = kD_x^2 \qquad \text{(from eq. 3.41)}$$

are merely approximations of the general relation:

$$\mathcal{E} = k(\lambda D + D^2) \qquad 3.42$$

where λ depends on radiation quality and has such a small value for X-rays that the linear term in D can be neglected as long as the dose is not too small, while in the case of neutrons it has such a large value that except for very large doses the quadratic term in D can be neglected.

The dual radiation action model of Rossi-Kellerer must be considered approximate because:

i) there are no correction for energy saturation (overkill),
ii) k must vary with radiation quality, and
iii) it assumes the existence of sites in which there is a constant probability of interaction between sub-lesions.

3.9.3 Chadwick and Leenhouts Molecular Theory of Radiation Action

Apart from the dimensions of the sensitive structure and their associated probability to damage, the Chadwick and Leenhouts/

and Leenhouts model is identical to Neary's model for chromosome aberrations, but based on the following assumptions:

i) the primary radiation action is the breakage of a molecular bond,
ii) the broken bond can be repaired or restituted,
iii) the critical molecule is the DNA double helix,
iv) the critical damage leading to cell death is a DNA double strand break,
v) a certain number of DNA double strand breaks lead to cell death.

This model contains implicitly factors governing the effect of oxygen, sensitisers and protectors on the survival curve. Aside from the difference in the detailed concept of dealing with a spherical molecular structure rather than an unidentified 'site' as in the Rossi-Kellerer case, the Chadwick-Leenhouts model can be written in exactly the same form as the original Neary model, but it has been developed further to allow explicitly for repair, etc.

3.9.4 Limitations of the Dual Action Models

Like almost all models of radiation action, the dual action models are based on the deposition of energy to produce the biological effect but take no account of a possible relationship between the action efficiency/

efficiency and the type of physical interactions involved. If such a relationship exists, then absorbed dose i.e. energy deposition would not quite be a suitable parameter for the specification of radiation quantity. The model also does not treat direct and indirect action explicitly which is necessary to account properly for the influence of modifying factors (e.g. O_2, water, etc.), though both the Rossi-Kellerer and Chadwick-Leenhouts models contain implicitly factors to allow for these modifying effects. The probability, k, that a track forms a lesion, used in the model is quality dependent, hence another setback to the model. The model of Rossi-Kellerer could be further critisised for the 'unidentified' (lack of detailed knowledge) sub-cellular region or 'site' which forms a basis for its formulation.

3.10 Relevant Work By Other Authors

Goodhead et al (1983) made a study to identify a single physical property of the radiation field that correlates with RBE. The property sought after was in terms of a minimum amount of energy deposition in a certain volume. In his earlier work (Goodhead et al, 1980), it was suggested tentatively that the predominant lethal lesions induced by radiation of low ionizing density (e.g. X and gamma-rays) arose from threshold/

from threshold energy concentrations of ~100 eV in ~ 3 nm. In his later work (Goodhead et al, 1985) it was further emphasised that at low doses, damage in mammalian cells is determined predominantly by very local properties of energy deposition over distances of 1 to 10 nm.

Watt et al (1984) suggested a tentative distance 'resonance' model as an alternative to the 'distance model' of dual action of Rossi-Kellerer. In this 'resonance' model, the maximum in the RBE-LET curve is suggested to be due to a 'resonance' match in the mean free path between interactions of the radiation and the mean interaction distance between sub-lesions in the site rather than due to competition between increased efficiency and saturation effects.

Cannell et al (1985) analysed the survival data of biological entities irradiated by fast ions and studied the intrinsic efficiency of their inactivation as a function of the specific primary ionization. They found that, only for targets containing double stranded DNA, there is a discontinuity in the plot of mean specific primary ionization against intrinsic efficiencies for damage at values of mean specific primary ionization of about 5.5 per $\mu g/cm^2$ in water or equivalent to a mean free path between ionizations of 1.8 nm. It was suggested that the mechanism of fast heavy ions inactivation in mammalian cells is dependent on the/

on the 'matching' of events spaced along the primary ion track with the strand separation distance and that the energy transfer per event is of minor importance.

Watt et al (1985) re-analysed published data for the inactivation of enzymes, viruses and higher cells by accelerated ions, X and gamma-rays. Results from this analysis indicate very strongly that for targets with double stranded DNA, especially mammalian cells, the dominant damage mechanism is caused by intra-track action in which an interaction is necessary in each of the two neighbouring strands spaced at about 1.8 nm apart in the DNA. They concluded that the mean free path between ionizations is the dominant fundamental physical parameter of the radiation which determines the radiation action and the effect will be a maximum when this 'matches' the strand spacing. The λ suggestion, with the backing of experimental data from other workers, that the effect of delta-rays may not be that significant in the inactivation of the biological targets was also put forward.

In order to find out if electrons with the optimum mean free path between ionizations (i.e. $\sim$ 0.5 ionizations per nm) have the same intrinsic efficiency for damage as other charged particles, Chen et al (1986), have made an extensive analysis of X and gamma-rays irradiation of mammalian cells. They found that the intrinsic efficiency for damage by electrons is nearly/

nearly an order of magnitude down compared to that for accelerated ions at the same specific primary ionization. A probable explanation given being that electrons are only capable of reaching the requisite specific primary ionization of about 0.5 per nm at the very end of their tracks, when their energies fall below 250 eV and hence their extrapolated range is only a few nanometers. Due to multiple scattering, only a small percentage ($\sim$ 10%) will then have sufficient projected range to penetrate both strands of the DNA, thereby reducing the probability of damage.

This is consistent and lends support to the deduction that the dominant damage mechanism is a process which reaches an optimum value when the mean free path between primary ionizations along the charged particle tracks corresponds to the spacing between strands in the double stranded DNA.

CHAPTER IV

THEORY OF RADIATION ACTION

4.1 Introduction

The requirement for a detailed understanding of the mechanisms of radiation action in biological media is fundamental to the assessment and control of damage by ionizing radiations. The action of ionizing radiation is not at all easy to understand because it is a highly complex chain of events following the initial interaction of the radiation with the biological media. It is made even more difficult to follow with the addition of modifying factors such as: damage to living cells can be repaired; the effect is dependent on the immediate chemical environment of the living cell and the dose-rate of the radiation. Also, the manifestation of damage may be immediate or delayed over a long period of time, even into future generations.

It is an experimental fact that exposure of mammalian cells to ionizing radiations can induce in the cells a variety of biological effects, including loss of proliferative capacity, mutation, chromosome aberrations and neoplastic transformation. Despite decades of investigation, the nature of the critical radiation lesions at the physical, chemical or biological stages remains uncertain. One sensible approach/

approach to the problem is to seek a single physical property of the radiation field that correlates with the relative damage efficiency of different radiations.

4.2 The Temporal Stages of Radiation Action

In trying to follow the development of radiation damage in as much detail as possible, it has been found to be very helpful, to separate the complex chain of events that follow the absorption of high energy radiation in matter into basically three main temporal stages, namely the physical stage, chemical stage and biological stage as can be seen in figure 4.1.

It would also be more convenient to classify further the action of radiation into a "direct action" and an "indirect action". The radiation action is termed as a direct action when the chain of events is initiated by the absorption of radiation energy in the biological system (e.g. DNA molecule) under investigation itself and consequently the resulting effect is termed "direct effect". On the other hand if the primary processes of radiation absorption occurs in the 'environment' (e.g. other biological molecules) of the system and as a result of intermolecular energy transfer mechanisms (such as the interaction of diffusing radicals with the system) it becomes damage, then the radiation action is termed indirect action and the resulting effect known as the "indirect effect".

4.2.1/

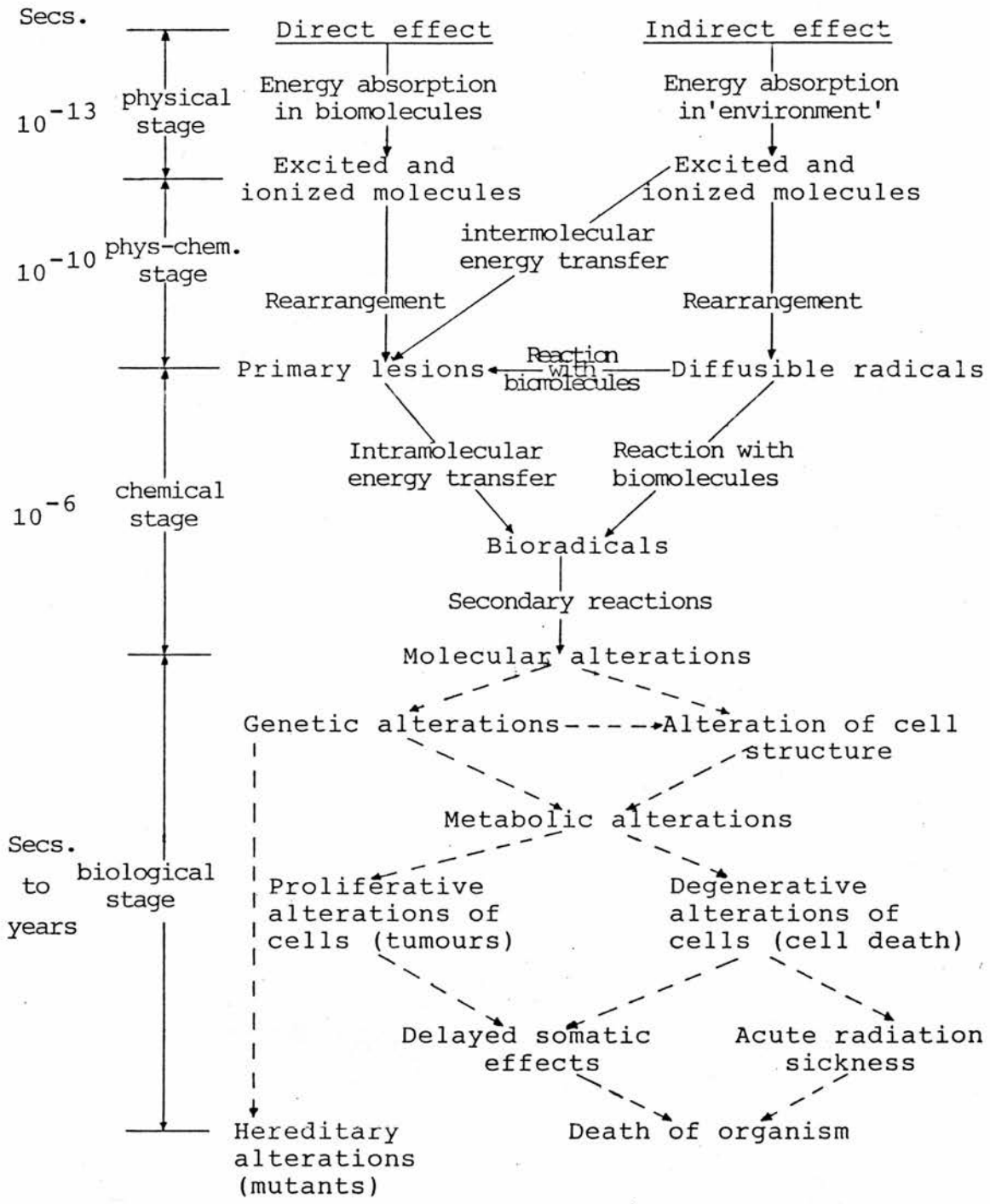

Fig. 4.1 The temporal stages of radiation action. (The reaction steps represented by broken lines are affected by metabolic processes). (Dertinger and Jung, 1970)

4.2.1 The Physical and Physico-chemical Stage

In this physical stage of radiation action, energy is transferred, through the many modes of interaction mechanisms, from the radiation to matter. These interaction mechanisms depend on the type and energy of the radiation and also on the atomic configuration of the absorbing medium. Some of the more important individual interaction processes are: photoelectric effect, Compton interaction, pair production as a result of the interactions of X and gamma-rays with matter; neutron scattering and neutron absorption for neutron interaction with matter; and for interactions of charged particles with matter (Sect. 3.3), nuclear collisions, nuclear reactions, nuclear scattering, Rutherford scattering, Lindhard scattering, etc. All of these processes consist of individual interactions, each of which has a distribution of possible energy transfer and they occur within a very short time (10^{-13} sec.) after the passage of the radiation. However, all these processes lead mainly to molecular excitations and ionizations. These resulting primary species (i.e. excited molecules and ion-pairs) are usually extremely unstable and promptly (10^{-10} sec.) undergo secondary reaction (such as de-excitation, recombination) either spontaneously or by collisions with molecules in their vicinity, to yield reactive secondary species. This is also known as the 'physico-chemical'/

chemical' stage and may consists of a single reaction or a complex succession of reactions.

4.2.2 The Chemical Stage

The chemical stage begins (10^{-6} sec.) when the system has finally re-established thermal equilibrium. The reactive species (usually free atoms or radicals) in this phase continue to react with each other and with their environment. Usually in the presence of water, H_2O, in the environment of the system (which is the case in all living cells), three main types of reactive species produced as a result of the absorption of the radiation are $\bar{e}_{aq}$ (hydrated electron), H. (hydrogen atom radical) and .OH (hydroxyl radical). It is the reaction of these reactive species with the system that produce molecular changes in the system. Also, reactions between these reactive species themselves can result to the formation of other molecular products, which could then react with the system;

e.g. $H. + H. \longrightarrow H_2$ (molecular hydrogen)

$$\bar{e}_{aq} + \bar{e}_{aq} \xrightarrow{2H_2O} H_2 + 2OH^-$$

$$\bar{e}_{aq} + H. \xrightarrow{H_2O} H_2 + OH^-$$

$$.OH + .OH \longrightarrow H_2O_2 \text{ (hydrogen peroxide)}$$

4.2.3/

4.2.3 The Biological Stage

Molecular changes occurring in a biological organism, regardless of their causes and modes of formation, may result in alterations in the system which, in going through the biological stage, finally leads to the development of the observed biological effect. During this stage of the development of the radiation damage, the metabolism of the affected organism is of particular importance. The initial primary processes of radiation absorption merely caused a small but significant injuries in the organism as a whole. However, the kind and the magnitude of the damage depend very much on whether the defect can be repaired, or whether the system, in attempting to operate under these perturbed conditions, will only tend to amplify the damage.

Though not without its limitations, this classification of the radiation action into its different temporal stages is of considerable assistance in any discussion of the complex succession of events following the initial absorption of radiation energy. An ideal biological investigation should lead to the elucidation of all the reaction steps in the different temporal stages shown in figure 4.1. Even though this aim has not yet been achieved, nevertheless, it still remains the main ultimate aim of research in radiation biology.

4.3 The Resonance/

4.3 The Resonance Model for Radiation Action of Yamaguchi et al (1983)

Yamaguchi et al (1983) proposed a new model for the analysis of survival curves of mammalian cells exposed to ionizing radiation. The model consists of three parts covering the physical, chemical and biological stages of radiation induced biological damage. In the physical stage the response is expressed by an analogue of the power absorption of a harmonic oscillator under resonance conditions comparable to the relation of the spatial distribution between ion clusters from ionizing particles and the critical elements of the biological system. Response in the chemical stage is explained in terms of the G-value of the Fricke dosimeter and response in the biological stage is related to a repair mechanism.

Since this work basically deals with the physical mechanisms of radiation action, therefore only the physical stage of the model of Yamaguchi is discussed at length with some suggested modifications.

4.3.1 The Physical Stage of Radiation Action of the Model of Yamaguchi

The RBE of mammalian cells has a peak at an LET of about 100-200 keV/μm (100-200 eV/nm) and it is independent of the presence or absence of oxygen and also its existence does not change with varying chemical/

chemical and biological conditions. Hence, Yamaguchi rightly concludes that this peak must occur as a manifestation of a basic radiation mechanism. In his model Yamaguchi considered the 'resonance' phenomenon between the basic biological structure and the spatial distribution of energy deposition.

In investigating the anology between the radiation action and the resonance phenomenon in terms of a simple mechanical harmonic oscillator with a damping force and considering the principle target to be the DNA, Yamaguchi deduced that F(L), the probability for lesions per traversal of nucleus of an ionizing particle of LET, L, is given by

$$F(L) = \frac{2kfL^2}{(L_o^2-L^2)^2 + (2kL)^2} \qquad 4.1$$

where $L=E/\lambda$ and $L_o=E/\lambda_o$;
and L_o is the 'natural LET', E the effective energy to produce an ion cluster, λ the average distance between ion clusters and λ_o is assumed to be the distance between DNA double-strands.

This is comparable to the mechanical oscillator resonance described by the power absorption of the system:

$$F(w) = \frac{2kf'w^2}{(w_o^2-w^2)^2 + (2kw)^2} \qquad 4.2$$

where/

where w_o and w are the natural and driving frequencies respectively, k the damping (resistance) coefficient and f' is the driving force strength and $f=f'/N$ is a dimensionless constant, N being the normalization constant of the power absorption.

It follows that if $F(L)\Delta L$ is the probability for lesions per traversal of nucleus of an ionizing particle of LET, $L+\Delta L$, then the number of lesions per unit absorbed dose, l_p, is expressed as

$$l_p = \frac{\rho \sigma_g}{16L} . F(L)\Delta L \qquad 4.3$$

$$= \frac{2krL}{(L_o^2 - L^2)^2 + (2kL)^2} \Delta L \qquad 4.3a$$

where $r = \rho \sigma_g \cdot \frac{f}{16}$; ρ is the density and $\sigma_g (\mu m^2)$ is the geometric cross-section of the sensitive structure (here assumed to be the cell as a whole).

The dimension of k is the same as L and the value of r characterizes the radiation effect concerned. Therefore, the number of lesions, $\varepsilon_p(D)$ at absorbed dose, D, due to this reaction mode becomes

$$\varepsilon_p(D) = l_p . D \qquad 4.4$$

4.3.2 Modification of the Radiation Action in the Physical Stage to the Model of Yamaguchi

From equation 4.3 it can be easily seen that the number of lesions, l_p, is dependent on LET of the radiation. Here an attempt is made to express the number of lesions in terms of the specific primary ionization, I_i, of the radiation field.

In his work, Watt et al (1985) showed that the specific primary ionization, I_i, is given by

$$I_i = \frac{L_\infty}{\bar{T}_\delta + W} \qquad 4.5$$

where L_∞ is the LET of the radiation, $\bar{T}_\delta$ is the frequency weighted average energy for the delta-ray spectrum and W is the mean energy required to produce an ion pair (taken to be 30 eV).

Note that Yamaguchi defined the LET, L, as follows

i.e. $L = E/\lambda$

where E is the effective energy to produce an ion cluster and λ is the average distance between ion clusters.

It can be easily seen that by definition $I_i = 1/\lambda$, Therefore,

$$L = EI_i \qquad 4.6$$

$$\text{or} \quad I_i = L/E \qquad 4.6a$$

which/

which is exactly similar to equation 4.5 above i.e. $E=\overline{T}_{\delta}+W$.

Therefore instead of using L, I_i is used in deriving the probability for lesions per primary ionization, $F(I_i)$

(from equation 4.1)

$$F(I_i) = \frac{2kfI_i^2}{(I_{i_o}^2-I_i^2)^2 + (2kI_i)^2} \qquad 4.7$$

and similarly from equation 4.3

$$l_p = \frac{\rho\,\sigma_g}{16I_i}.F(I_i)\Delta I_i \qquad 4.8$$

$$= \frac{2krI_i}{(I_{i_o}^2-I_i^2)^2 + (2kI_i)^2}\Delta I_i \qquad 4.8a$$

It follows from equation 4.8a that the number of lesions per unit absorbed dose, l_p, is maximum when $I=I_{i_o}$; and since $I_{i_o}=1/\lambda_o$, therefore the value of l_p is maximum when the average distance between ionizations, λ, is equal to λ_o, the distance between the DNA double strands.

4.4 Discussion

The physical stage of the 'resonance' model of the radiation action of Yamaguchi (also the above modified model)/

model) shows that the total number of lesions, $\varepsilon_p(D)$ at absorbed dose, D, is at a maximum when the average distance between ionizations, λ, is equal to the distance between the DNA double strands, λ_o; but $\varepsilon_p(D)$ is also totally dependent on the absorbed dose, D, i.e. the energy deposition along the particle tracks. This is however, quite in contradiction with the physical mechanism of damage suggested in this work. Though they both are at their optimum when the mean free path between primary ionizations 'matches' the strand separation in the DNA, but in the physical mechanism of damage proposed in this work, the energy transfer per event is of minor importance i.e. increasing the energy transfer per event beyond the minimum threshold needed to break the DNA strand will not result to any significant increase in the efficiency for damage of the cells.

But maybe more important is the fact that in Yamaguchi's model, as can be seen in equation 4.3a, the number of lesions per unit absorbed dose, l_p, is at its maximum when $L=L_o$ ($\lambda=\lambda_o$). l_p will decrease for values of L greater than or less than L_o. Whereas in the physical mechanism of damage suggested in this work the intrinsic efficiency of damage keeps on increasing (until it reaches a saturation value) as L becomes larger than L_o, but its rate of increase is significantly reduced as compared to when L is less than L_o.

CHAPTER V

COLLECTION AND CORRELATION OF DATA

5.1 Correlation of Data

Sets of survival data for charged particle irradiations of mammalian cells have been collated (tables 5.1 — 5.4). Cell lines that were of interest were those of Chinese hamster V79,lung cells; Chinese hamster $CH2B_2$ cells; Chinese hamster M3-1, bone marrow cells; and human kidney T1 cells.

The cells were all irradiated in vitro. They were asynchronous and aerobic i.e. irradiated in air or in oxygen and no added chemical protectors or sensitisers were present.

5.2 Determination of D_o (D_{37})

The values of D_o which were used in this work were either from the original authors or, if they were not quoted, were determined from the given survival curves. Theoretically, D_o, is the dose corresponding to an observed survival fraction (in the linear portion of the survival curve) of 1/e i.e. 37%. D_{37} on the other hand is the dose required to reduce the survival from 100% to 37%. Therefore it can be seen that (see figure 5.1) for a pure exponential survival curve $D_o=D_{37}$; but for shouldered survival curves D_{37} is always/

Table 5.1. Cross-section ratio and damage efficiency per primary ionization in Chinese hamster V79 cells.

Reference	Ions	E_i (MeV)	D_o (Gy)	$\bar{L}_T$ (eV/nm)	$1/\bar{L}_T$ (nm/eV)	$1/\bar{I}_s$ (nm)	ε_R	β^2	E_δ (keV)
Perris et al. (1985)	p	3.0	2.13	11.73	8.525×10^{-2}	2.247×10^{1}	1.726×10^{-2}	0.0064	6.54
	p	7.4	1.61	5.811	1.721×10^{-1}	5.495×10^{1}	1.155×10^{-2}	0.0159	16.2
Hall et al. (1978)	p	160	1.40	0.521	1.919×10^{0}	9.091×10^{2}	1.191×10^{-3}	0.2700	378
	p	160	1.56	0.521	1.919×10^{0}	9.091×10^{2}	1.069×10^{-3}	0.2700	378
Wainson et al. (1972)	p	8	3.50	5.461	1.831×10^{-1}	5.917×10^{1}	4.993×10^{-3}	0.0168	17.5
	p	90	3.78	0.789	1.267×10^{0}	5.882×10^{2}	6.680×10^{-4}	0.1673	205
Cox et al. (1977)	^{4}He	11.7	1.04	47.58	2.102×10^{-2}	5.522×10^{0}	1.464×10^{-1}	0.0062	6.42
	^{4}He	34.9	1.75	20.27	4.933×10^{-2}	1.626×10^{1}	3.706×10^{-2}	0.0185	19.2
Bird et al. (1975)	^{4}He	39.7	1.06	18.27	5.473×10^{-2}	1.848×10^{1}	5.516×10^{-2}	0.0210	21.9
Thacker et al. (1979)	^{4}He	7.6	0.75	65.72	1.522×10^{-2}	3.601×10^{0}	2.804×10^{-1}	0.0041	4.17
	^{4}He	5.8	0.65	80.07	1.249×10^{-2}	2.755×10^{0}	3.942×10^{-1}	0.0031	3.18
	^{4}He	24.3	1.30	27.02	3.701×10^{-2}	1.138×10^{1}	6.652×10^{-2}	0.0129	13.4
Hall et al. (1972)	^{4}He	5.2	0.66	86.76	1.157×10^{-2}	2.475×10^{0}	4.206×10^{-1}	0.0028	2.85
Bird et al. (1975)	^{7}Li	68.9	0.67	41.43	2.414×10^{-2}	8.130×10^{0}	1.979×10^{-1}	0.0208	21.7
	^{11}B	101	0.48	121.1	8.258×10^{-3}	2.747×10^{0}	8.074×10^{-1}	0.0194	20.2
	^{12}C	107	0.63	176.9	5.653×10^{-3}	1.871×10^{0}	8.986×10^{-1}	0.0189	19.7
	^{20}Ne	123	1.15	603.7	1.657×10^{-3}	5.106×10^{-1}	1.680×10^{0}	0.0131	13.5
	^{40}Ar	204	2.58	1789.0	5.590×10^{-4}	1.659×10^{-1}	2.218×10^{0}	0.0108	11.2
Thacker et al. (1979)	^{10}B	107	0.86	107.4	9.311×10^{-3}	3.181×10^{0}	3.996×10^{-1}	0.0225	23.5
	^{10}B	49.6	0.70	193.2	5.176×10^{-3}	1.527×10^{0}	8.832×10^{-1}	0.0106	10.9
	^{14}N	51.8	1.22	438.6	2.280×10^{-3}	6.318×10^{-1}	1.150×10^{0}	0.0079	8.13

Table 5.2. Cross-section ratio and damage efficiency per primary ionization in Chinese hamster $CH2B_2$ cells. (Skarsgard et al., 1967)

Ions	E_i (MeV)	D_o (Gy)	$\bar{L}_T$ (eV/nm)	$1/\bar{L}_T$ (nm/eV)	$1/\bar{I}_s$ (nm)	ε_R	β^2	E_δ (keV)
^4He	40	1.65	18.17	5.504×10^{-2}	1.859×10^{1}	3.524×10^{-2}	0.0211	22.0
^6Li	58	1.43	42.06	2.378×10^{-2}	7.981×10^{0}	9.412×10^{-2}	0.0204	21.3
^6Li	30	1.06	70.95	1.409×10^{-2}	4.165×10^{0}	2.142×10^{-1}	0.0106	11.0
^{11}B	102	1.07	120.0	8.333×10^{-3}	2.777×10^{0}	3.588×10^{-1}	0.0196	20.4
^{12}C	106	1.00	178.4	5.605×10^{-3}	1.852×10^{0}	5.708×10^{-1}	0.0187	19.5
^{16}O	131	1.42	329.3	3.037×10^{-3}	9.893×10^{-1}	7.420×10^{-1}	0.0174	18.1
^{20}Ne	153	2.02	523.6	1.910×10^{-3}	6.144×10^{-1}	8.294×10^{-1}	0.0162	16.9
^{40}Ar	230	5.00	1688.0	5.924×10^{-4}	1.802×10^{-1}	1.080×10^{0}	0.0122	12.7

Table 5.3. Cross-section ratio and damage efficiency per primary ionization in Chinese hamster M3-1 cells. (Todd, 1975)

Ions	E_i (MeV)	D_o (Gy)	$\bar{L}_T$ (eV/nm)	$1/\bar{L}_T$ (nm/eV)	$1/\bar{I}_s$ (nm)	ε_R	β^2	E_δ (keV)
^2H	13.2	1.18	6.38	1.569×10^{-1}	4.902×10^{1}	1.729×10^{-2}	0.0139	14.4
^4He	26.3	1.07	25.38	3.942×10^{-2}	1.232×10^{1}	7.588×10^{-2}	0.0140	14.5
^7Li	46.1	0.71	57.16	1.750×10^{-2}	5.465×10^{0}	2.576×10^{-1}	0.0139	14.5
^{11}B	72.4	0.49	156.5	6.390×10^{-3}	1.996×10^{0}	1.022×10^{0}	0.0140	14.5
^{12}C	78.8	0.80	223.2	4.480×10^{-3}	1.400×10^{0}	8.928×10^{-1}	0.0140	14.5
^{14}N	91.0	1.15	301.9	3.312×10^{-3}	1.032×10^{0}	8.400×10^{-1}	0.0138	14.3
^{16}O	105.0	1.18	384.4	2.602×10^{-3}	8.129×10^{-1}	1.042×10^{0}	0.0140	14.5
^{20}Ne	132.0	1.57	578.2	1.730×10^{-3}	5.404×10^{-1}	1.178×10^{0}	0.0140	14.5
^{40}Ar	228.0	4.33	1696.0	5.896×10^{-4}	1.791×10^{-1}	1.253×10^{0}	0.0121	12.6

Table 5.4. Cross-section ratio and damage efficiency per primary ionization in human kidney T1 cells. (Todd, 1967)

Ions	E_i (MeV)	D_o (Gy)	$\bar{L}_T$ (eV/nm)	$1/\bar{L}_T$ (nm/eV)	$1/\bar{I}_s$ (nm)	ε_R	β^2	E_δ (keV)
^2H	13.2	0.97	6.38	1.569×10^{-1}	4.902×10^{1}	2.104×10^{-2}	0.0139	14.4
^4He	26.3	0.86	25.38	3.942×10^{-2}	1.232×10^{1}	9.440×10^{-2}	0.0140	14.5
^7Li	46.1	0.56	57.16	1.750×10^{-2}	5.465×10^{0}	3.266×10^{-1}	0.0139	14.5
^{11}B	72.4	0.46	156.5	6.390×10^{-3}	1.996×10^{0}	1.089×10^{0}	0.0140	14.5
^{12}C	78.8	0.51	223.2	4.480×10^{-3}	1.400×10^{0}	1.400×10^{0}	0.0140	14.5
^{14}N	91.0	0.92	301.9	3.312×10^{-3}	1.032×10^{0}	1.050×10^{0}	0.0138	14.3
^{16}O	105.0	1.07	384.4	2.602×10^{-3}	8.129×10^{-1}	1.150×10^{0}	0.0140	14.5
^{20}Ne	132.0	1.07	578.2	1.730×10^{-3}	5.404×10^{-1}	1.729×10^{0}	0.0140	14.5
^{40}Ar	228.0	1.94	1696.0	5.896×10^{-4}	1.791×10^{-1}	2.798×10^{0}	0.0121	12.6

Fig. 5.1 Typical survival curves of mammalian cells irradiated by ionizing radiations.

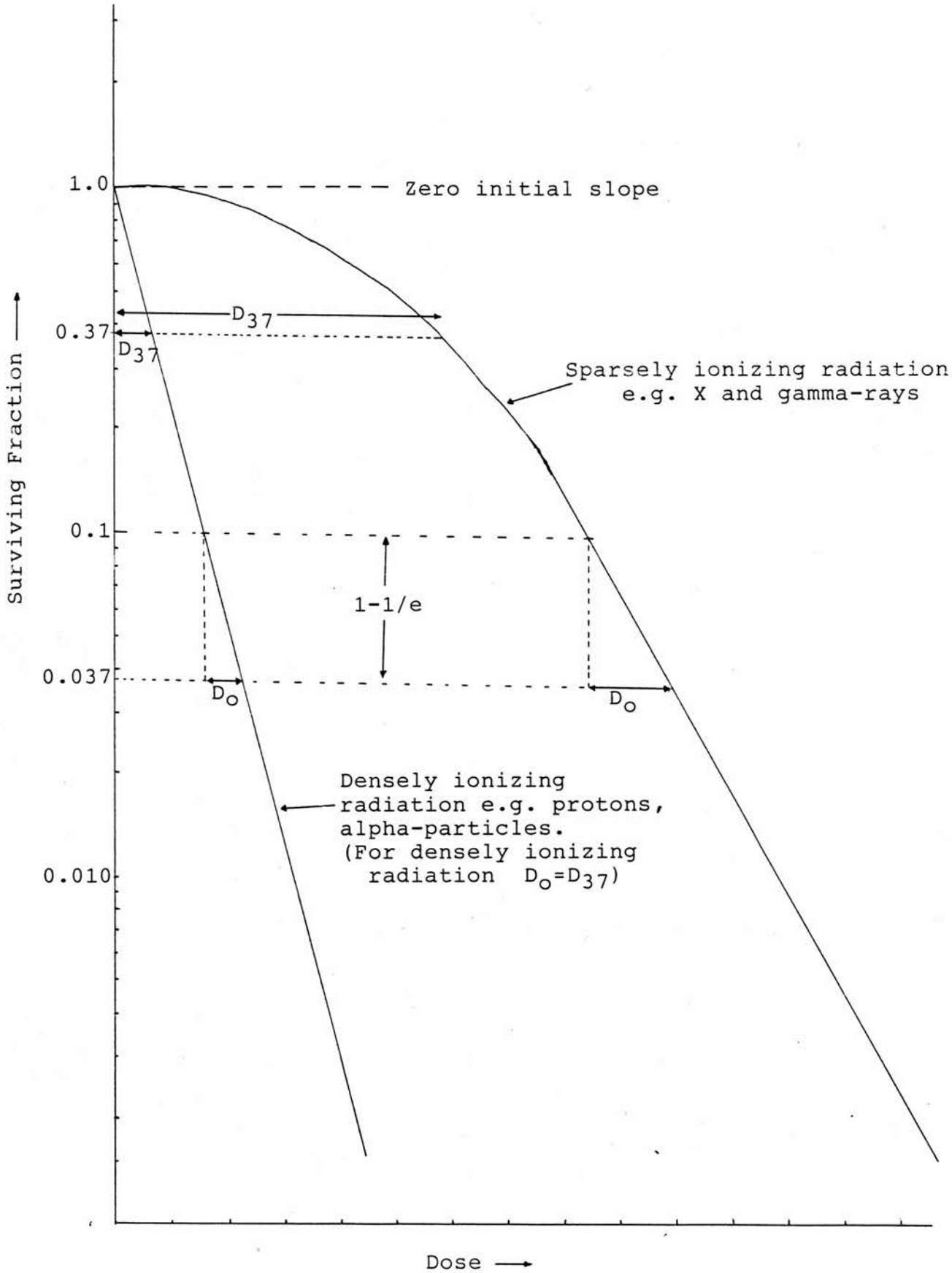

is always (sometimes considerably) larger than D_o.

When values of D_o (D_{37}) were determined from the given survival curves (i.e. their values were not quoted by the authors), there is bound to be some error in the values of the D_o (D_{37}) obtained. The error was found to vary from a few percent to not more than 10%. The magnitude of this error was determined by comparing the values of D_o (D_{37}) obtained from the survival curves to those given by the original authors (when they are available).

Generally, the survival curves of mammalian cells exposed to low LET radiations e.g. X and gamma-rays will have an initial slope equal to zero i.e. shouldered curves, and therefore the value of D_o and D_{37} (fig. 5.1) will differ. The survival curves of mammalian cells irradiated by high LET radiations e.g. protons, heavy ions, etc., are usually pure exponential i.e. a straight line with a definite initial slope and hence the values of D_o and D_{37} are equal.

5.3 Determination of the Intrinsic Efficiency for Inactivation, ε_R

The effect cross-section, σ_e, by the individual charged particle is calculated from the formula

$$\sigma_e = \frac{1.6 \times 10^{-9}}{D} \bar{L}_T \qquad 5.1$$

where/

where $\bar{L}_T$ is the track average LET in keV/μm for the relevant charged particle energy spectrum, σ_e is in cm^2 and the dose, D, in gray.

ε_R, the total intrinsic efficiency for inactivation is then given by

$$\varepsilon_R = \frac{\sigma_e}{\sigma_g} \qquad 5.2$$

where σ_g is the geometrical cross-section of the cell nuclei and a nominal value of 5×10^{-7} cm^2 is taken as a compromise between the uncertainty in nuclear size in different experimental setups i.e. the major and minor diameter of the cells.

Therefore the values of ε_R for the inactivation of the different cell lines by the various charged particles are calculated from

$$\varepsilon_R = \frac{1.6 \times 10^{-9}}{D} \bar{L}_T \times \frac{1}{5 \times 10^{-7}} \qquad 5.3$$

and the results tabulated in tables 5.1 – 5.4

The values of: $\bar{L}_T$, the track average LET; keV/μm or eV/nm,

$\bar{I}_s$, the specific primary ionization; nm^{-1},

E_δ, energy/

E_δ, energy of delta-rays; keV,

β^2, the ratio of v/c; v the velocity of the charged particle and c the velocity of light.

for the different types of charged particles at different energies were obtained from the personal data collection of Watt, D.E. (personal communication) and also tabulated in tables 5.1 – 5.4

5.4 Determination of the Intrinsic Efficiency of Damage for the Delta-Rays, $\bar{\varepsilon}_j$.

From the work of Watt et al (1985) it was shown that the total probability of damage, ε_R is given by

$$\varepsilon_R = P(i) + I_i \bar{d}\, \overline{P(j)} \qquad 5.4$$

where P(i) is the intrinsic efficiency of damage for the radiation on the primary target alone, in which $I_i \bar{d}$ ionizations occur on average; $\bar{d}$ is the mean chord length of the targets (taken to be 4000 nm), and P(j) is the mean intrinsic efficiency of damage for the delta-ray spectrum.

P(i) could not be determined without a foreknowledge of the actual inactivation mechanism; but in the saturation condition i.e. $I_i > 0.55$ nm^{-1} ($1/I_i < 1.8$ nm), P(i)=1. Therefore from equation 5.4

$\overline{P(j)}$ =/

$$\overline{P(j)} = \frac{\varepsilon_R - P(i)}{I_i \bar{d}}$$

$$= \frac{\varepsilon_R - 1}{4000 \text{ nm} \times I_i}$$

$$= \bar{\varepsilon}_j \qquad 5.5$$

where $\bar{\varepsilon}_j$ represents the mean intrinsic efficiency of damage for a single delta-ray with average energy representative of the delta-ray spectrum.

Using equation 5.5, values of $\bar{\varepsilon}_j$ (beyond the saturation condition) were calculated for all the cell lines and tabulated in table 5.5.

5.5 Symbols used in Graphs

The symbols used for plotting the points in the graphs were as follows:

p	for	protons
d	"	deuterons
α	"	alpha-particles
L	"	lithium ions
B	"	boron ions
C	"	carbon ions
N	"	nitrogen ions
O	"	oxygen ions
#	"	neon ions
and A	"	argon ions

5.6/

Table 5.5 The calculated values of the mean intrinsic efficiency of damage, $\bar{\varepsilon}_j$, by delta-rays.

Cell lines	Ions	ε_R	I_i (nm^{-1}) x 10^{-3}	E_δ (keV)	$\bar{\varepsilon}_j = (\varepsilon_R - 1)/I_i \bar{d}$
V79	^{40}Ar	2.218	6027.7	11.2	5.052×10^{-5}
	^{20}Ne	1.680	1957.9	13.5	8.683×10^{-5}
	^{14}N	1.150	1582.8	8.13	2.369×10^{-5}
$CH2B_2$	^{40}Ar	1.080	5549.0	12.7	3.604×10^{-6}
M3-1	^{11}B	1.022	501.1	14.5	1.098×10^{-5}
	^{16}O	1.042	1230.2	14.5	8.535×10^{-6}
	^{20}Ne	1.178	1850.4	14.5	2.405×10^{-5}
	^{40}Ar	1.253	5582.8	12.6	1.133×10^{-5}
T1	^{11}B	1.089	501.1	14.5	4.440×10^{-5}
	^{12}C	1.400	714.4	14.5	1.399×10^{-4}
	^{14}N	1.050	968.7	14.3	1.290×10^{-5}
	^{16}O	1.150	1230.2	14.5	3.048×10^{-5}
	^{20}Ne	1.729	1880.4	14.5	9.849×10^{-5}
	^{40}Ar	2.798	5582.8	12.6	8.052×10^{-5}

5.6 Plotting the Graphs

Graphs of $1/\bar{I}_S$, $1/\bar{L}_T$, $\bar{L}_T$ and Z^2/β^2 all against ε_R were plotted using the methods of least squares. Each graph was assumed to be two separate straight lines intersecting at the point of inflexion. Each straight line was determined as follows:

The general regression line is given by

$$y' = b(x-\bar{x}) + \bar{y}$$

where

$$\bar{x} = \frac{1}{n}\sum x \qquad \text{and} \qquad \bar{y} = \frac{1}{n}\sum y$$

(n being the number of points)

and $b = S_{xy}/S_{x^2}$

where,

$$S_{xy} = \frac{1}{n-1}\left[\sum xy - \frac{1}{n}\sum x \sum y\right]$$

and

$$S_{x^2} = \frac{1}{n-1}\left[\sum x^2 - \frac{1}{n}\left(\sum x\right)^2\right]$$

In this work x and y are both in logarithmic scale, therefore the regression line now becomes

$$\log y' = b(\log x - \overline{\log x}) + \overline{\log y}$$

where,

$$\overline{\log x} = \frac{1}{n}\sum \log x \qquad \text{and} \qquad \overline{\log y} = \frac{1}{n}\sum \log y$$

and/

and

$$S_{xy} = \frac{1}{n-1}\left[\sum \log x \log y - \frac{1}{n}\sum \log x \sum \log y\right]$$

$$S_{x^2} = \frac{1}{n-1}\left[\sum \log x^2 - \frac{1}{n}\left(\sum \log x\right)^2\right]$$

The regression lines for the various graphs were calculated and tabulated in tables 5.6 and 5.6a. The values of the x-axis parameters at the points of inflexion for the plots of $1/\overline{I}_S$, $1/\overline{L}_T$, $\overline{L}_T$ and Z^2/β^2 all against ε_R for the different cell lines were also calculated (from their respective regression lines) and tabulated in tables 5.6 and 5.6a.

The uncertainties in the calculated values of the x-axis parameters were simply determined as follows:

Since the values of x-axis parameters were determined from the points of intersections of the regression lines

i.e. $y' = b(x-\overline{x}) + \overline{y}$

therefore $x = y'/b - \overline{y}/b + \overline{x}$

and since there is only one value of b, $\overline{y}$ and $\overline{x}$ for each of the regression line therefore their mean deviation, σ could not be determined. Hence the error in x, Δx, is assumed to be equal to the error in y, Δy, and since in all cases

$$y = \varepsilon_R/$$

Table 5.6 The calculated regression lines used in plotting the graphs.

cell lines	Graph	Regression lines	Value of x at point of inflexion
V79	$1/\bar{I}_S$ Vs ε_R	i) $\log y_1' = -1.127(\log x - 1.196) - 1.244$ ii) $\log y_2' = -0.3795(\log x + 0.0628) + 0.0731$	1.18±0.12 nm
T1	$1/\bar{I}_S$ Vs ε_R	i) $\log y_1' = -1.2166(\log x - 0.7930) - 0.6010$ ii) $\log y_2' = -0.3941(\log x - 0.1074) + 0.1583$	2.00±0.20 nm
M3-1	$1/\bar{I}_S$ Vs ε_R	i) $\log y_1' = -1.1902(\log x - 0.7930) - 0.7022$ ii) $\log y_2' = -0.1799(\log x + 0.1924) + 0.0124$	1.82±0.18 nm
$CH2B_2$	$1/\bar{I}_S$ Vs ε_R	i) $\log y_1' = -1.2165(\log x - 0.7004) - 0.7674$ ii) $\log y_2' = -0.2185(\log x + 0.320) - 0.059$	1.64±0.16 nm
V79	$\bar{L}_T$ Vs ε_R	i) $\log y_1' = 1.356(\log x - 1.306) - 1.244$ ii) $\log y_2' = 0.1708(\log x - 2.3545) + 0.0732$	184.59±18 eV/nm
T1	$\bar{L}_T$ Vs ε_R	i) $\log y_1' = 1.2164(\log x - 1.7018) - 0.6010$ ii) $\log y_2' = 0.3983(\log x - 2.5910) + 0.1583$	157.40±16 eV/nm
M3-1	$\bar{L}_T$ Vs ε_R	i) $\log y_1' = 1.1905(\log x - 1.7018) - 0.7022$ ii) $\log y_2' = 0.1913(\log x - 2.681) + 0.0124$	169.63±17 eV/nm
$CH2B_2$	$\bar{L}_T$ Vs ε_R	i) $\log y_1' = 1.2328(\log x - 1.813) - 0.7674$ ii) $\log y_2' = 0.2406(\log x - 2.8213) - 0.059$	191.87±19 eV/nm

Table 5.6a The calculated regression lines used in plotting the graphs (contd.).

cell lines	Graphs	Regression lines	Value of x at point of inflexion
			nm/eV
V79	$1/\bar{L}_T$ Vs R	i) $\log y_1' = -1.233(\log x + 1.306) - 1.244$ ii) $\log y_2' = -0.3989(\log x + 2.549) + 0.0731$	$5.12\times10^{-3}\pm0.5\times10^{-3}$
T1	$1/\bar{L}_T$ Vs R	i) $\log y_1' = -1.2164(\log x + 1.7018) - 0.6010$ ii) $\log y_2' = -0.3998(\log x + 2.5998) + 0.1583$	$6.42\times10^{-3}\pm0.6\times10^{-3}$
M3-1	$1/\bar{L}_T$ Vs R	i) $\log y_1' = -1.1905(\log x + 1.7018) - 0.7022$ ii) $\log y_2' = -0.1912(\log x + 2.6836) + 0.0124$	$5.90\times10^{-3}\pm0.6\times10^{-3}$
$CH2B_2$	$1/\bar{L}_T$ Vs R	i) $\log y_1' = -1.2328(\log x + 1.813) - 0.7674$ ii) $\log y_2' = -0.2244(\log x + 2.821) - 0.059$	$5.11\times10^{-3}\pm0.5\times10^{-3}$
V79	Z^2/B^2 Vs R	i) $\log y_1' = 1.0847(\log x - 2.3502) - 1.189$ ii) $\log y_2' = 0.3385(\log x - 3.6525) + 0.0731$	2821±282
T1	Z^2/B^2 Vs R	i) $\log y_1' = 1.0287(\log x - 2.9994) - 0.4176$ ii) $\log y_2' = 0.5318(\log x - 3.6923) + 0.1583$	3090±309
M3-1	Z^2/B^2 Vs R	i) $\log y_1' = 1.1827(\log x - 2.7572) - 0.7022$ ii) $\log y_2' = 0.1202(\log x - 3.6923) + 0.0119$	2106±211
$CH2B_2$	Z^2/B^2 Vs R	i) $\log y_1' = 1.2054(\log x - 2.8482) - 0.7674$ ii) $\log y_2' = 0.1865(\log x - 3.9267) - 0.0591$	2217±222

$$y = \varepsilon_R = \frac{1.6 \times 10^{-9}}{D} \bar{L}_T \times \frac{1}{5 \times 10^{-7}} \qquad \text{(from eq. 5.3)}$$

and here the major contribution of error is in determining the dose, D, i.e ΔD has a maximum error of about 10%. Therefore the error for each of the calculated x-axis parameters were also assumed to be about 10% and these were included in tables 5.6 and 5.6a.

Analysis of the plotted graphs for all the cell lines investigated were carried out in the next chapter. To make it more systematic all the graphs for the different cell lines were grouped into five groups i.e. $1/\bar{I}_S$ vs ε_R; $1/\bar{L}_T$ vs ε_R; $\bar{L}_T$ vs ε_R; E_δ vs ε_R; and Z^2/B^2 vs ε_R and each group was analysed separately.

CHAPTER VI

RESULTS AND THEIR ANALYSIS

6.1 The Intrinsic Efficiency for Inactivation, ε_R, as a Function of the Mean Free Path Between Primary Ionizations, $1/\bar{I}_s$

Figures 6.1 – 6.4 give the plots of $1/\bar{I}_s$ against ε_R for the different cell lines investigated. It is very clear indeed that in each of these graphs there exist a point of inflexion. The value of $1/\bar{I}_s$ at which the points of inflexion occur varies between 1.18 nm and 2.0 nm as can be seen in table 5.6. Except for the plot of the data for V79 cells, the others give values of $1/\bar{I}_s$ very close to that of the strand spacing of a double stranded DNA in the cells i.e. 1.8 nm.

It may be worth pointing out that for the V79 cells, if the points in the graph corresponding to protons with energies of 160 MeV were neglected, then the value of $1/\bar{I}_s$ at the point of inflexion will undoubtedly be much closer to 1.8 nm. This could well be justified because except for the 160 MeV protons, the energies for all the other charged particles quoted by the authors were energies at the surface of the cells; whereas the 160 MeV was given as the initial energy of the particle. Perris et al (1985), showed that the energies of the particles at the surface of the cell could well be different from their initial energies due to kinematics and the/

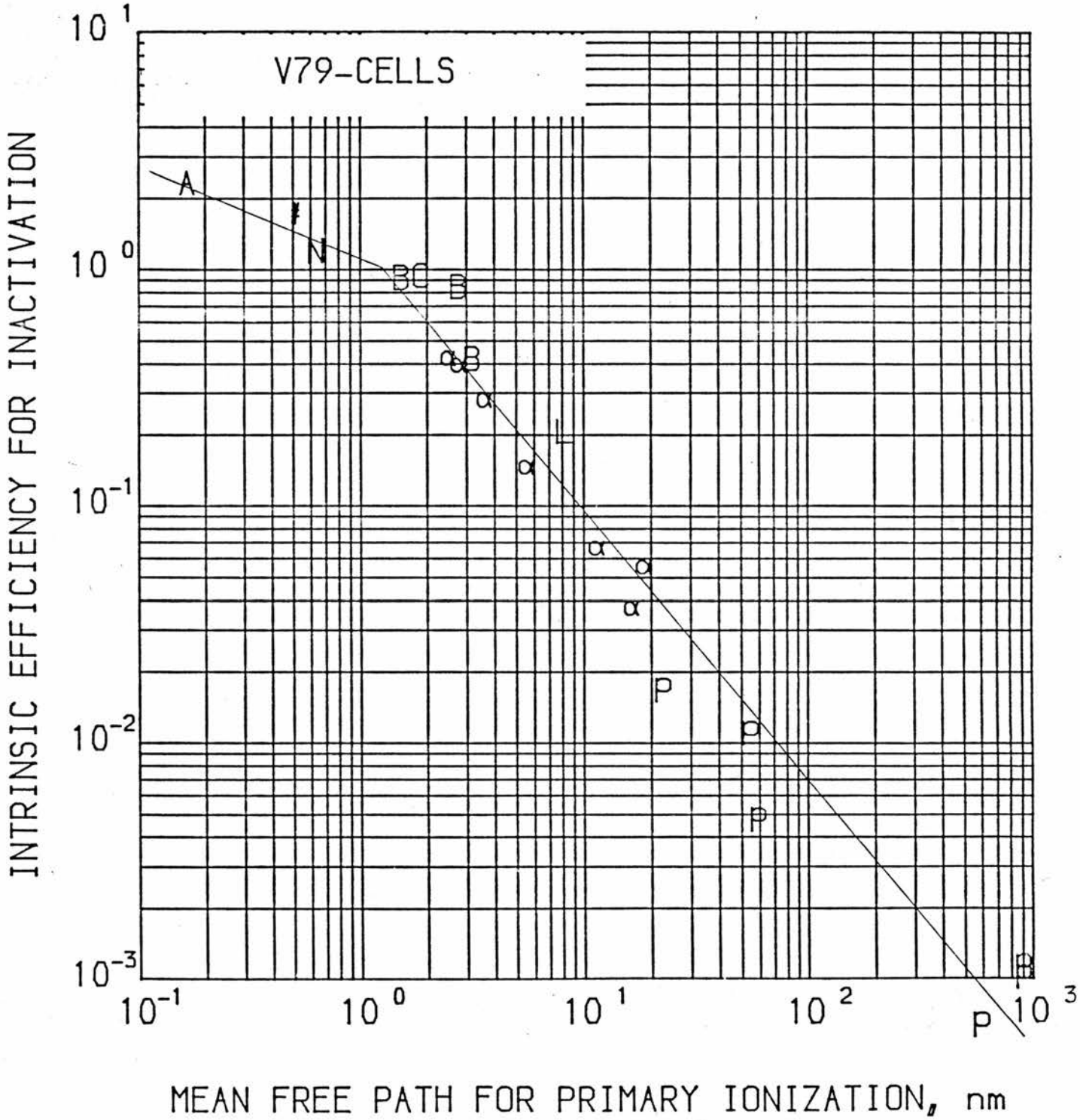

Fig. 6.1 Intrinsic efficiency for inactivation of V79 cells as a function of mean free path between primary ionization.

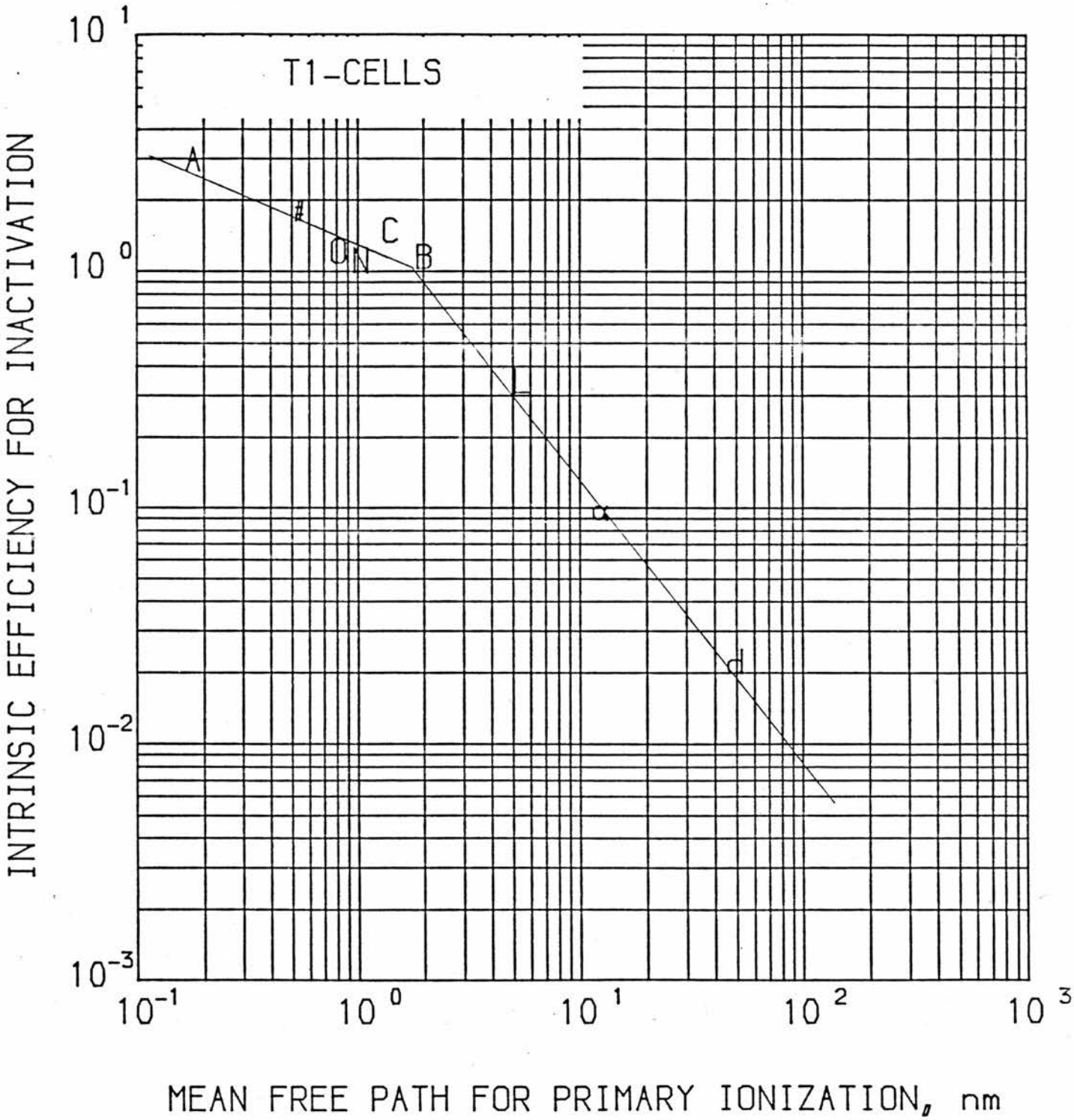

Fig. 6.2 Intrinsic efficiency for inactivation of T1 cells as a function of mean free path between primary ionization.

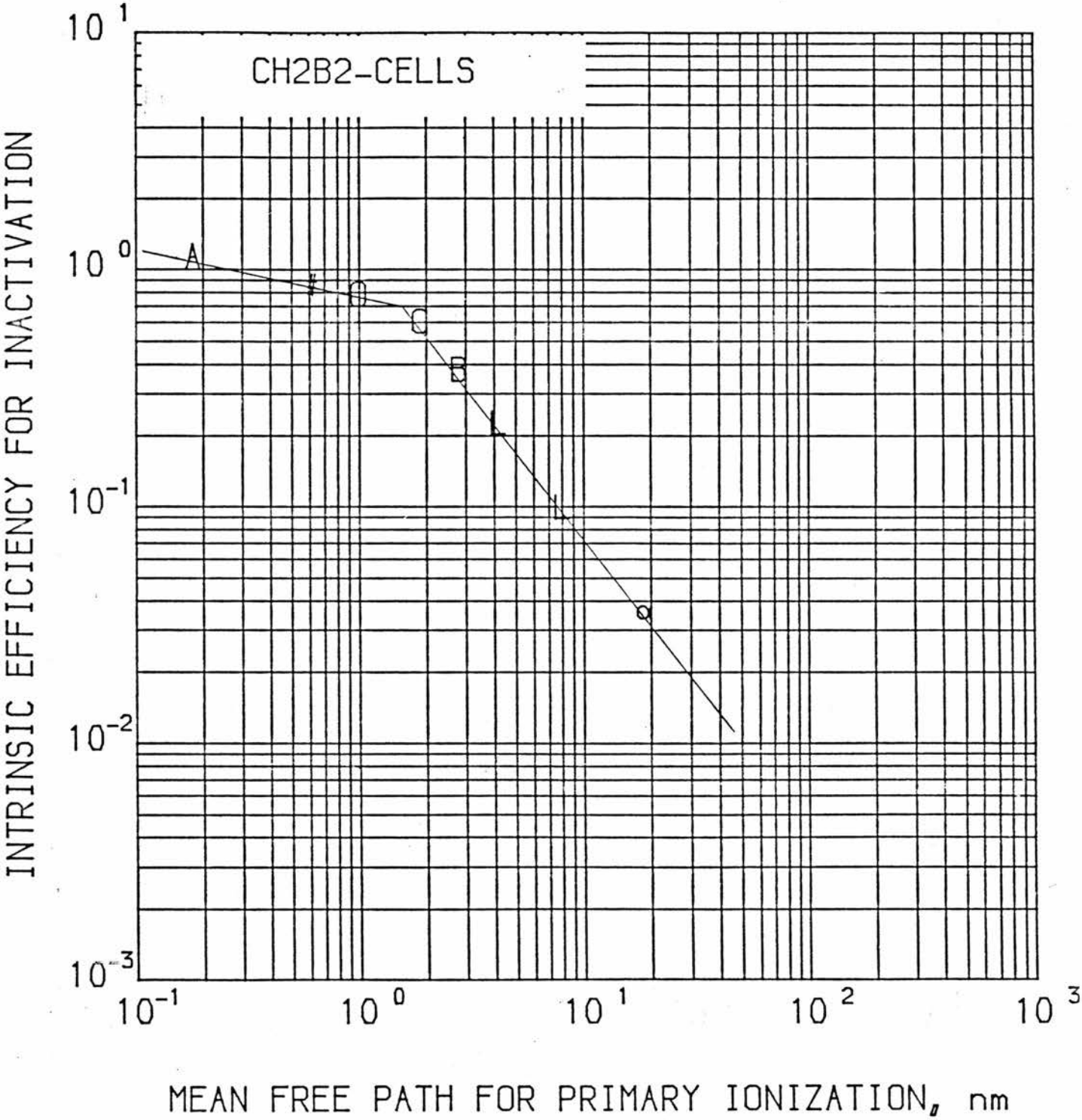

Fig. 6.3 Intrinsic efficiency for inactivation of $CH2B_2$ cells as a function of mean free path between primary ionization.

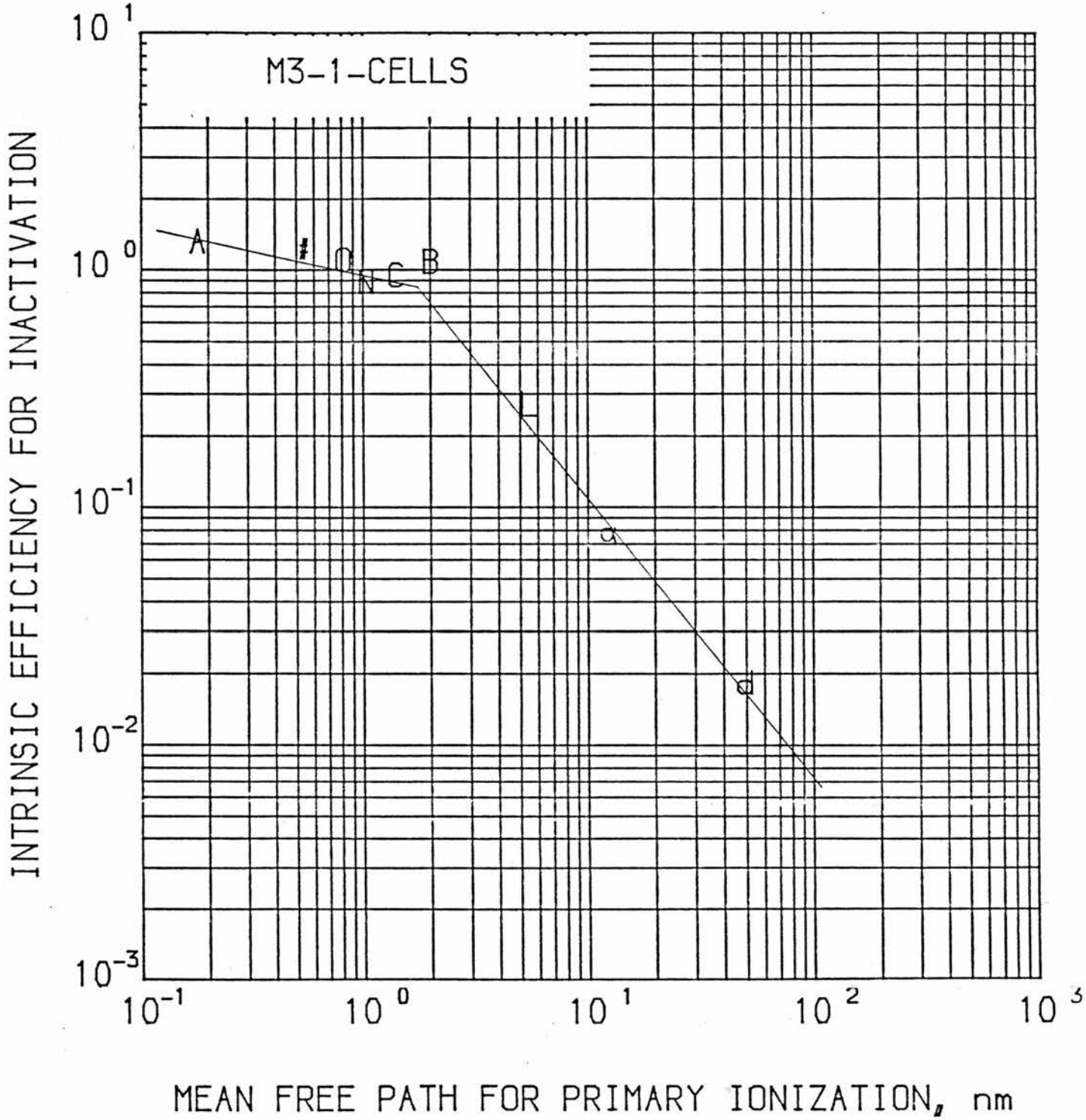

Fig. 6.4 Intrinsic efficiency for inactivation of M3-1 cells as a function of mean free path between primary ionization.

and the presence of absorbing media such as gold (foil) target (to scatter the particle beam), mylar window, air, etc. in their paths. In their work, the initial energies of the protons used in inactivating the cells were reduced from their initial energies of 8 and 4 MeV to 7.4 and 3.0 MeV at the surface of the cells respectively. If the points due to the 160 MeV protons were omitted, the value of $1/\overline{l}_s$ at the point of inflexion was calculated to be 1.54 nm.

Apart from the slight misfit of the data for the V79 cells, the fact remains that the point of inflexion exists and that the optimum efficiency for inactivation occurs at a value of mean free path between primary ionizations corresponding to this point. The most acceptable explanation for this observation is that the optimum efficiency for inactivation occurs when the mean free path between primary ionizations of the incident radiation matches the strand separation of the double stranded DNA in the cells.

This not only suggests that the optimum efficiency for inactivation is independent of ion (radiation) type but it is also quite independent of the energy deposition distribution. The parameter that is of importance is the linear spatial distribution of events and when this matches the strand separation in the DNA i.e. an event every 1.8 nm, an optimum efficiency for the inactivation of the cells will be observed.

6.2 The Intrinsic Efficiency for Inactivation, ε_R, as a Function of the Reciprocal of LET, $1/\bar{L}_T$

Results for the plots of $1/\bar{L}_T$ against ε_R are given by figures 6.5 – 6.8 and in table 5.6a. The plots show the points of inflexion occurring somewhere between 5×10^{-3} and 6.5×10^{-3} nm/eV for the various cell lines. Here again, all the graphs show clearly the existence of the points of inflexion even though it is quite difficult to visualize the significance of the values of $1/\bar{L}_T$ of between 5×10^{-3} and 6.5×10^{-3} nm/eV within which they occur. It can only be said from observing the results, that for optimum intrinsic efficiency for inactivation, the path (track) length of the ionizing radiation per every eV of energy transferred is between 5×10^{-3} and 6.5×10^{-3} nm for the different cell lines.

6.3 The Intrinsic Efficiency for Inactivation, ε_R, as a Function of the Track Average LET, $\bar{L}_T$

The plotted graphs for ε_R as a function of $\bar{L}_T$ (figures 6.9 – 6.12) show that the optimum values of $\bar{L}_T$ with respect to its intrinsic efficiency for inactivation varies between 150 and 190 eV/nm (table 5.6) for the different cell lines. The graphs also show that beyond this optimum value of $\bar{L}_T$, a further large increase in $\bar{L}_T$ will only result in a very slight increase in the intrinsic efficiency for inactivation ($\geqslant 10^3$ eV/nm to increase/

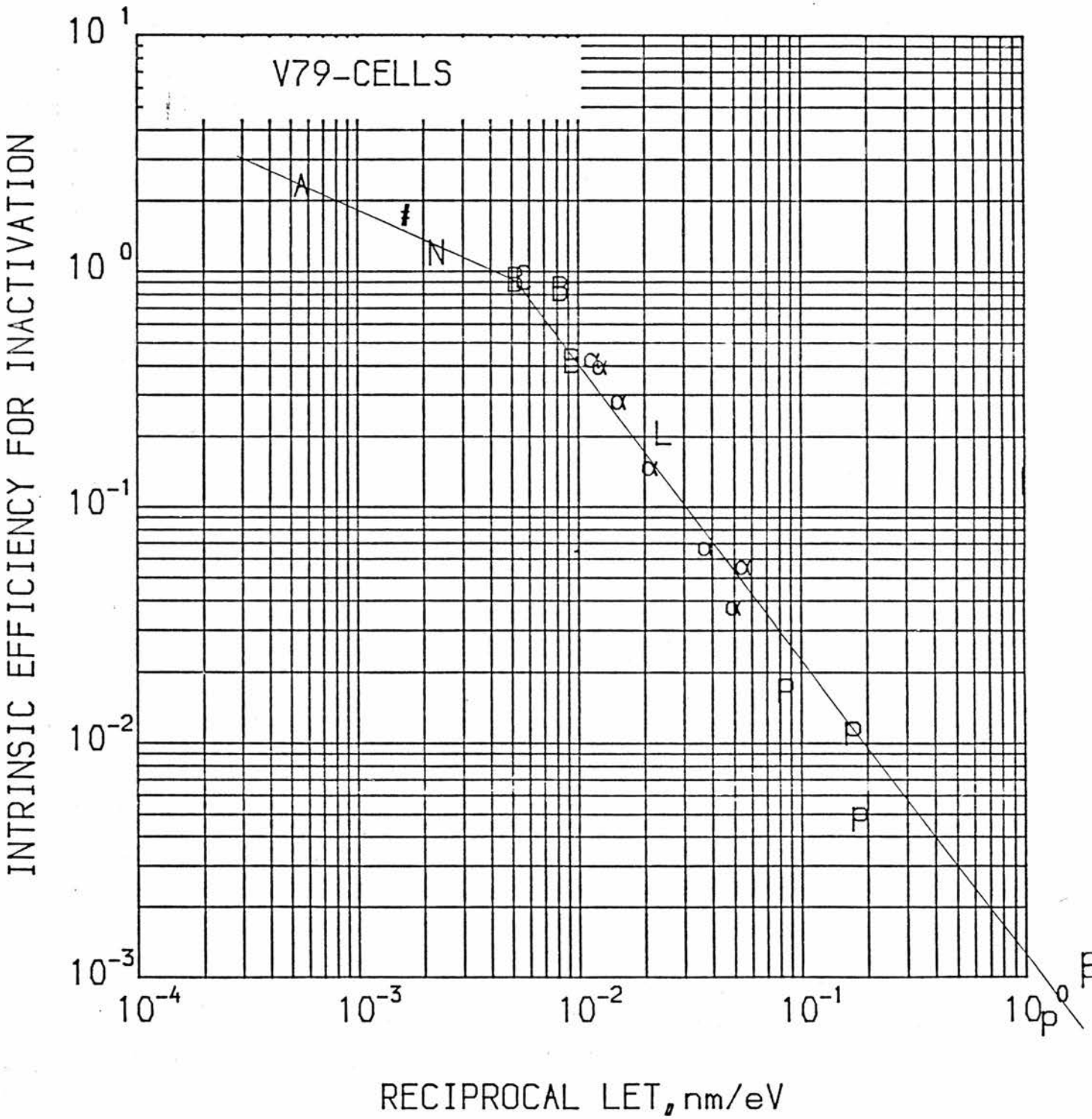

Fig. 6.5 Intrinsic efficiency for inactivation of V79 cells as a function of 1/LET.

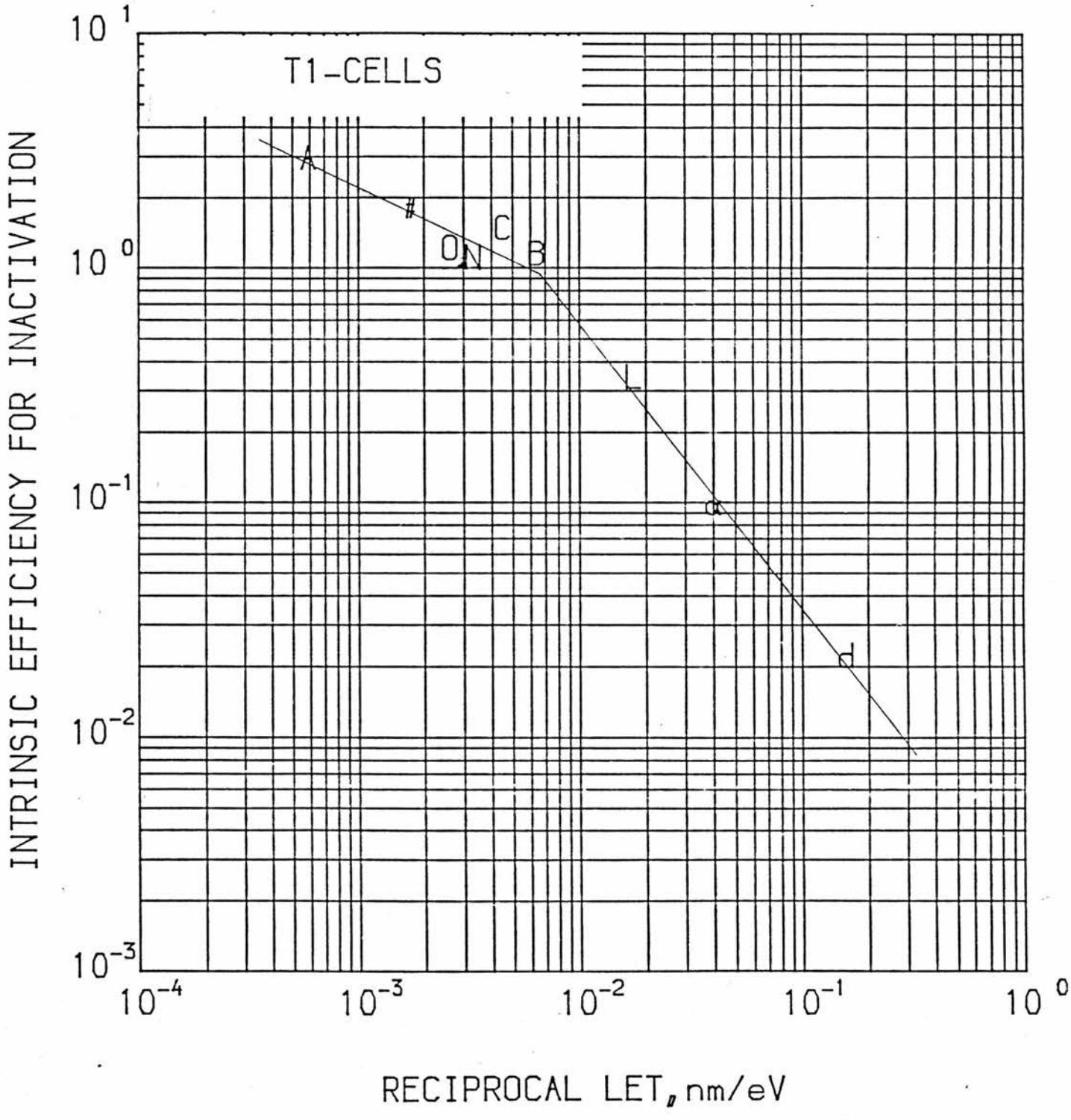

Fig. 6.6 Intrinsic efficiency for inactivation of T1 cells as a function of 1/LET.

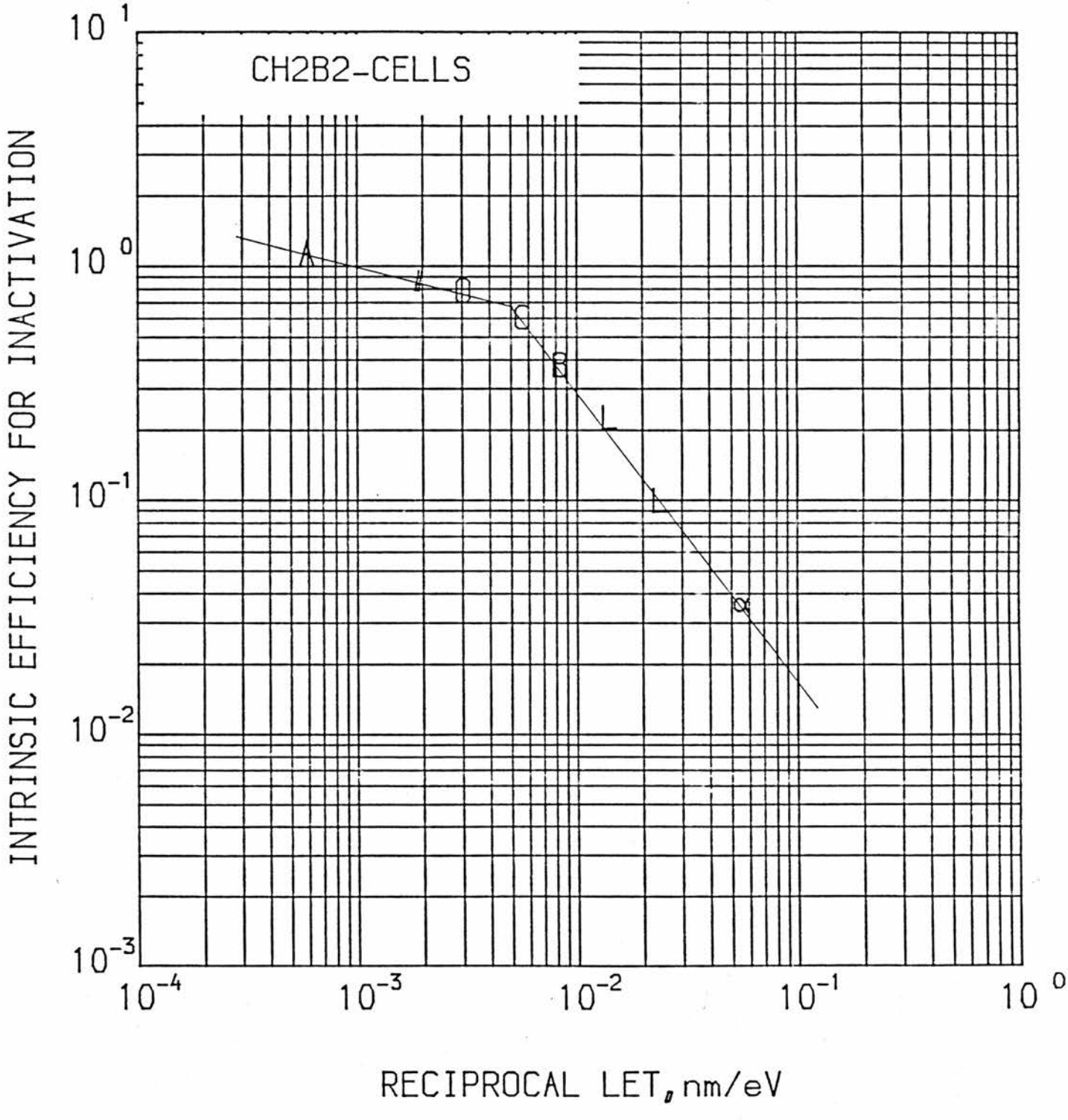

Fig. 6.7 Intrinsic efficiency for inactivation of $CH2B_2$ cells as a function of 1/LET.

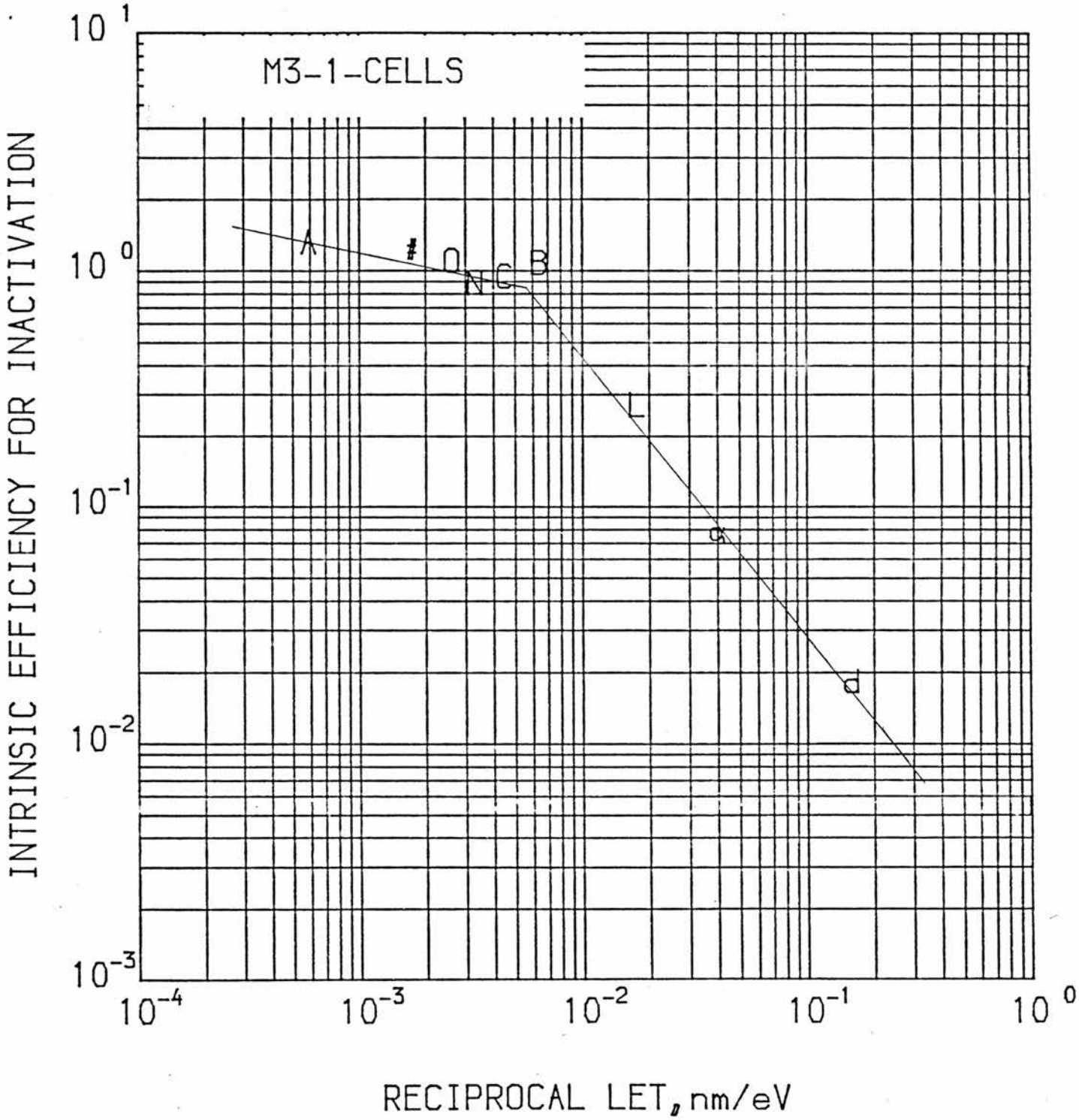

Fig. 6.8 Intrinsic efficiency for inactivation of M3-1 cells as a function of 1/LET.

to increase ε_R from 1.0 to 2.0). This agrees with the already established fact (Goodhead et al, 1980; Yamaguchi et al, 1983) that the RBE for mammalian cells has a peak at an LET of about 100 – 200 eV/nm (100 – 200 keV/μm) in the plot of the RBE-LET curve.

Plainly, the results suggest that heavy charged particles which are most effective in the inactivation of mammalian cells are those with LETs in the range of 150 to 190 eV/nm.

In their work, Watt et al (1984), tentatively suggested that the above mentioned maximum value of RBE to be due to a resonance match in the mean free path between interactions of the radiation and the mean interaction distance between sub-lesions, in other words the distance between the strands of the DNA, assuming that the sub-lesion is a breakage in the strand. It follows that by coupling these two observations i.e. optimum intrinsic efficiency for inactivation occurs when i) values of $1/\bar{I}_s$ equal to 1.8 nm (DNA strand separation) and ii) values of $\bar{L}_T$ between 150 and 190 eV/nm; together would lead to the conclusion that the optimum energy transfer (or deposition) for breakage of adjacent strands in the double stranded DNA is between 270 and 342 eV i.e. (1.8x150 and 1.8x190)

6.4 Intrinsic/

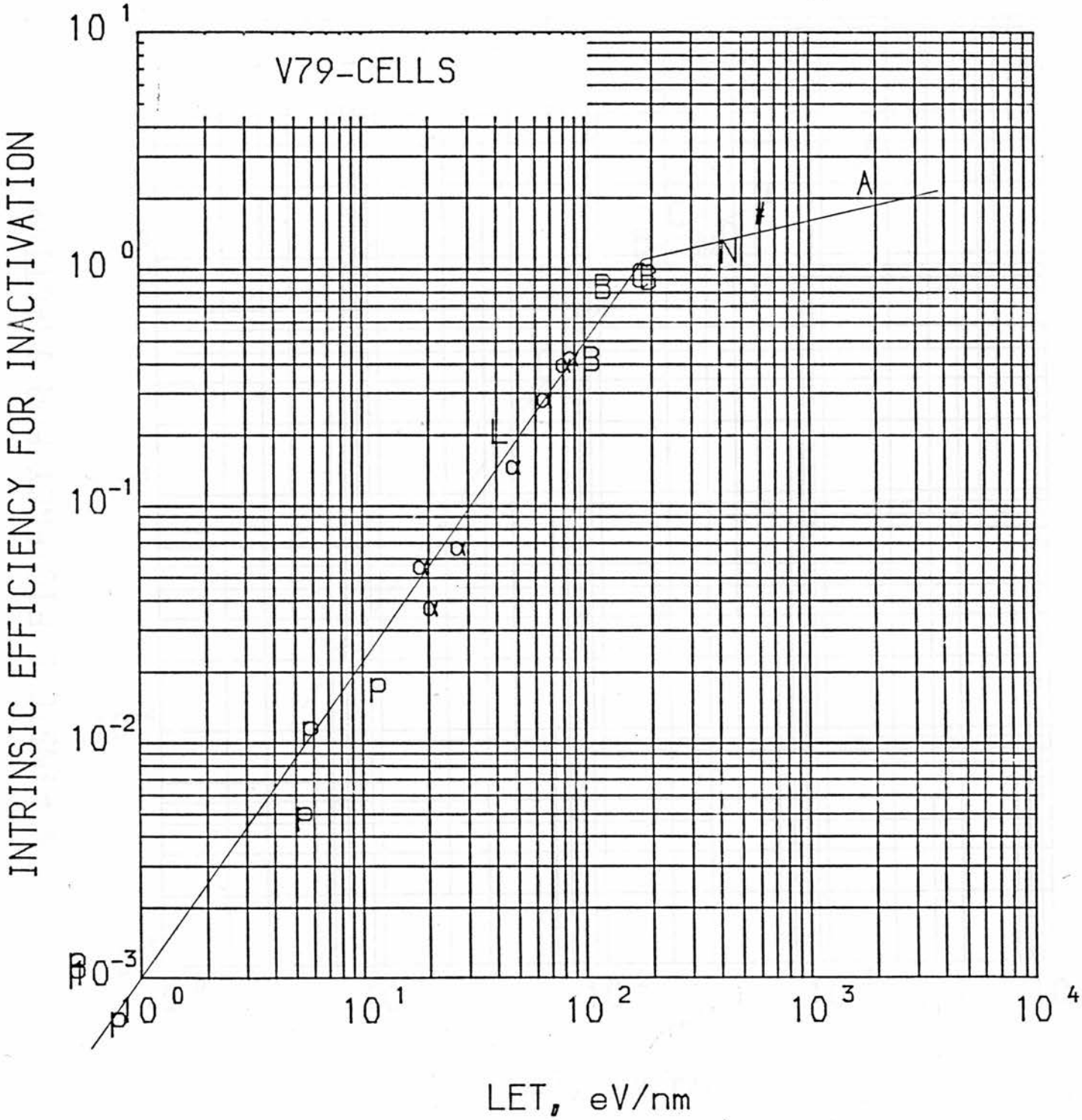

Fig. 6.9 Intrinsic efficiency for inactivation of V79 cells as a function of LET.

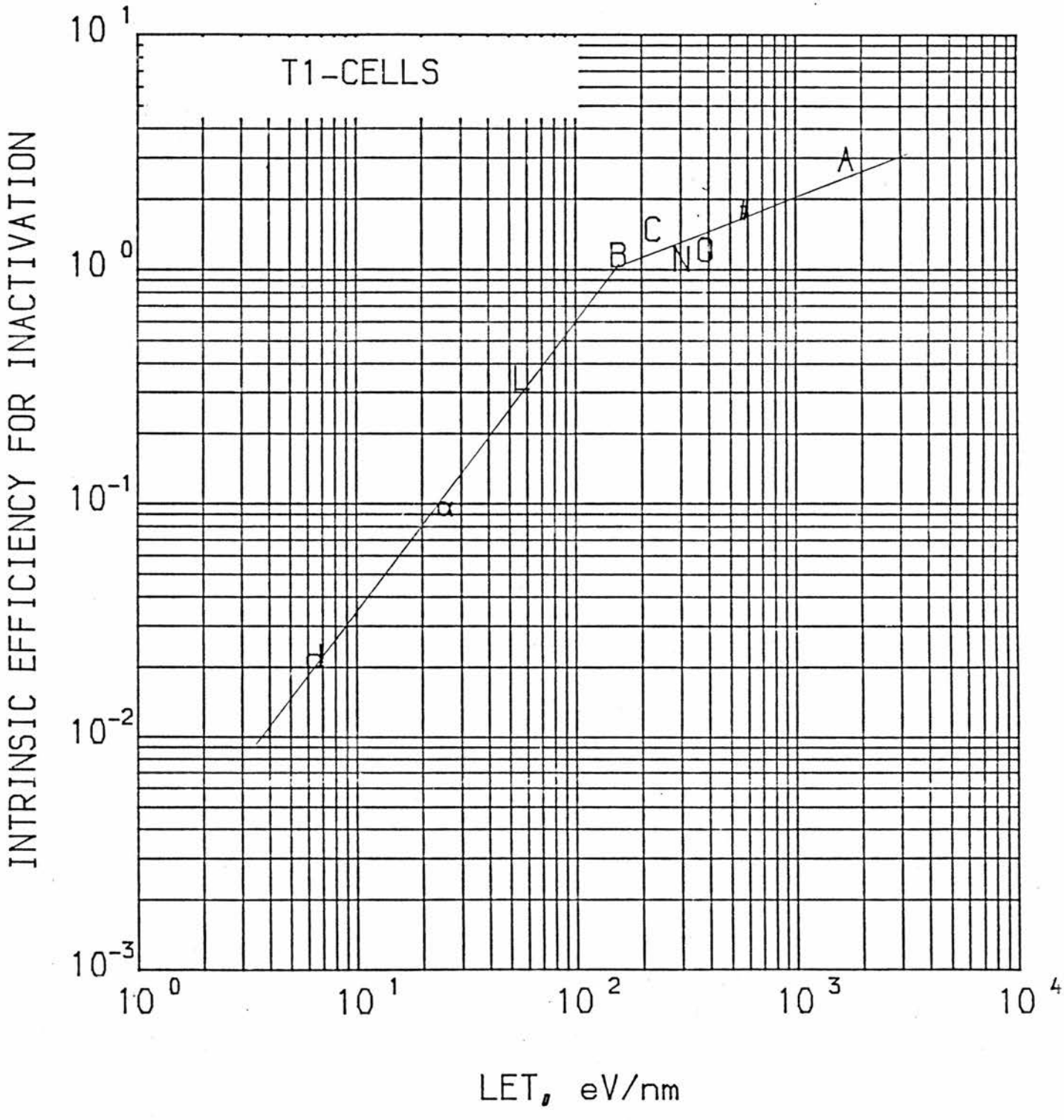

Fig. 6.10 Intrinsic efficiency for inactivation of T1 cells as a function of LET.

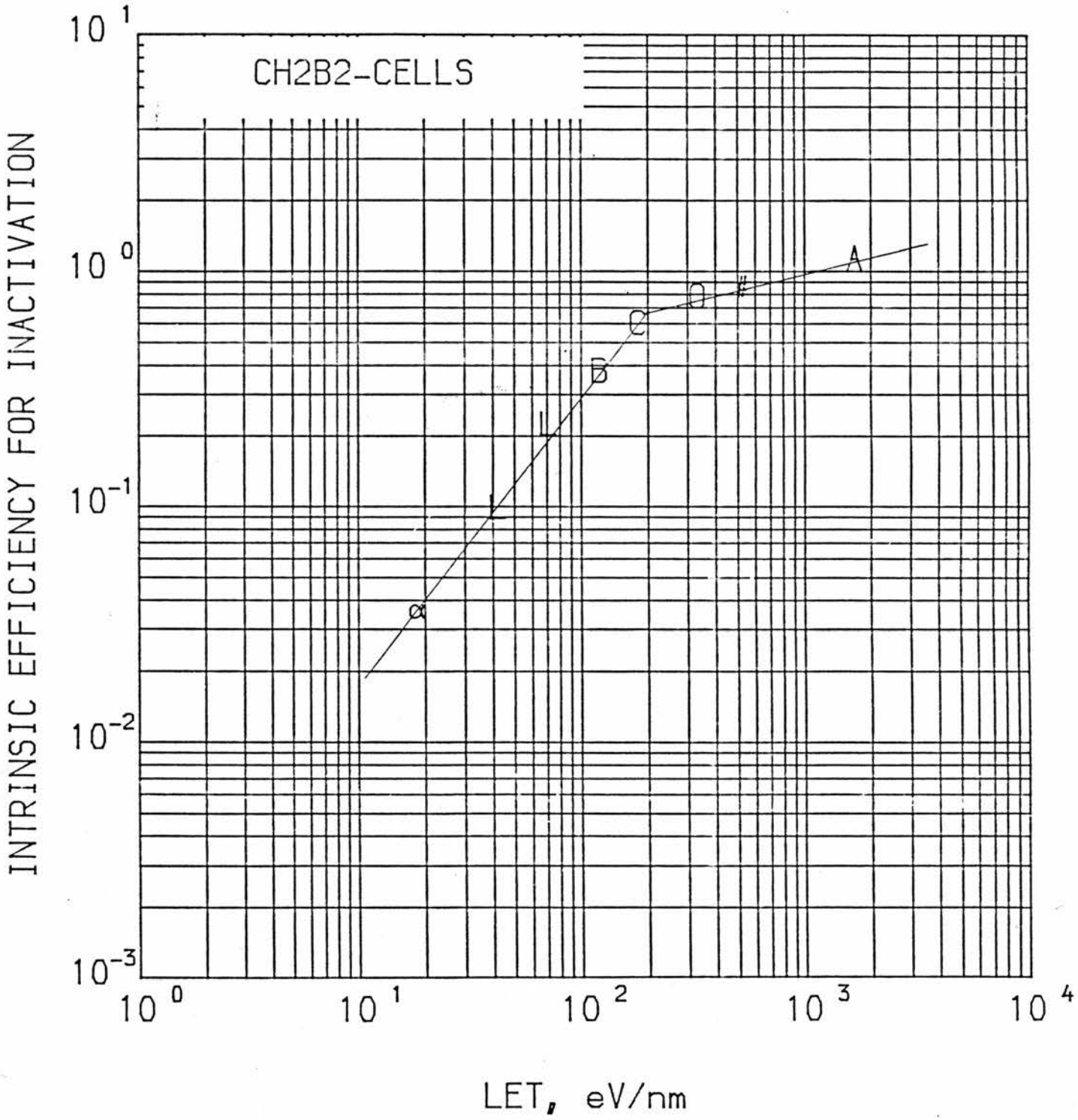

Fig. 6.11 Intrinsic efficiency for inactivation of $CH2B_2$ cells as a function of LET.

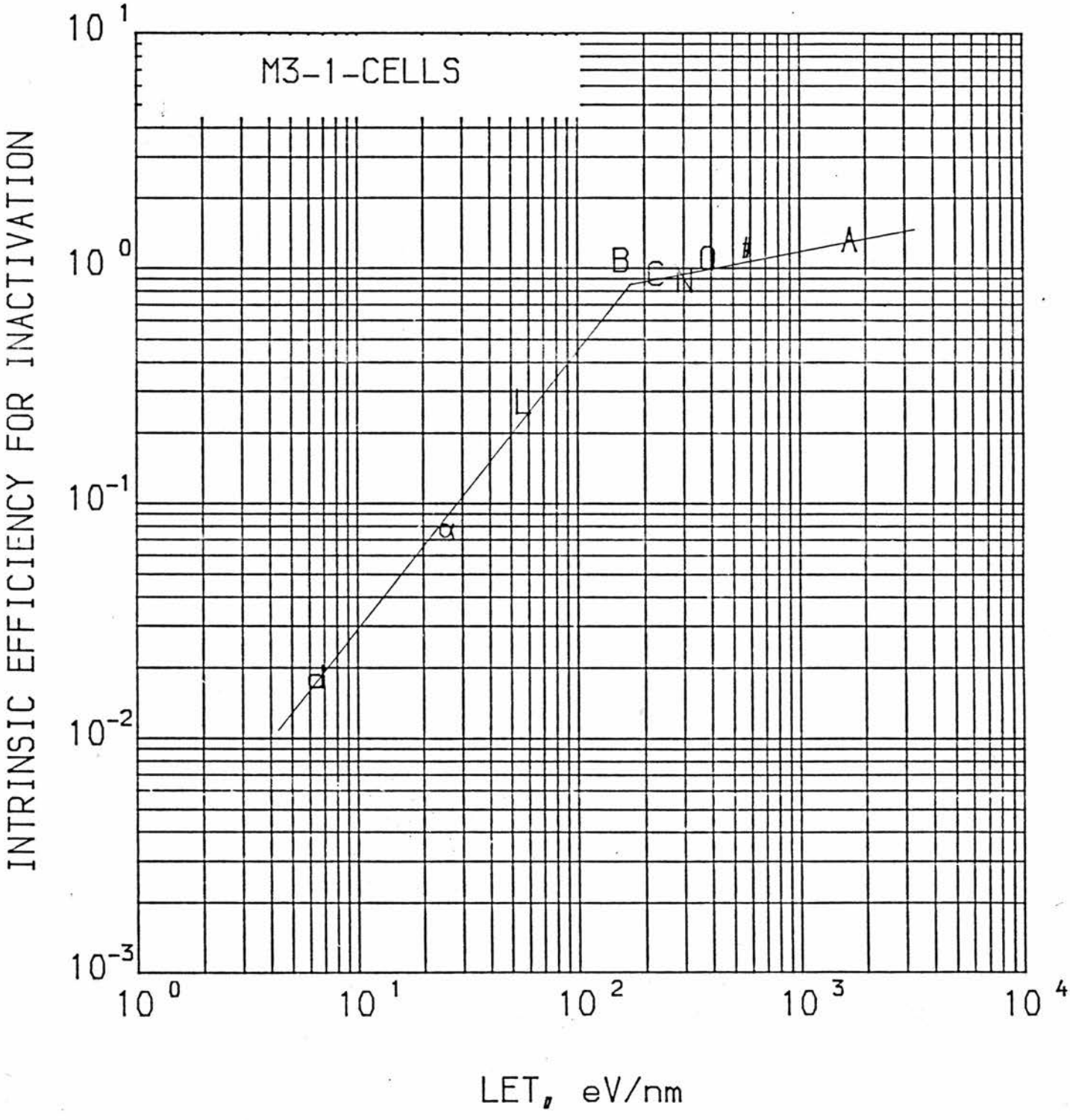

Fig. 6.12 Intrinsic efficiency for inactivation of M3-1 cells as a function of LET.

6.4 Intrinsic Efficiency for Inactivation, ε_R, and the Mean Intrinsic Efficiency of Damage by Delta-Rays, $\bar{\varepsilon}_j$, both as Functions of the Energy of Delta-Rays, E_δ

The plots of E_δ against ε_R (figures 6.13–6.16) and E_δ against $\bar{\varepsilon}_j$ (figure 6.17) seem to show that the contribution of damage by delta-rays to the total damage when mammalian cells are irradiated by heavy charged particles are of little if any significance. This conclusion is reached from the observations that there is no clear relationship between the total intrinsic efficiency for inactivation, ε_R, and the energy of the delta-rays, E_δ; and also between the mean intrinsic efficiency of damage by a single delta-ray, $\bar{\varepsilon}_j$, (beyond the saturation condition) and E_δ. If the contribution of damage due to delta-rays is significant, ε_R and $\bar{\varepsilon}_j$ should both be directly (on log log plot) proportional to E_δ or at least the value of ε_R and $\bar{\varepsilon}_j$ corresponding to the most energetic delta-rays should be comparable if not greater than those for the low energy delta-rays. However, the results (for V79 cells) show that the most energetic delta-rays ($\sim$400 keV) correspond to the minimum values of ε_R. Also in the plot of E_δ against $\bar{\varepsilon}_j$, it seems that $\bar{\varepsilon}_j$ is not dependent on E_δ at all; delta-rays with about the same E_δ can result in $\bar{\varepsilon}_j$ in the range of 4×10^{-6} to 10^{-4}.

Another thing which is of relevance is that the value of $\bar{\varepsilon}_j$ is at least an order of magnitude lower than/

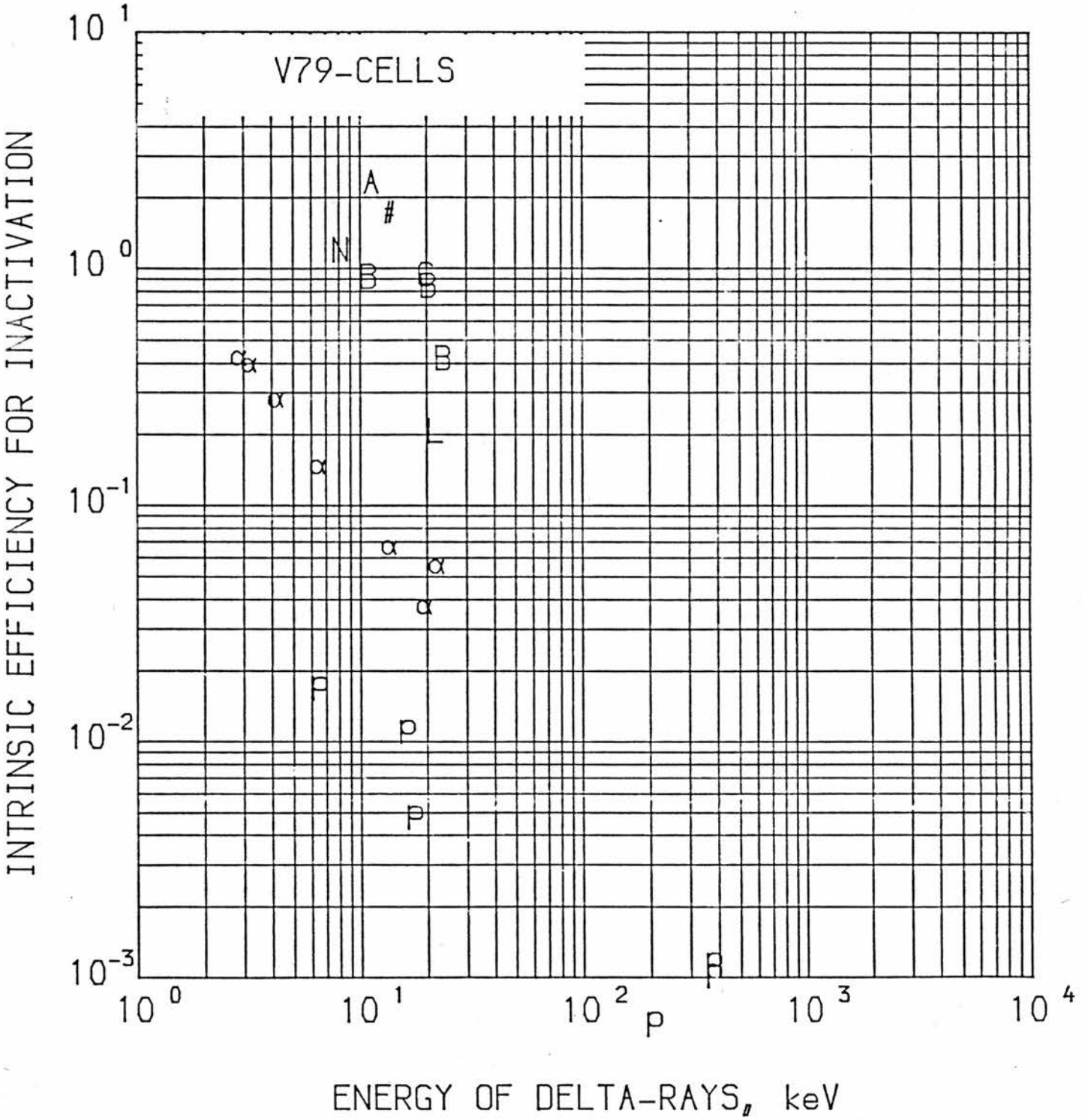

Fig. 6.13 Intrinsic efficiency for inactivation of V79 cells as a function of the energy of delta-rays.

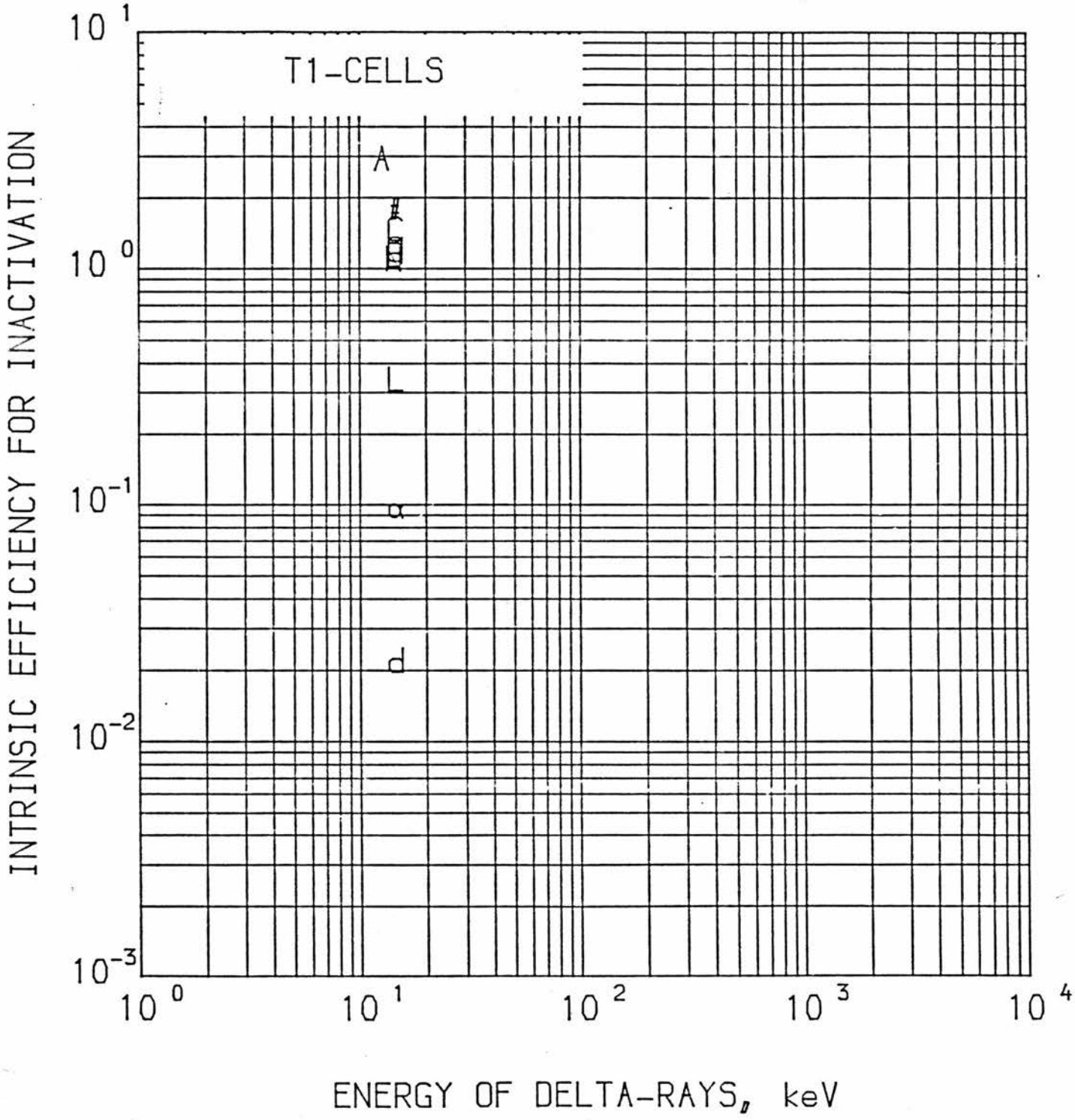

Fig. 6.14 Intrinsic efficiency for inactivation of T1 cells as a function of the energy of delta-rays.

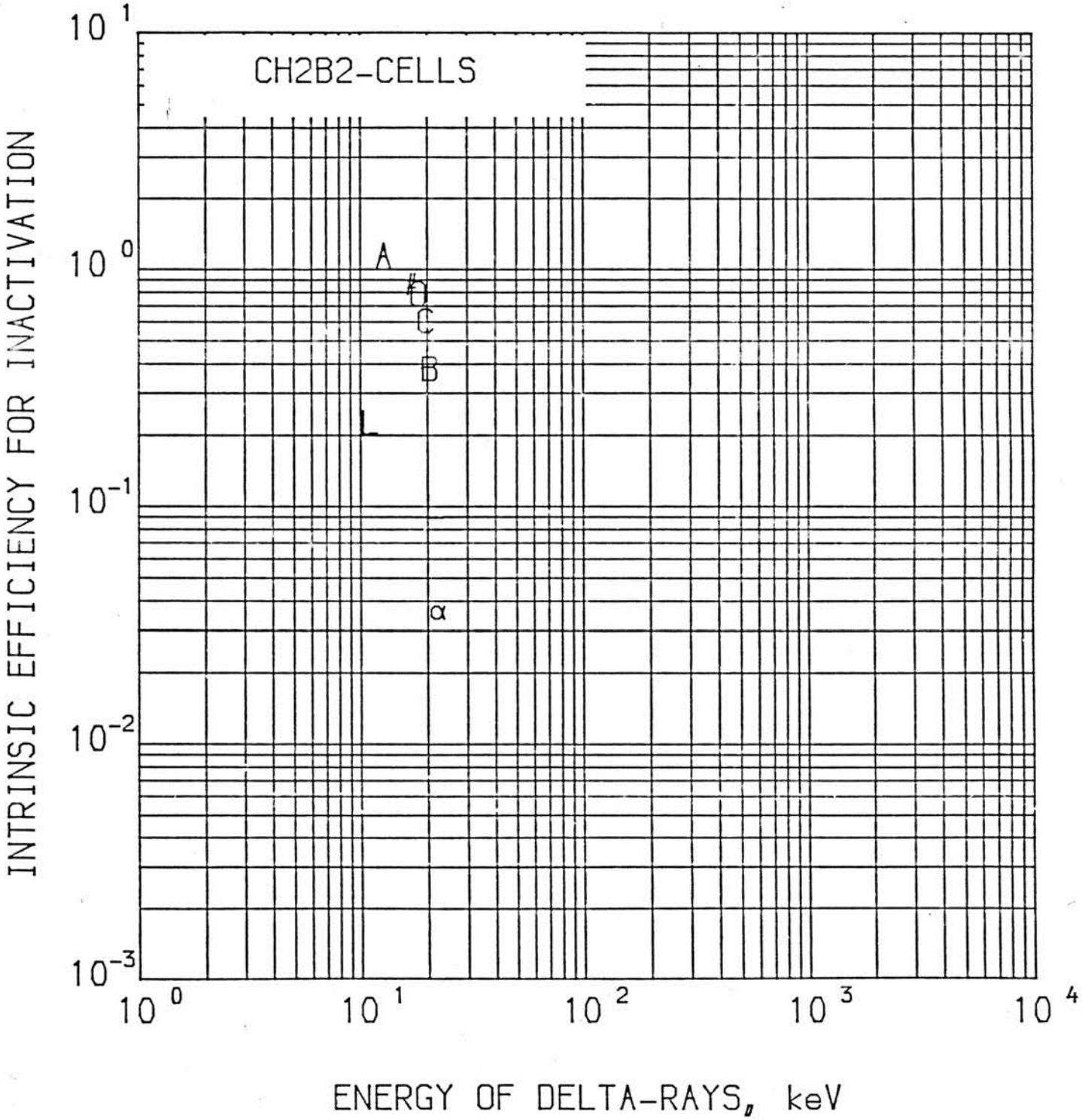

Fig. 6.15 Intrinsic efficiency for inactivation of $CH2B_2$ cells as a function of the energy of delta-rays.

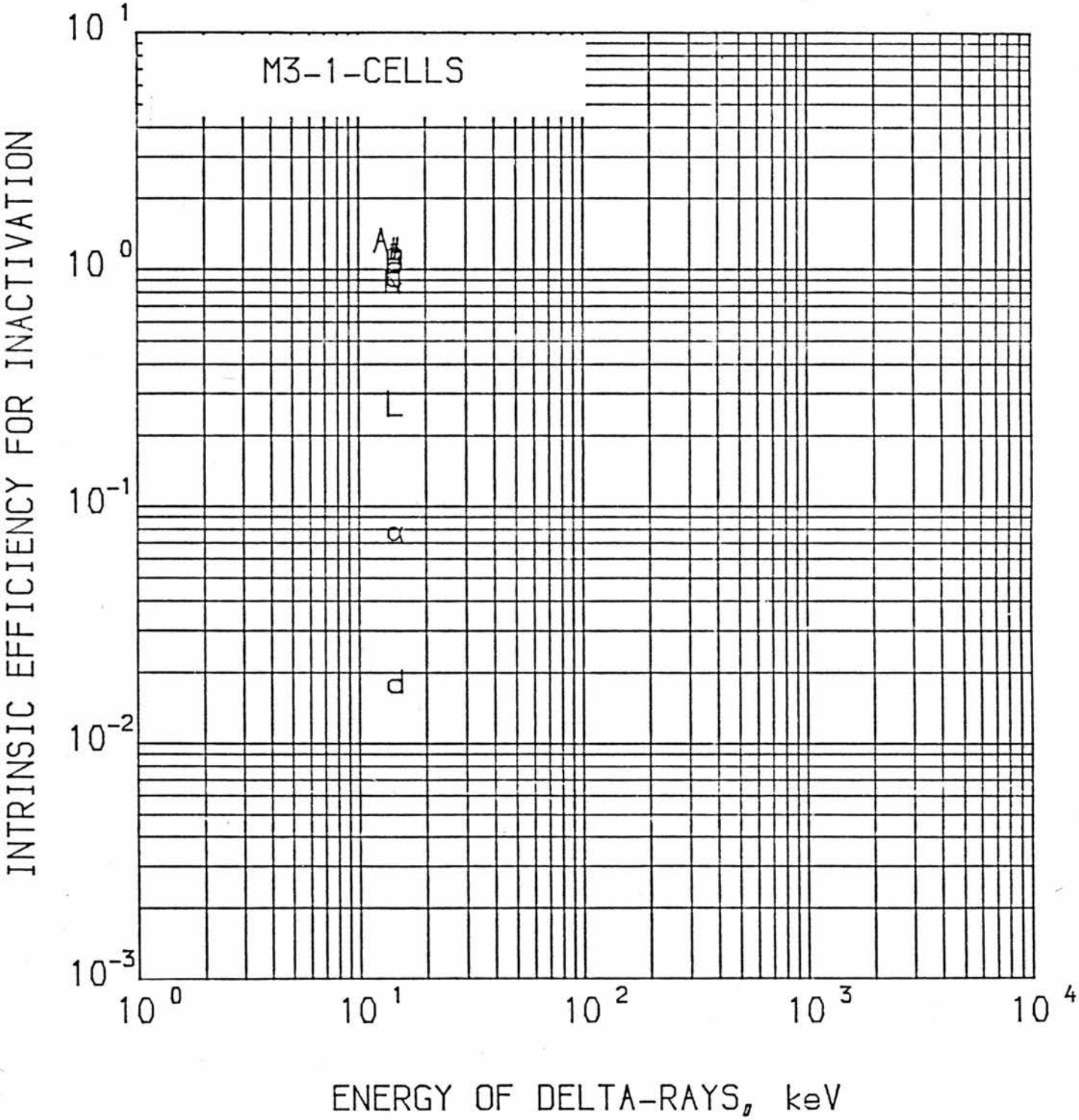

Fig. 6.16 Intrinsic efficiency for inactivation of M3-1 cells as a function of the energy of delta-rays.

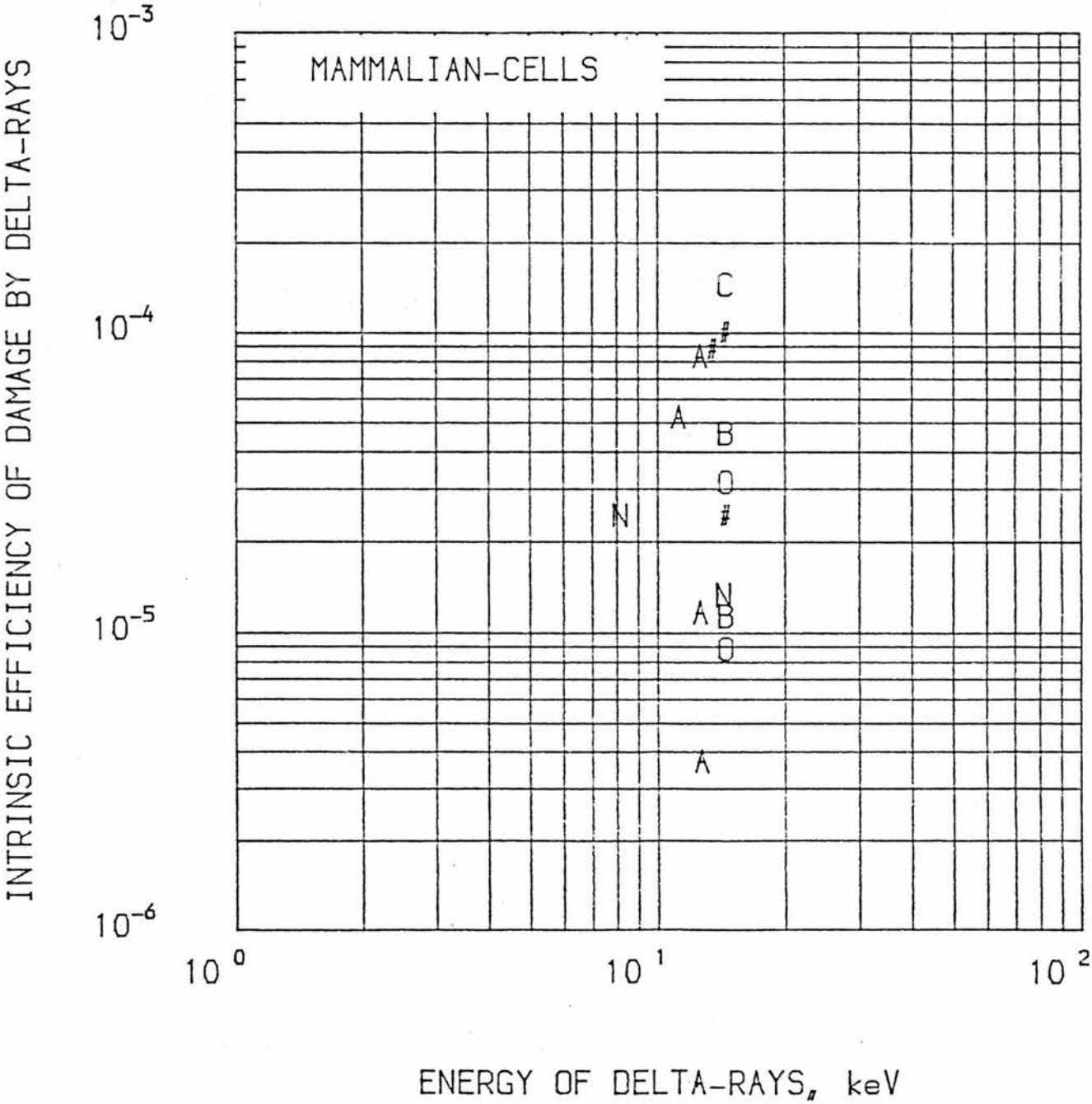

Fig. 6.17 Intrinsic efficiency of damage by delta-rays for mammalian cells as a function of the energy of delta-rays.

than ε_R which is why the contribution of $\bar{\varepsilon}_j$ to ε_R is not that significant. This agrees with the work of Chen et al (1985). The result is not quite that conclusive because in this work data for the values of $\bar{\varepsilon}_j$ for much more energetic delta-rays were not obtained. However, Watt et al (1985), showed that even with delta-rays of energies up to 1 MeV the values of $\bar{\varepsilon}_j$ were still in the range of 10^{-4}.

6.5 Intrinsic Efficiency for Inactivation, ε_R, as a Function of Z^2/β^2

To find out if Z^2/β^2 is a suitable quality parameter, graphs of ε_R as a function of Z^2/β^2 for the different cell lines were plotted and the results can be seen in figures 6.18–6.21. Careful study of these graphs show that Z^2/β^2 is just as good a quality parameter as is $1/\bar{I}_S$ or $\bar{L}_T$. Again the graphs clearly show the existence of the points of inflexion and values of Z^2/β^2 at which they occur are given in table 5.6a. Since Z^2/β^2 reflects the total yield (number) of delta-rays, therefore the results suggest that there is an optimum value for the yield of delta-rays at which optimum damage occurs. In section 6.4 it is suggested ε_R is not dependent on the energy, E_δ, of the delta-rays but here it suggests that ε_R is dependent on the total yield of delta-rays.

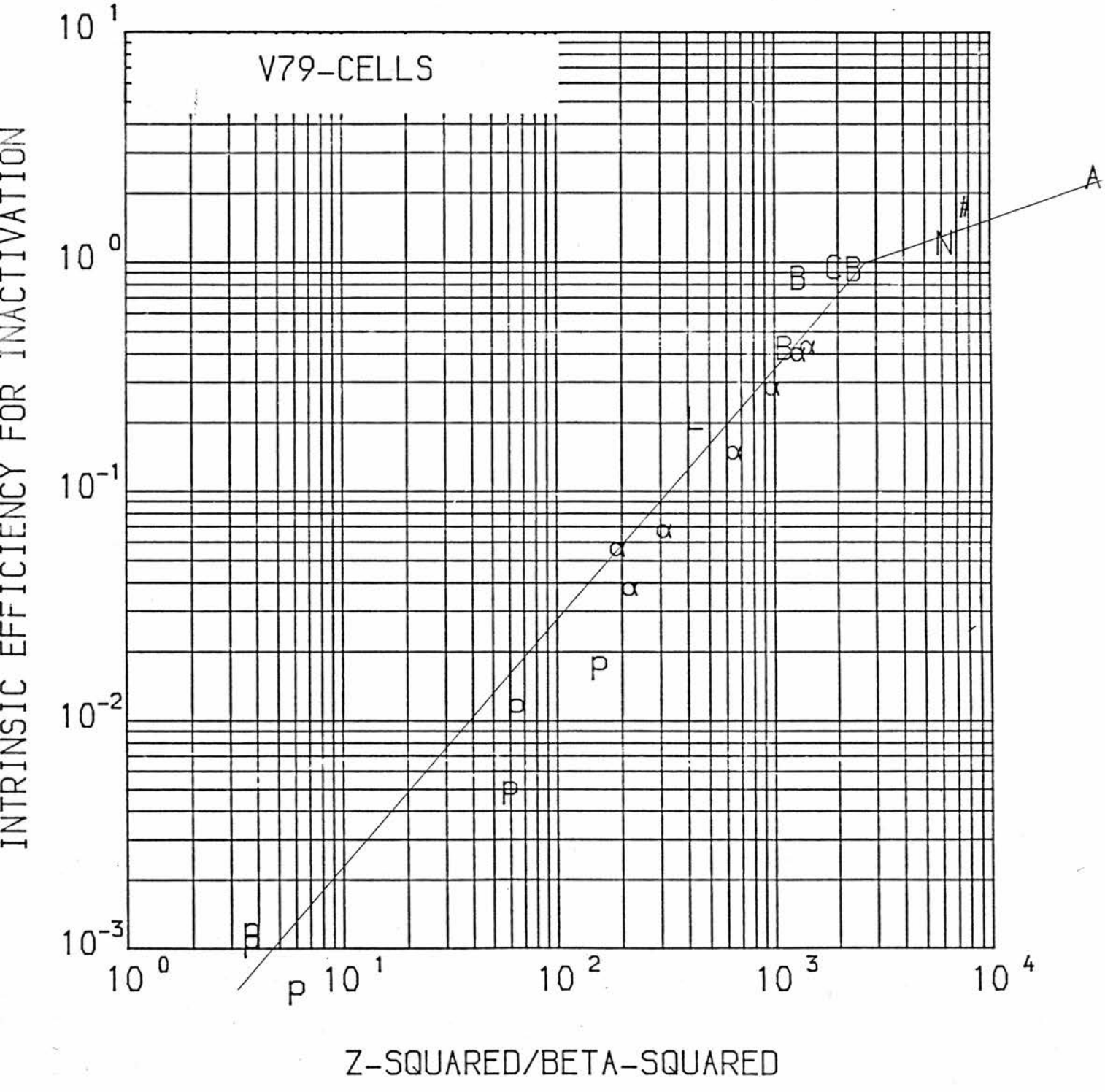

Fig. 6.18 Intrinsic efficiency for inactivation of V79 cells as a function of Z^2/β^2.

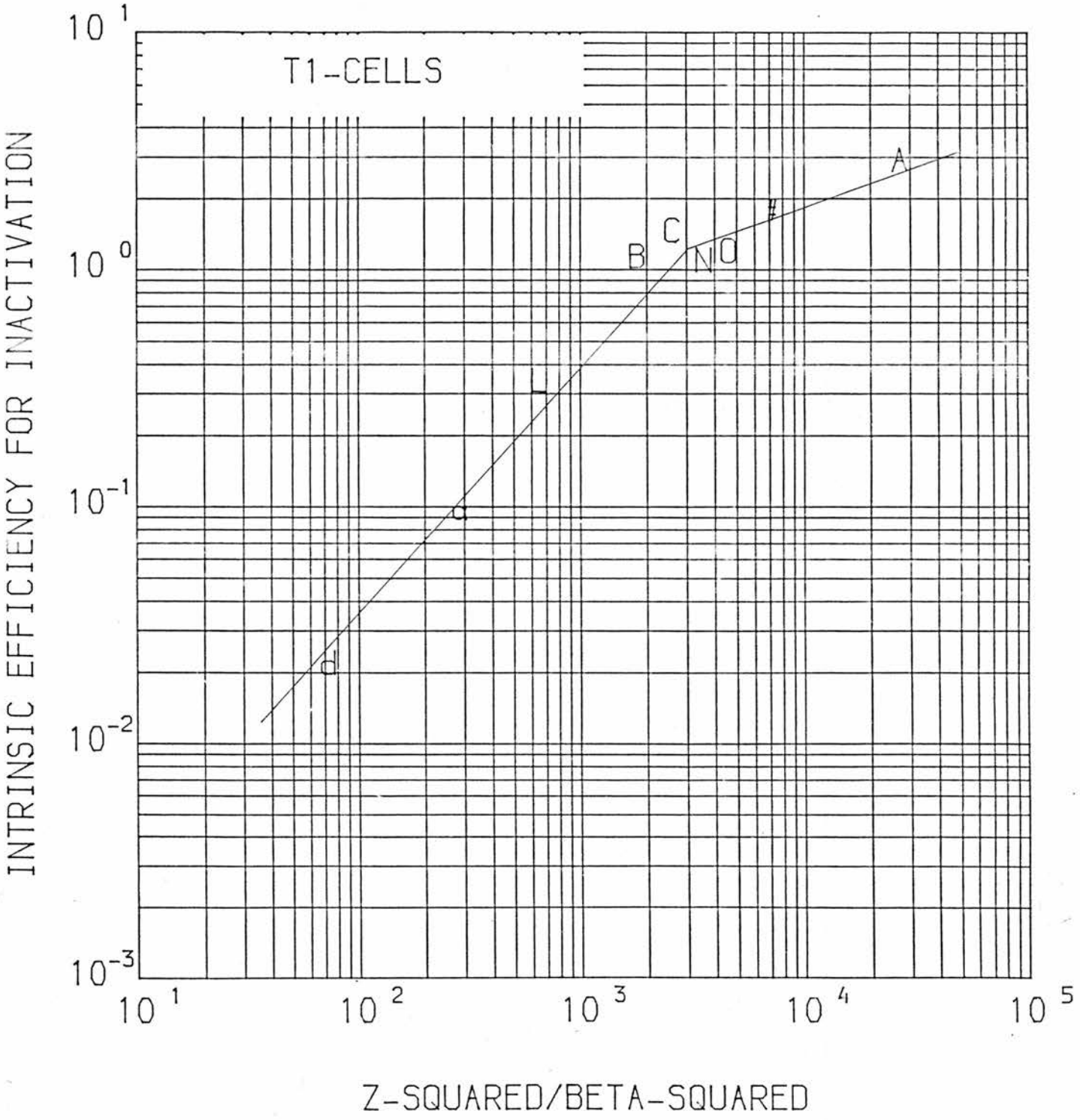

Fig. 6.19 Intrinsic efficiency for inactivation of T1 cells as a function of Z^2/β^2.

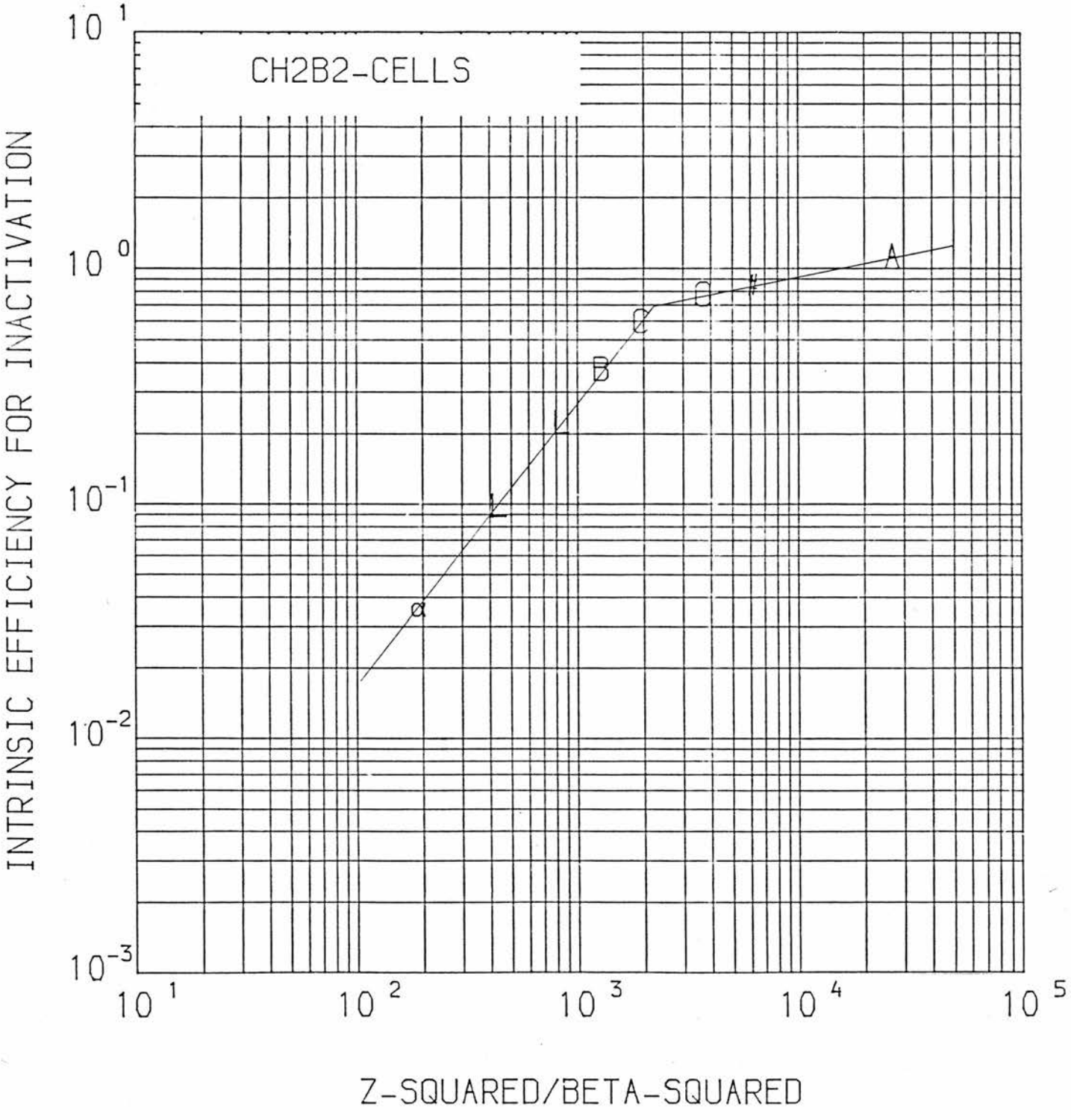

Fig. 6.20 Intrinsic efficiency for inactivation of $CH2B_2$ cells as a function of Z^2/β^2.

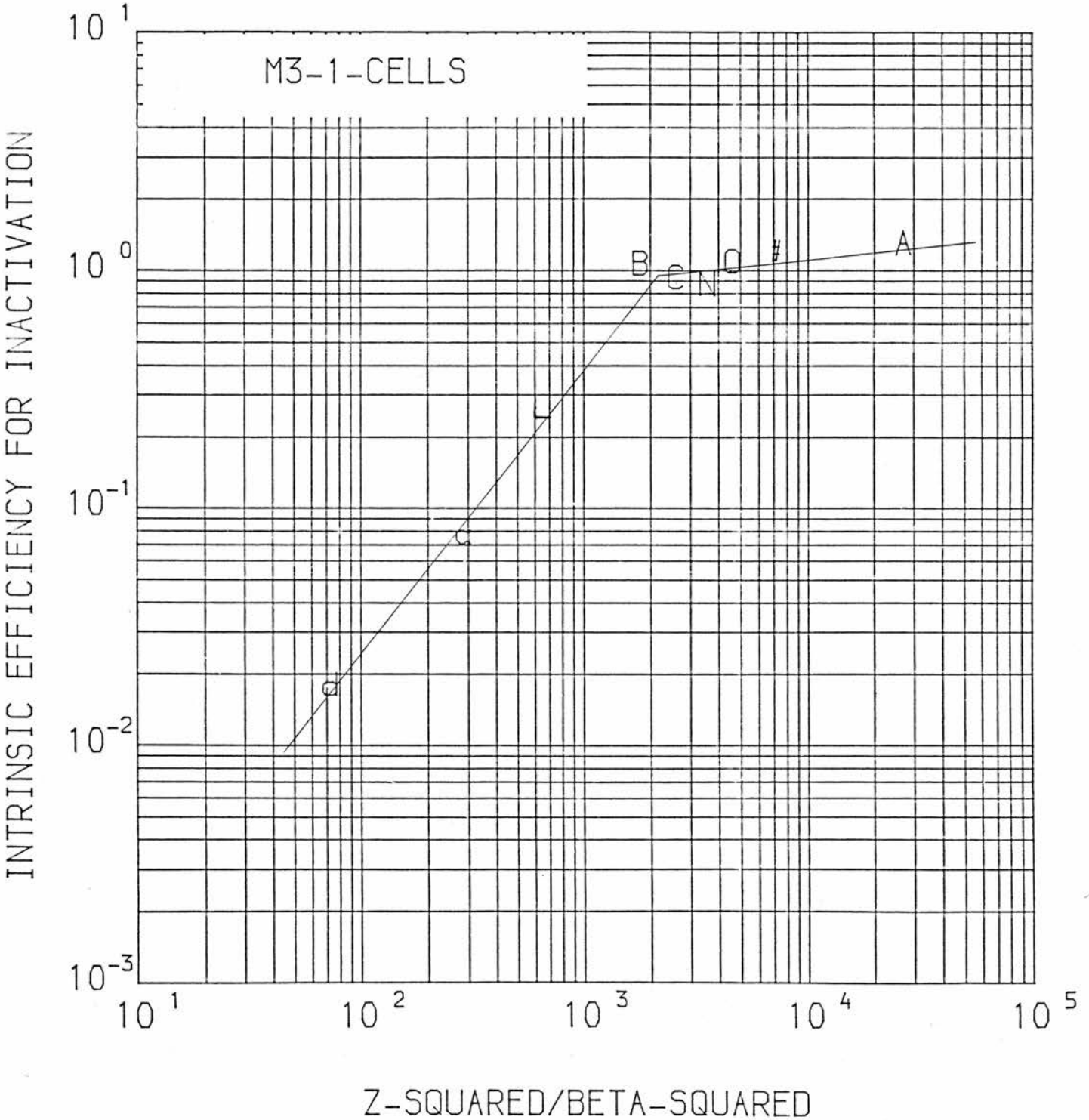

Fig. 6.21 Intrinsic efficiency for inactivation of M3-1 cells as a function of Z^2/β^2.

CHAPTER VII

DISCUSSIONS, CONCLUSIONS AND PROPOSALS FOR FUTURE WORK

7.1 Discussions and Conclusions

The first thing worth pointing out is that even though results from this work suggest that the optimum intrinsic efficiency for inactivation, ε_R, occurs when the mean free path between primary ionizations, $1/\bar{I}_s$, of the radiation matches the strand separation in the DNA, it does not mean that radiation with a mean free path between ionizations other than this particular value of 1.8 nm will not cause any damage to the cells. As can be seen from the results, ε_R increases at a certain constant rate as $1/\bar{I}_s$ decreases until $1/\bar{I}_s$ is approximately 1.8 nm, then the rate of increase of ε_R with further decrease in $1/\bar{I}_s$ is markedly less. It is not unreasonable to assume that ε_R will saturate to some value ε_{R_s} say, where a further decrease in $1/\bar{I}_s$ (or increase in $\bar{I}_s$) will only result in a waste of energy or what is termed as an overkill.

Results from data obtained from a single author show a very similar trend to those obtained by correlating data from several authors. The data for the V79 cells were obtained from several authors whereas the data for $CH2B_2$, T1 and M3-1 cells were each compiled by a single author. One only has to compare the plots/

the plots of the data obtained by the two methods and will find that they are similar in every respect right down to the points where the inflexion occurs (within experimental and plotting error). One can still argue that this is not a true comparison because it compares one set of data from one cell line to another set of data from a different cell line. The only way to get over this is then to carry out the experiments and obtain a complete set of data for the V79 cells and compare it to the set of data for the V79 cells above; it is doubtful if they will be much different from each other. What may be concluded from this observation is that uncertainties due to the use of different sub-cell lines, differences in the cell culture and irradiation techniques and statistical and environmental variations of each of the different laboratories are of little if any significance at all.

All the results (graphs) from this work conclusively point to one thing. There exists a physical mechanism of damage which results to optimum damage at the corresponding optimum values of be it $1/\bar{I}_S$, $\bar{L}_T$ or Z^2/β^2. The most acceptable explanation of all these observations is that optimum damage occurs when the spatial distribution of events (interactions) matches the interaction distance between sub-lesions, in the case of mammalian cells, the strand separation in the double stranded DNA. This consequently relegates the spatial/

the spatial distribution of energy of the incident radiation, which was previously thought to be of considerable importance, to a much lesser role in the inactivation of mammalian cells by heavy charged particles.

It may be said that results from this work seem to point out, though more work is necessary to prove it conclusively, that the contribution to the total intrinsic efficiency for inactivation by delta-rays is quite insignificant when mammalian cells are irradiated by accelerated heavy ions.

Study of the plots of all the data for $1/\bar{I}_S$, $\bar{L}_T$ and Z^2/β^2 show that all three are comparatively satisfactory quality parameters; ε_R is linearly dependent (on log-log plots) on all three. Though in this work $1/\bar{I}_S$ is preferred above the other two because it is in the same dimension as the proposed dominant physical mechanism of damage (i.e $1/\bar{I}_S$ = 1.8 nm).

Finally, with all the overwhelming evidence from the results of this work it is concluded that the dominant physical mechanism of damage in the inactivation of mammalian cells by heavy charged particles is the matching between the mean free path between primary ionizations of the incident radiation and the strand separation in the double stranded DNA of the cells.

7.2/

7.2 Proposals for Future Work

At the beginning of this work it was intended to treat the inactivation of mammalian cells by protons, alpha-particles and heavy ions separately. Unfortunately, there wasn't enough published data for proton and alpha-particle inactivation of mammalian cells to cover the necessary energy range so as to be a complete set on their own. Therefore, it is hoped that future work on the inactivation of mammalian cells by protons in the energy range of the lower keVs to tens of MeV (LETs of ~ 10 to 10^3 eV/nm) and of alpha-particles in the energy range of tens of keV to 100 MeV (LETs of 100 to 10^3 eV/nm) will be carried out. This will give a complete set of data covering the ranges of $\bar{I}_S$, $\bar{L}_T$, etc. of interest. Though it can be visualized as pointed out by Neary, (1970) , that there might be the problem of whether the very low energy particles will have track lengths large enough compared to the thickness of the cell layers so that they may be considered as track segment experiments. But still, attempts should be made where possible to obtain survival data for irradiation with these lower energy particles.

Another very interesting piece of work which could be done is to carry out a very similar analysis on chromosome aberrations and mutations of mammalian cells with double stranded DNA. Since both chromosome aberrations and mutations are not dependent on the breakage of adjacent strands/

strands of the double stranded DNA (as such breakages are assumed to inactivate the cells) an absence of the points of inflexion at $1/\bar{I}_s$=1.8 nm in the plots of chromosome aberrations or mutations against $1/\bar{I}_s$ will undoubtedly support the suggestion that optimum damage to the cells occurs when the mean free path between primary ionizations equals the strand separation in the DNA.

In addition to the above it will also be worth looking into the contributions made by delta-rays to the total intrinsic efficiency for inactivation not only as a function of their energy as was done here but also as a function of their mean free path between events and event cross-sections or even as a function of their extrapolated range as electrons are found to be most damaging towards the end of their track (Chen et al, 1985). Also it may be conclusive to study the relationship (beyond the saturation condition) between the energy of delta-rays, E_δ, of much more energetic delta-rays and the intrinsic efficiency for damage of the delta-rays, $\bar{\varepsilon}_j$. In this work, the relationship between E_δ and $\bar{\varepsilon}_j$ was only observed for delta-rays with energies, E_δ, of not more than 20 keV as the contributions to the total intrinsic efficiency for damage, ε_R, by much more energetic delta-rays (up to $\sim$ 400 keV) occurs before the saturation condition and therefore $\bar{\varepsilon}_j$ could not be determined.

It makes/

It makes one wonder if it is possible to alter slightly the strand separation in the DNA such as when at different stages of the cell-cycle or by chemical or whatever means (but still maintaining the basic functions of the cells); then carrying out a similar analysis on these cells with altered DNA strand separation will provide absolute proof (or disprove) of the physical mechanism of damage proposed in this work.

Finally, taking it a step further, it might also be interesting to investigate if similar physical mechanisms of damage do occur in other targets; say the breakage of adjacent chemical bonds or chains in polymers or any other organic material to produce an effect, preferably a desired effect such as the vulcanization of rubber.

APPENDIX I

Limitations of the Fixed-frequency Cyclotron

The limit of the maximum energy attained by particles in a fixed-frequency cyclotron is set by a fundamental phenomenon of nature described by the theory of relativity. The kinetic energy of any object is associated both with its mass and with its velocity and since the latter cannot exceed that of light, an increase in energy of a body moving at a speed near this limit shows up largely as an increase in its mass. Consequently, this increase in mass brings about a change in the frequency of revolution of the particle i.e. the revolution frequency of a fast particle in a cyclotron is less than that of a slow one, and if the oscillator has been adjusted to be in synchronism with ions just starting out, it will be at the wrong frequency for the more energetic ions which have gained somewhat in mass. The onset of this difficulty is gradual, the ions slowly slipping out of phase until ultimately traversal of the dee-to-dee gap brings about deceleration. The limit thus set is about 15 MeV for protons, 25 MeV for deutrons and 50 MeV for alpha-particles. It would be absurd to use a cyclotron to accelerate electrons because their mass is already trebled at energies of only about 1 MeV.

This problem is however, overcome, by the introduction of the synchrocyclotron. The synchrocyclotron avoids the energy limitation of the fixed-frequency cyclotron by the expedient of varying the frequency of the oscillator. As acceleration proceeds and the revolution frequency drops because/

because of the increase in mass, a tuning element slowly lowers the frequency of the oscillator so that the particles and the voltage always stay in phase. One pays a price for the greater energy however; the output of high energy ions is vastly reduced, since each group of ions must be shepherded carefully to high energy and then the oscillator returned to the starting frequency before it can pick up another group.

APPENDIX II

A Computer Program for plotting the graph.

```
C     PROGRAM ICRUA.FOR
C     A LOG/LOG VERSION. NOW MODIFIED FOR CROSS-SECTION RATIOS OF
C       BIOLOGICAL EFFECTS, ETC.
C     CHECK VALUES OF MOL/ATOMIC WT. (W), SCALES (SX1,SX2,SY1,SY2)
C     DATA FILES GIVE N1,N2, E(keV),STOPPING POWER(MeV.CM2/GM).
C     IF CROSS-SECTIONS(*10-15) ARE REQUIRED AS INPUT/OUTPUT
C       PUT W=0.0.
C     STOPPING CROSS-SECTIONS ARE IN eV.CM2/1.0E15 ATOMS.
C     STOPPING POWERS ARE IN MeV.CM2/GM.
C     PARTICLE ENERGIES ARE IN keV.
      REAL SX1,SX2,SY1,SY2,SG
      REAL X(50),Y(50),E(50),BS(50),ST(50),FP(50),TD(50),SR(50)
      INTEGER K,L,N,J,IN,M(50),IZ(50)
      CHARACTER*20 STPFIL(15)
C     READS LIST OF DATA FILES BY NAME.
C     POSITIONS X,Y SCALE TITLES AUTOMATICALLY FROM SX1,SX2,SY1,SY2.
      OPEN(UNIT=32,STATUS='OLD',ACCESS='SEQUENTIAL',FILE='V79.DAT')
      KE=1
C     NOTE KE IS THE NUMBER OF DATA FILES.
      W=32.0
      RNA=602.2/W
      SX1=0.1
      SX2=1.0E3
      SY1=1.0E-3
      SY2=10.0
C     IT,IX FORM THE SUPERFIXES FOR THE SCALES.
      IT=IFIX(ALOG10(SY1))
      IX=IFIX(ALOG10(SX1))
C     XK1,XK2,YK1,YK2 DEFINE MASK CO-ORDINATES.
      XK1=1.05*SX1
      XK2=XK1*10.0**(0.5*ALOG10(SX2/SX1))
      YK1=SY1*10.0**(0.91*ALOG10(SY2/SY1))
      YK2=SY2*0.99
      CALL PAPER(1)
      CALL PSPACE(0.25,1.0,0.15,0.95)
      CALL MAPXYL(SX1,SX2,SY1,SY2)
C     RX1,RY1 GIVES MID-PT. OF MASK.
      RX1=XK1*10.0**(0.5*ALOG10(XK2/XK1))
      RY1=YK1*10.0**(0.5*ALOG10(SY2/YK1))
      CALL CTRMAG(20)
      CALL MASK(XK1,XK2,YK1,YK2)
      CALL THICK(1)
      CALL AXNOTA(0)
      CALL BLUPEN
      CALL XGRATL
      CALL AXNOTA(1)
      CALL YGRATL
      CALL BLKPEN
C     THE FOLLOWING CALCULATES THE ORDINATE NOTATION.
C     LENGTH OF Y SCALE = AY*10.0**IBY
      FX1=SX1*0.43
      HKY=IFIX(ALOG10(SY2/SY1))
      DO 827 KY=0,HKY
      FY1=SY1*10.0**KY
```

```
      CALL POSITN(FX1,FY1)
      CALL TYPENI(10)
      CALL SUPFIX
      CALL TYPENI(IT+KY)
      CALL NORMAL
827   CONTINUE
C     THE FOLLOWING CALCULATES THE ABSCISSA SCALE.
      RNY=SY1*0.7
      HKX=IFIX(ALOG10(SX2/SX1))
      DO 818 J=0,HKX
      FX1=0.7*SX1*10.0**J
      CALL POSITN(FX1,RNY)
      CALL TYPENI(10)
      CALL SUPFIX
      CALL TYPENI(IX+J)
      CALL NORMAL
818   CONTINUE
      CALL POSITN(RX1,RY1)
      CALL TCSCEN('V79-CELLS',9)
      ZX1=SX1*10.0**(0.5*ALOG10(SX2/SX1))
      ZY1=SY1*0.3
      CALL POSITN(ZX1,ZY1)
      CALL TCSCEN('MEAN FREE PATH FOR PRIMARY IONIZATION, nm',41)
      TX1=0.316*SX1
      TY1=SY1*10.0**(0.5*ALOG10(SY2/SY1))
      CALL POSITN(TX1,TY1)
      CALL CTRORI(90.0)
      CALL TCSCEN('INTRINSIC EFFICIENCY FOR INACTIVATION',37)
      CALL CTRORI(0.0)
      CALL UNMASK(0)
      DO 839 KJ=1,KE
      READ(32,17) STPFIL(KJ)
17    FORMAT(A20)
      READ(32,*) W1,W2
      READ(32,*) N
      READ(32,*) SG
      DO 276 K=1,N
      READ(32,*) M(K),IZ(K),E(K),BS(K),ST(K),FP(K),TD(K),SR(K)
      X(K)=FP(K)
      Y(K)=SR(K)
276   CONTINUE
      IF (KJ.GT.3) GOTO 839
      IF (KJ.EQ.1) CALL REDPEN
      IF (KJ.GT.1) CALL BLKPEN
      DO 376 K=1,N
      IF (M(K).EQ.1) MF=112
      IF (M(K).EQ.2) MF=100
      IF (M(K).EQ.6) MF=76
      IF (M(K).EQ.7) MF=76
      IF (M(K).EQ.10) MF=66
      IF (M(K).EQ.11) MF=66
      IF (M(K).EQ.12) MF=67
      IF (M(K).EQ.14) MF=78
      IF (M(K).EQ.16) MF=79
      IF (M(K).EQ.19) MF=70
      IF (M(K).EQ.20) MF=35
      IF (M(K).EQ.40) MF=65
      IF (M(K).EQ.48) MF=84
```

```
      IF (M(K).EQ.58) MF=73
      IF (M(K).EQ.84) MF=75
      IF (M(K).EQ.129) .OR. M(K).EQ.132) MF=88
      IF (M(K).EQ.207) MF=80
      IF (M(K).EQ.238) MF=85
      IF (M(K).NE.4) GOTO 277
      CALL CTRFNT(2)
      MF=97
      CALL PLOTNC(X(K),Y(K),MF)
      GOTO 376
277   CONTINUE
      CALL CTRFNT(1)
      CALL PLOTNC(X(K),Y(K),MF)
376   CONTINUE
839   CONTINUE
      CLOSE(UNIT=32)
      CALL GREND
      STOP
      END
```

REFERENCES

Alper, T. : "Cell Survival After Low Doses of Radiation". John Wiley & Sons, Bristol (1975).

Al-Affan, I.A.M. and Watt, D.E. : Determination of Quality Factors by Microdosimetry. Submitted to Nucl. Instr. Meth. (Nov. 1985).

Al-Kazwini, A.T. : Ranges and Cross-sections for Inactivation of Solid Enzymes by Low Energy H, He and N Ions. Ph.D Thesis, Univ. of Dundee, 1983.

Al-Shaibani, H.M.A. : Cross-sections for Inactivation of Enzymes by Low Energy Ions. Ph.D Thesis, Univ. of Dundee, 1979.

Alvarez, L.W. : The Design of a Proton Linear Accelerator. Phys. Rev. 70, (1946), pp. 799-800.

Al-Wajidi, T.A.M. : Cross-sections for Inactivation of Ribonuclease in Solution by Low Energy X-Rays (10 keV to 70 keV). Ph.D Thesis, Univ. of Dundee, 1984.

Barendsen, G.W. : RBE-LET Relations for Induction of Reproductive Death and Chromosome Aberrations in Mammalian Cells. IN Sixth Symposium on Microdosimetry. Edts., Booz, J. and Ebert, H.G.. Vol. I, pp. 55-68. Harwood Academic Publishers Ltd., London (1978)

Bettega, D., Birattari, C., Bombana, M., Fuhrman-Conti, A.M., Gallini, E., Pelluchi, T. and Tallone Lombardi, L. : Relative Biological Effectiveness For Protons of Energies up to 31 MeV. Rad. Res. 77, (1979), pp. 85-97.

Bettega, D. and Tallone Lombardi, L. : Physical and Radiobiological Parameters of Proton Beams up to 31 MeV. Il Nuovo Cimento, Vol. 20, No. 3, (1983), pp. 907-916.

Bird, R.P. and Burki, H.J. : Survival of Synchronized Chinese hamster Cells Exposed to Radiation of Different LET. Int. J. Radiat. Biol., Vol.27, No.2, (1975), pp. 105-120.

Burrill, E.A. : Van der Graaff and Other Direct Electron Accelerators. Sect. 2.2.1.2 IN "Engineering Compedium on Radiation Shielding", Vol. I, Springer-Verlag, Berlin (1968).

Cannell, R.J. and Watt, D.E. : Biophysical Mechanisms of Damage by Fast Ions to Mammalian Cells in vitro. Phys. Med. Biol. 30, (1985), pp. 255-258.

Chadwick, K.H. and Leenhouts, H.P. : "The Molecular Theory of Radiation Biology", Springer-Verlag, Berlin (1981).

Chapman, J.D., Blakely, E.A., Smith, K.C. and Urtasun, R.D. : Radiobiological Characterization of the Inactivating Events Produced in Mammalian Cells By Helium and Heavy Ions. Int. J. Radiat. Oncol. Biol. Phys., Vol.3, (1977), pp. 97-102.

Chen, C.Z. and Watt, D.E. : Biophysical Mechanism of Radiation Damage to Mammalian Cells By X and Gamma-Rays. Int. J. Radiat. Biol., Vol. 49, No. 1, (1986), pp. 131-142.

Cox, R., Thacker, J. and Goodhead, D.T. : Inactivation and Mutation of Cultured Mammalian Cells By Aluminium Characteristic Ultrasoft X-Rays. II. Dose-response of Chinese hamster and Human Diploid Cells to Aluminium X-Rays and Radiation of Different LET. Int. J. Radiat. Biol. 31, (1971), pp. 561-576.

Cunningham, J.W. : Quantitative Analysis of Damage to Enzymes, Viruses, Bacteria and Higher Cells By Ionizing Radiation. Ph.D Thesis, Univ. of Dundee, 1982.

Curtis, S.B. : Calculated LET Distributions of Heavy Ion Beams. Int. J. Radiat. Oncol. Biol. Phys., Vol. 3, (1977), pp. 87-91.

Dertinger, H. and Jung, H. : "Molecular Radiation Biology". English Univ. Press Ltd., London (1970).

Fry, D.W. : The Linear Electron Accelerator. Philips Tech. Rev., 14, (1952), pp. 1-12.

Ginzton, E.L., Hansen, W.W and Kennedy, W.R. : A Linear Electron Accelerator. Rev. Sci. Instr., 19, (1948), pp. 89.

Goodhead, D.T. and Thacker, J. : Inactivation and Mutation of Cultured Mammalian Cells By Aluminium Characteristic Ultrasoft X-Rays. I. Properties of Aluminium X-Rays and Preliminary Experiments With Chinese hamster Cells. Int. J. Radiat. Biol., 31, (1977), pp. 541-559.

Goodhead,D.T., Munson, R.J., Thacker, J. and Cox, R. : Mutation and Inactivation of Cultured Mammalian Cells Exposed to Beams of Accelerated Heavy Ions. IV. Biophysical Interpretation. Int. J. Radiat.Biol., 37, (1980), pp.135-168.

Goodhead, D.T. and Charlton, D.E. : Analysis of High LET Radiation Effects in Terms of Local Energy Deposition. Radiat. Prot. Dosim., Vol. 13, No. 1-4, (1985), pp.253-258.

Goodhead, D.T. and Brenner, D.J. : Estimation of a Single Property/

Kiefer, J. : On The Interpretation of Heavy Ion Survival Data. IN "Proceedings 8th Symposium on Microdosimetry", Edts., Booz, J. and Ebert, H.G., pp. 729-742. EUR 8395 (Harwood Academic, London, 1983).

Lawrence, E.O. and Edlefsen, N.E. : On The Production of High Speed Protons. Science 72, (1930), pp. 376.

Lawrence, E.O. and Livingston, M.S. : The Production of High Speed Protons Without the Use of High Voltages. Phys. Rev. 38, (1931), pp. 834.

Lawson, J.D. : "The Physics of Charged Particle Beams". Oxford Univ. Press, 1977.

Lea, D.E. : "Actions of Radiation on Living Cells", 2nd Edition, Cambridge Univ. Press, 1962.

Livingood, J.J. : "Principles of Cyclic Particle Accelerator". D. Van Nostrand, 1961.

Livingston, M.S. and Blewitt, J.P. : "Particle Accelerators". McGraw Hill, New York (1962).

Livingston, M.S. : Ion Sources for Cyclotrons. Rev. Mod. Phys. 18, (1946), pp. 293-299.

McMillan, E.M. : Particle Acceleratos. Part XII IN "Experimental Nuclear Physics", Vol. III, Edt., Segre, E. John Wiley & Sons, New York (1959).

Munson, R.J., Bance, D.A., Stretch, A. and Goodhead, D.T. : Mutation and Inactivation of Cultured Mammalian Cells Exposed to Beams of Accelerated Heavy Ions. I. Irradiation Facilities and Methods. Int. J. Radiat. Biol., Vol. 36, No. 2, (1979), pp. 127-136.

Property of Low LET Radiations Which Correlates With Biological Effectiveness. Phys. Med. Biol., Vol. 28, No. 5, (1983), pp. 485-492.

Gordon, H.S. and Behman, G.A. : Particle Accelerator. Chap.8 IN "Nuclear Physics", Edt. Curtiss, L.F., American Institute of Physics Handbook, McGraw Hill, New York (1963).

Hall, E.J. : "Radiology for the Radiologist". Harper & Row Publishers Inc., New York (1978a).

Hall, E.J., Kellerer, A.M., Rossi, H.H. and Lam, Y.P. : The Relative Biological Effectiveness of 160 MeV Protons. Int. J. Radiat. Oncol. Biol. Phys., Vol. 4, (1978), pp.1009-1013.

Hall, E.J., Gross, W., Dvorak, R.F., Kellerer, A.M. and Rossi, H.H. : Survival Curves and Age Response Functions for Chinese hamster Cells Exposed to X-Rays or High-LET Alpha-Particles. Radiat. Res. 52, (1972), pp. 88-98.

Katz, R., Sharma, S.C. and Homayoonfar, M. : Chap. 6 IN Topics in Radiation Dosimetry, Supple. 1, Edt. Attix, F.H.. Academic Press Inc., London (1972).

Katz, R., Ackerson, B., Homayoonfar, M. and Sharma, S.C. : Inactivation of Cells By Heavy Ion Bombardment. Rad. Res. 47, (1971), pp. 402-425.

Kellerer, A.M. and Rossi, H.H. : The Theory of Dual Radiation Action. IN Current Topics in Radiation Research, Vol. 8, Edts., Ebert, M. and Howard, A., pp. 85-156. North Holland, Amsterdam (1974).

Neary, G.J. : Int. J. Radiat. Biol. 9, (1965), pp.477-502.

Neary, G.J. : Irradiation Of Simple Biological Specimens By Charged Particles. IN "The Uses of Cyclotrons in Chemistry, Metallurgy and Biology", Edt., Amphlett, C.B., pp.194-203. Butterworths, London (1970).

Panofsky, W. : The Linear Accelerator. Scientific American, Oct. 1954, pp. 40-44.

Patterson, H.W. and Thomas, R.N. : "Accelerator Health Physics". Academic Press, N. York & London (1973).

Perris, A., Pialoglou, P., Katsanos, A.A. and Sideris, E.G. : Biological Effectiveness of Low Energy Protons. I. Survival of Chinese hamster Cells. (Unpublished report- Nov. 1985).

Raju, M.R. : Chap. 4 IN "Heavy Particle Radiotherapy". Academic Press (1980).

Rossi, H.H. : Microdosimetry and Radiabiology. Radiat. Prot. Dosim., Vol. 13, No. 1-4, (1985), pp. 259-265.

Sinclair, W.K. : Experimental RBE Values of High LET Radiations at Low Doses and the Implications for Quality Factor Assignment. Radiat. Prot. Dosim., Vol. 13, No. 1-4, (1985), pp. 319-326.

Skarsgard, L.D., Kihlman, B.A., Parker, L., Pujara, C.M. and Richardson, S. : Survival, Chromosome Abnormalities and Recovery in Heavy Ion and X-Irradiated Mammalian Cells. Rad. Res. Supple. 7, (1967), pp. 208-221.

Stephens, K.G., Wilson, I.H. and Moruzzi, J.L. (Edts.) : "Low Energy/

Energy Ion Beams". Institute of Physics Conference Series Number 38, (1977).

Suit, H.D., Goitein, M., Tepper, J.E., Verhey, L., Koehler, A.M., Schneider, R. and Gragoudas, E. : Clinical Experience and Expectation With Protons and Heavy Ions. Int. J. Radiat. Oncol. Biol. Phys., Vol. 3, (1977), pp. 115-125.

Sutcliffe, J.F. : Inactivation Mechanisms By Low Energy Heavy Ions in Ribonuclease. Ph.D Thesis, Univ. of Dundee, 1974.

Takatsuji, T., Takekoshi, H. and Sasaki, M.S. : Induction of Chromosome Aberrations By 4.9 MeV Protons in Human Lymphocytes. Int. J. Radiat. Biol., Vol. 44, No. 6, (1983), pp.553-562.

Thacker, J., Stretch, A. and Stephens, M.A. : Mutation and Inactivation of Cultured Mammalian Cells Exposed to Beams of Accelerated Heavy Ions. II. Chinese hamster V79 Cells. Int. J. Radiat. Biol., Vol. 36, No. 2, (1979), pp. 137-148.

Todd, P : Medical College of Virginia Quarterly I, pp.2-14, 1966.

Todd, P.W. : Heavy Ion Irradiation of Cultured Human Cells. Rad. Res. Supple. 7, (1967), pp. 196-207.

Todd, P.W. : Heavy Ion Irradiation of Human and Chinese hamster Cells in Vitro. Rad. Res. 61, (1975), pp.288-297.

Wainson, A.A., Lomanov, M.F., Shmakova, N.L., Blokhin, S.I. and Jarmonenko, S.P. : The RBE of Accelerated Protons in Different/

Different Parts of the Bragg Curve. British J. of Radiology 45, (1972), pp. 525-529.

Watt, D.E., Cannel, R.J. and Thomas, G.E. : Ion Beams in Quality Determination for Radiation Protection. IN Int. Symp. on 3-day in Depth Review on the Nuclear Accelerator Impact in the Interdisiplinary Field, Laboratori Nazionali diLegnaro, Padova, Italy (1984), pp. 267-282.

Watt, D.E., Al-Affan, I.A.M., Chen, C.Z. and Thomas, G.E. : Identification of Biophysical Mechanisms of Damage By Ionising Radiation. Radiat. Prot. Dosim., Vol. 13, No. 1-4, (1985), pp. 285-294.

Wideroe, R. : Radiat. Clin. Biol. 36, (1968), pp. 308

Yamaguchi, H. and Waker, A.J. : A Resonance Model For Radiation Action. IN Microdosimetry, Proceedings of the 8th Symp., Edts., Booz, J. and Ebert, H.G., (1982), pp.497-506.

Zimmer, K.G. : "Studies in Quantitative Radiation Biology", Oliver & Boyd, London (1961).

Zirkle, R.E. and Tobias, C.A. : Effects of Ploidy and LET on Radiobiological Survival Curves. Arch. Biochem. Biophys. 47, (1953), pp. 282-306.